UNIVERSITY OF FORESTRY (LTU) – SOFIA

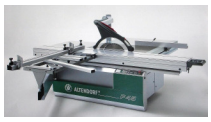

FACULTY OF FOREST INDUSTRY

DEPARTMENT OF

MECHANICAL ENGINEERING AND AUTOMATION OF PRODUCTION

STEFAN HRISTOV **STEFANOV**

associate professor, PhD, mechanical engineer, engineer-mathematician

INTEGRATION OF DAMAGE DIFFERENTIALS (IDD) FOR FATIGUE LIFE ASSESSMENT UNDER ANY LOADING

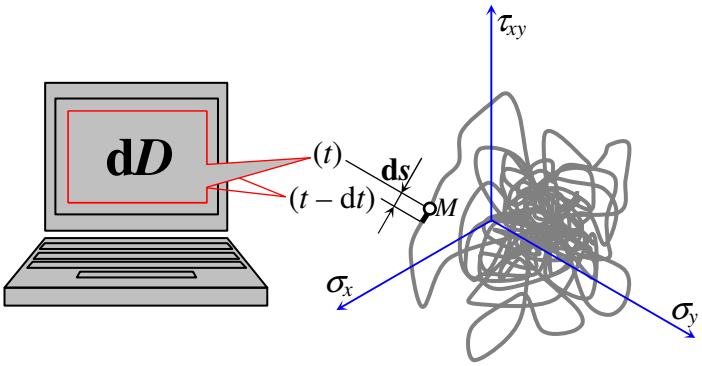

AUTHOR'S SUMMARY

of the THESIS

presented for conferring DSc degree on the author

Area of Higher Education: „5. Technical Sciences"

Professional Field: „5.13. General Engineering"

Scientific Speciality: „02.01.32 Machines and Technical Equipment for the Forestry, Wood Industry, Woodworking and Furniture Industry"

Sofia, 2011

***

The phrase ‘any loading’ in the title of the thesis means the following:

‘variable (with respect to the t time) plane state of stress having components $\sigma_x(t)$, $\sigma_y(t)$ and $\tau_{xy}(t)$ that may vary in any way: cyclic or non-cyclic (in the second case, deterministic or random); one of the three components may remain constantly zero, or two of the three components may remain constantly zero (then the state of stress is uniaxial or pure shear); in the general case, the oscillograms of the stresses $\sigma_x(t)$, $\sigma_y(t)$ and $\tau_{xy}(t)$ are all of them non-zero and have non-cyclic, arbitrary (or random) and non-proportional variations’.

In order to avoid such a long description, the short phrase ‘any loading’ has been preferred.

In fact, ‘any loading’ means ‘any stressing’ but the fatigue researchers say much oftener ‘loading’ for ‘stressing’. With that, it is expected to be understandable that fatigue ‘loading’ does not mean loads as definitely variable forces and/or moments but variable stresses causing fatigue of the material. Those stresses are caused by forces and/or moments that may even be constant (for example, constant forces on a carriage axle cause variable stresses due to the rotating bending).

The above paragraph is an answer to an otherwise just remark of the scientific jury member Professor L. Lazov: why ‘loading’ after talking about stresses?

By the way, the author had put the term ‘stressing’ instead of ‘loading’ in the title of his first publication [176] in *J. Fatigue*.

***

To facilitate the readers looking for details in the thesis, the pagination of the thesis is also given in the Contents of this summary together with its own pagination.

FOREWORD

The phenomenon of **fatigue of materials** due to variability of loading was realized in 19th century. Most of the fractures of engineering structures are due to fatigue and the consequences are disastrous. How to envisage in what operational lifetime fatigue failure would occur, i.e. how to assess the fatigue life, has been one of the most important engineering problems for the last two centuries. *There was not any uniform and all-acknowledged solution under any loading including the general multiaxial case of non-proportional, non-cyclic and arbitrary wave-forms of the stress components*. According to the thesis, the lack of solution was since the fatigue life had not been searched by means of an integral of fatigue damage differentials. Such a possibility had not been revealed and exploited before but it can be practically implemented nowadays thanks to the computers.

The thesis opens a **new scientific research line** under the IDD abbreviation. The underlying statement is that only the universal mathematical way of the calculus from differentials to an integral can establish a uniform and all-acknowledged solution to the problem of fatigue life evaluation under any loading. *The new line proposed would re-direct a vast world-wide research experience, accumulated for nearly two centuries, into another course. The basic notion of that experience is loading cycle and therefore the hitherto existing approach is called Cycle Counting Approach* (*CCA*). *In the thesis, another, new and radically different IDD approach is proposed: the basic, general notion is loading differential, while loading cycle remains as a particular notion, and the damage differentials per the separate loading differentials are integrated* (*summed*). That such differentials are introduced for fatigue life assessment may have the same importance which the differentials introduced in the mathematics and exact sciences generally have: decisive.

The development of the IDD approach and creating unique IDD software has been done by the author only what has inevitably engaged a lot of time: about 30 years. Since everything proposed here is entirely original and without any existing analog, the colleagues in the world and in Bulgaria have taken an explainable position of waiting for results. Thus, the IDD work continued most of the time without any collaborators, nor any financial or other support. Nevertheless, the IDD approach has become well-known and discussed in the world.

What is said above, as well as the necessity of juxtaposition to the nearly two-century CCA experience, explain the inevitable fact of a comparatively large volume of the thesis: 353 pages (with expanded line spacing and with an IDD-software manual included). But the colleagues that will study it, as well as the members of the scientific jury, will quickly orientate themselves to the main points. To help them, this Summary, this Foreword and an extended peculiar Preview serve. Then, the Conclusion and the Contributions (i.e. novelties presented separately) can be read. Afterwards, the details can be entered: the new notions, the mathematical instruments, the software created for practical application of the author's IDD method, the verifications carried out and their results, and so on. The volume of these details has been compressed to an acceptable minimum.

The IDD site cited above has been organized in a way as to also facilitate the study of the thesis. Besides, the site offers the IDD software as freeware. As well, the site gives the files involved in the sections of the thesis and in the verifications.

Eventually, this foreword hints that the thesis is expected to evoke great interest and opinions under considerable scientific responsibility on the part of the scientific jury members and the other colleagues. To all of them the author renders homage and his expectation of a just evaluation.

CONTENTS

(In the parentheses at the right margin, the page numbers of the thesis are put. Some of the contents items of the thesis are not included in this summary.)

PREVIEW

A treatise on the differentials and integrals

Mankind had been at a standstill in science and technology for millennia in succession by year 1600, i.e. by 17th century. *This related to non-development of mathematics*. *What actually happened to the human being's thinking after 1600* so that, in four centuries only comparatively to millennia of standstill, a lot of sciences suddenly progressed and enabled the contemporary scientific and technological miracles?

What happened in 17th century is that *the idea of infinitely little quantities* (*infinitesimals*) *was carried out*. *This was an infinitely great jump of the mankind*. The calculus was developed starting with the notion of a derivative function $f(x) = \mathrm{d}F(x)/\mathrm{d}x$ and its primitive function $F(x)$. The famous Newton-Leibniz theorem is well known: a definite integral with a variable upper limit $x_{\max}$ is a function $F(x_{\max})$ from which $f(x)$ is obtained by differentiation. This is a key interpretation for the thesis giving a surprising result discussed below.

After the fundamental Newton-Leibniz theorem, what was revolutionarily developed is *the general and universal mathematical way for obtaining relations searched among variables*: *namely as integral results from integration of relations found on a differential level*, *under any integration conditions*. Respectively, *if the differential and integral approach is not applied to a scientific field, then there will not be any uniform, all-acknowledged and universal method in a general formulation of the problem i.e. under general integration conditions*. Instead, there will be: hundreds of methods proposed in particular formulations, i.e. individual results under conditions which would have been particular integration conditions if researchers had integrated; hundreds of attempts to carry particular solutions onto a higher level of generalization what actually are trials to inductively adapt results from simpler integration conditions to more complicated ones; thousands of written papers resulted from scattering efforts.

Hence, it becomes apparent why IDD is proposed for fatigue life assessment under general (any) kind of loading: because namely in this field of research the general deductive mathematical way from differentials (of fatigue damage) to an integral had not been applied, namely under general (any) integration conditions (of loading). Instead, researchers went inductively from particular solutions to adapting them in a more general formulation, in many different scattering ways, without reaching a general and uniform method. To happen so was for historical and technological reasons (the future computers were still missing). Yet it is the high time to try with fatigue damage differentials and their numerical integration.

Retrospection of IDD

For taking up an exact attitude towards the proposed IDD method, it is of importance to know how the method was initiated and developed, and what a reception it had.

After additional mathematical education for graduated engineers held in the so-called 'Block B' of the Technical University of Sofia, the author started 1976 postgraduate (doctoral) studies. This happened at Department of Strength of Materials of the same Technical University of Sofia, in the research line of fatigue life. The director of the doctoral studies was the department head Professor Petar Levchev Ganev.

After the literature review done it became apparent that nobody had searched for fatigue life by means of an integral of fatigue damage differentials. At the root of fatigue life knowledge the empirical relation lies which is known as S-N line or Wöhler line. All the following studies were mostly on it. The S-N line represents an exponential relation between σ_{a} and N where σ_{a} is the amplitude of a cyclically varying stress and N is number of cycles to fatigue rupture.

Yet, from the IDD point of view, the *S-N* line i.e. the empirical relation $N = N(\sigma_a)$ can be treated as an integral result from summing (integrating) fatigue differentials per stress differentials $\mathrm{d}\sigma$ during time differentials $\mathrm{d}t$. The integration condition of this result is a simple particular case of cyclic σ variation: $\sigma(t) = \sigma_a \sin \omega t$. *However, no one had looked at the S-N line namely from this point of view*. Therefore, no question had been brought up for a differential $\mathrm{d}\sigma$ entailing some fatigue differential so that the Wöhler relation $N = N(\sigma_a)$ would result from integration of such differentials under the condition $\sigma(t) = \sigma_a \sin \omega t$. If this had been done, other integrations would immediately have been also done under any other non-cyclic (non-periodical, non-sinusoidal) $\sigma(t)$ oscillograms. Instead, a different thing happened: after the pressing question arose of how to predict fatigue life under an arbitrary, non-cyclic, deterministic or random $\sigma(t)$ oscillogram, *a process started for adapting the integral result from the case* $\sigma(t) = \sigma_a \sin \omega t$.

In other words, all the researchers directed themselves to looking for cycles with different amplitudes $\sigma_{a,i}$ *in a non-cyclic oscillogram* $\sigma(t)$. The latter was considered as a loading with a variable amplitude which accepted the different values $\sigma_{a,i}$, i.e. $\sigma(t)$ was replaced by a series of cycles with $\sigma_{a,i}$ amplitudes. The next adaptation to the *S-N* line was developed as follows. Researchers assumed that a so-called (relative) fatigue damage $1/N(\sigma_{a,i})$ occurs per one cycle with $\sigma_{a,i}$. The $N(\sigma_{a,i})$ life, shorter denoted as N_i, is taken from the *S-N* line. If the same cycle repeats itself to failure, the latter would occur in N_i cycles and the cumulative (relative) damage $D_\Sigma = \Sigma(1/N_i)$ would reach its full value 1 (i.e. 100 %). Thus, $n_i < N_i$ repetitions of $\sigma_{a,i}$ would make damage $n_i.(1/N_i) = n_i/N_i$. After summing such n_i/N_i damages from the different (grouped) $\sigma_{a,i}$ amplitudes, then the life is determinable from the equation $\Sigma(n_i/N_i) = 1$.

Such an approach dates back to the 20s of XX century after a similar idea of Palmgren. It was developed by Miner in the 40s. That is why determination of the life so that $\Sigma(n_i/N_i) = 1$ (or some revised value instead of 1) is called the rule of Miner (or Palmgren-Miner). Following the vein of the above treatise, the Miner rule is a way of adapting the integral result (the *S-N* line) under the particular integration condition $\sigma(t) = \sigma_a \sin \omega t$ to an arbitrary condition $\sigma(t)$. And, under such an interpretation, what happened later becomes already recognizable: a lot of methods were proposed for distinguishing cycles in a non-cyclic oscillogram and counting them. Such processing is also called schematization or decomposition of the non-cyclic oscillogram. In the last decades, the Rain-Flow Method of the CCA (the cycle counting approach) is the most popular. In Europe there is also Eurocode 3:1993 Reservoirs Standard (according to a note of Professor Lazov during preliminary discussions on the thesis).

In contrast to that all, the sacred calculus equation $\mathrm{d}F(x) = f(x)\mathrm{d}x$ was addressed. Analogously and merely, the equation $\mathrm{d}D(\sigma) = R(\sigma)\mathrm{d}\sigma$ was built. Here, $D(\sigma)$ is (relative) fatigue damage which changes by the differential $\mathrm{d}D(\sigma)$ per $\mathrm{d}\sigma$; $R(\sigma)$ is derivative of $D(\sigma)$ and as such is intensity of fatigue damage. Correspondingly, the $D(\sigma)$ damage function is the primitive of the $R(\sigma)$ damage intensity. If integrating $\mathrm{d}D(\sigma) = R(\sigma)\mathrm{d}\sigma$ under the condition $\sigma(t) = \sin \omega t$ for one cycle i.e. for one time-period T, then a relative fatigue damage per one cycle will be obtained. It is $1/N(\sigma_a)$. Vice versa, if differentiating suitably this specific integral result $1/N(\sigma_a)$ as a primitive, then the derivative $R(\sigma)$ can be determined according to the Newton-Leibniz theorem.

Hence, the determination of the damage intensity $R(\sigma)$ (*and thereafter operation on differential level of damage*) *can be done by relevant differentiation of a concrete* $1/N(\sigma_a)$ *primitive represented by the S-N line. After that,* $dD(\sigma) = R(\sigma)d\sigma$ *can be integrated under any arbitrary stress-time function* $\sigma(t)$. *Thus, there is no need of preliminary distinguishing and counting cycles i.e. no need of CCA* (*what is the surprising result mentioned above*). *And thus, the thesis advances a radically different idea of using an S-N line from cyclic loadings for fatigue life evaluation under arbitrary non-cyclic loading*.

The σ stress above is meant to represent a uniaxial state of stress i.e. one-component loading. The development of the engineering in 20th century posed the question of the fatigue life under multiaxial stress at surface points where, besides $\sigma(t) \equiv \sigma_x(t)$, also $\sigma_y(t)$ and $\tau_{xy}(t)$ may act. *In case the three* $\sigma_x(t)$, $\sigma_y(t)$ *and* $\tau_{xy}(t)$ *oscillograms vary proportionally, the stressing is tantamount to one-component loading*. Indeed, it is again represented by a single variable. If the latter is denoted as s, then again it comes to a single $s = s(t)$ oscillogram. Again one *S-N* line can be used. The next problem is that, in the general case, the multiaxial (multi-component) loading is non-proportional: with three totally different $\sigma_x(t)$, $\sigma_y(t)$ and $\tau_{xy}(t)$ oscillograms.

How did researchers start evaluating the fatigue life under multiaxial non-proportional loading? Again in the vein of the above treatise, what happened is expectable: without any loading and damage differentials defined in this general case, and therefore without any integration under arbitrary three-component conditions $\sigma_x = \sigma_x(t)$, $\sigma_y = \sigma_y(t)$ and $\tau_{xy} = \tau_{xy}(t)$, researchers started creating numerous methods. And, if under uniaxial loading many tens of criteria were proposed, then under two-component and three-component loading their number would increase to the second and third power. It became very complicated while doing trials to generalize some results from one-component loading to two- or three-component loading. Such trials required certain concepts (theories) for fatigue equivalence between multiaxial non-proportional loading and one-component loading, respectively for reducing the loading multiaxiality. Many concepts and many corresponding conceptual problems appeared.

Whereas, *if integrating fatigue damage from a differential level of multiaxial stressing, directly under arbitrary* $\sigma_x(t)$, $\sigma_y(t)$ *and* $\tau_{xy}(t)$ *oscillograms, then any necessity of reducing the loading multiaxiality drops out, neither is there any need of looking for cycles and counting them*. The mentioned conceptual problems do not appear.

But how to define a loading (stressing) differential (labeled with ds) under three components $\sigma_x(t)$, $\sigma_y(t)$ and $\tau_{xy}(t)$? Under one only component $\sigma(t) \equiv \sigma_x(t)$, the differential ds is quite simple according to above: it is $d\sigma$. However, under three components, the definition of ds is not that simple at all: the three stresses are tensor-like dependent on (variant of) the choice of the x and y axes. Hence *it is first to solve the problem of how to compose a three-component loading differential* ds *which is independent of* x *and* y. *The next problem*: *provided that* ds *is defined, how to compose the damage differential* dD?

These problems were a true challenge to the author's mathematical setting from the 'Block B' (and after some accumulated professional experience in algorithms and computer programming in a computer-processing center). A term of *trajectory* was introduced as a path described in the σ_x-σ_y-τ_{xy} coordinate system. It is obvious that while the describing running (current) point of the trajectory is going away from the coordinate origin, the damage intensity is rising. Then it stands to reason to associate the cumulative damage with accumulation of a (curvilinear) integral along the trajectory: the latter is composed by infinitesimal segments that are, in fact, stressing differentials ds. Per every ds, a damage differential dD is added with a damage intensity which steeply rises while σ_x, σ_y and τ_{xy} rise. However, this σ_x-σ_y-τ_{xy} trajectory is, as already understood, tensor-like *variant*, i.e. it will radically change if different x and y axes are chosen.

Therefore another, *invariant* trajectory must be introduced. This is the trajectory of the principal stresses σ' and σ'' i.e. the trajectory described in the σ'-σ'' coordinate plane. However, the rotation of the principal axes ' and " would be omitted in this way. How should it be accounted?

After all, to the attention of the director Prof. Ganev and of the department, a three-component differential $\mathrm{d}s$ in the coordinate system ε'-ε''-$\mathrm{d}\gamma$ was submitted; ε' and ε'' are the principal strains, and $\mathrm{d}\gamma$ is a shear-strain differential. Addressing strains instead of stresses was influenced by Prof. Ganev who searched for application of an ε_x-ε_y hysteresis loop discovered by him. The idea of $\mathrm{d}s$ in ε'-ε''-$\mathrm{d}\gamma$ coordinates remains the same in σ'-σ''-$\mathrm{d}\tau$ coordinates as presented in the thesis.

The director and the department took intense interest in the $\mathrm{d}s$ differential proposed. The multiaxial (three-component) loading could already be represented as a multitude of $\mathrm{d}s$ differentials. They are technically formed as finite Δs differences that are short enough and of a sufficiently great number. Thus IDD was formed as a numerical method enabled only by means of a computer. By the way, for the necessity of a computer, the IDD method would not have been proposed for practical application earlier than e.g. 1970. In fact, the method hit upon the beginning of the mass computerization and the entailed possibility of numerical differentiation and integration in a large volume. On this basis, also in other scientific fields, methods were developed that had been unthinkable before. And, finally, contemporary kinds of software appeared for finite elements (FE) modeling.

The idea of $\mathrm{d}s$ and the first computer programming already done were published 1978. This is the registered beginning of the IDD method (the name 'IDD' was accepted 2009 and it substituted the previous name 'Integral Method'). After $\mathrm{d}s$, the damage differential $\mathrm{d}D$ was also postulated, first in the simplest way from above: $\mathrm{d}D(s) = R(s)\mathrm{d}s$. This was a hypothesis (published 1979) that the same damage intensity $R(s)$ could be used under different integration conditions. The PhD dissertation was successfully defended 1980.

The director envisaged a great future for IDD in combination with input S-N lines obtained in an accelerated manner based on his ε_x-ε_y hysteresis loop. Unfortunately, he fell ill 1984 and passed away 1985. The new department head, Prof. Stoyan Nedelchev, did such a personnel policy (in a communist manner) that the final result for the author was leaving the Technical University. The author's career continued at the Faculty of Forest Industry of the University of Forestry where the author became an associate professor 1991.

At that time Bulgaria opened itself to the world and the author returned to the method in order to popularize it internationally. It seemed that the very idea to sum fatigue damage differentials directly under any loading, without any cycle counting or reducing stress multiaxiality, would find the same respect and support as in the Department of Strength of Materials 1978 - 1984. Introducing the damage differentials and an integral of them seemed to have the same revolutionary importance for the fatigue life research like the importance of introducing differentials and integrals into the mathematics and related exact sciences. It seemed that the Integral Method (IDD) would immediately be taken up from the world fatigue life research authorities and institutions.

In 1993 there was a two-month author's study visit to the one of European centers of fatigue research: the Prof. Zenner's IMAB-institute in Clausthal, Germany. Prof. Zenner, as one of the world fatigue research authorities, and his collaborators showed some interest to the Integral Method. But they only wished success in its development: they had their own scientific program and financing, and each colleague had his own task.

The author was successful to have four papers published in *Int. J. Fatigue* 1993 – 1997. Each publication took one-year effort. The referees showed reserves about the unknown author from Bulgaria who tried to propose something nontraditional.

The fourth paper was dedicated to the interesting characteristic loading case in which the principal axes rotate but the principal stresses remain constant. This case was revealed thanks to IDD and the paper emphasized that it remained undeservedly unnoticed; that it is very important because it is a 'maximized' case. A lot of fatigue life criteria should be approbated under such loading to check their validity. Then, many of them would fail.

After this fourth paper, *Int. J. Fatigue* did not admit to publication a fifth paper submitted. In it, the point was openly set that the whole world fatigue life evaluation experience should be redirected to relations on differential level from where free integration should be done as a uniform method under any sorts of loading. Another paper, 'Fatigue Life Prediction without Cycle Counting (Using an Integral)', was also denied. A situation became apparent that the Integral Method is not accepted by the authors and supporters of the many existing CCA methods established also by government standards.

But later, already on a regional level in Bulgaria, the paper 'Fatigue Life Prediction without Cycle Counting (by Means of the Integral Method)' was accepted and published in the *J. Theoretical and Applied Mechanics* (of the Bulgarian Academy of Sciences).

In the meantime, Prof. Ewald Macha from the Technical University of Opole, Poland, took an interest in the Integral Method. This stimulated building a team with the author leading and with participation of Prof. Macha and his Polish collaborators for doing "Development of the Integral Method for Fatigue Life Prediction under Multiaxial Non-proportional Arbitrary or Random Loading". Under this title, the Bulgarian Science Fund granted some financing ('TH-545/95' contract with the University of Forestry). However, for the post-communist crisis and inflation in Bulgaria at that time, the resources quickly exhausted. Besides, a negative situation occurred in the relations with the Polish colleagues (details, including curious ones, can be read in the thesis).

Another stimulus appeared in connection with Prof. De Mare and his collaborators from Sweden. It turned out that they, independently and in a later time, enabled fatigue life prediction under one single oscillogram by using its instantaneous ordinates instead of amplitudes, what is the same with the Integral Method. Respectively, they also defined damage intensity although they did not call it so: it is their function $g(s)$ which equals the IDD $R(s)$ intensity in the particular case of zero static level of the oscillogram. They had not initiated the idea of loading and damage differentials and correspondingly they did not talk about an integral of such differentials.

Prof. De Mare was contacted for cooperation. An invitation followed and financing on Swedish part was provided to the author for a study visit to Sweden and participation in the Workshop 'Statistical Methods in Fatigue of Materials' 1998. A talk was given in which the Integral Method was briefly represented and its point of intersection with the Swedish authors' model was shown. A call was extended for joint effort for a new approach to fatigue life prediction starting from differential level. The response was reserved. After all, the Swedish colleagues did not show any intention to generalize their method to something more than its original direction.

It became more and more apparent that whether the Integral Method would really be the right new approach or not is on the one hand only. On the other hand the circumstance was that a global acknowledgment of the Integral Method would require from the other authors to reevaluate, readjust or even deny their own concepts. However, they made their careers and obtained finances thanks to their concepts. Hence, the reserved attitude or even a preliminary negative aptitude to IDD seems to be logical. The author nearly gave up next trials.

In 1998, a second two-month study visit to the Prof. Zenner's institute, Germany, was enabled again. A touch with the University of Braunschweig was enabled, as well, and a talk was also given there. On a conference in Sheffield, UK, IDD was also talked. Within the period 1999 – 2003, the author was to the US for two years and a half. In 2002, he was a visiting professor at the Illinois Institute of Technology, Department of Mechanical, Materials and Aerospace Engineering (MMAE). Some attempts were made to engage MMAE and other American colleagues with the Integral Method. But they kindly denied for being busy in their own tasks and projects. After all, persistent IDD f0llowers were not found.

Thus, the work on IDD broke again. Subsequently, the method proved to be already well-known and discussed in the world. There was the acknowledgement that the IDD concept is far beyond the scope of the previous studies. There was, as well, negative reaction on the part of persistent CCA followers. This additionally showed that the work must continue, and cooperation and IDD adherents should be found. Besides, an IDD public defense procedure should be evoked as an additional way to engage the attention and valuation of more people.

A next stimulus appeared again. It came on the part of a doctorand (postgraduate student), assistant professor Boyan Stoychev, from the Department of Engineering Mechanics at the Technical University of Gabrovo, Bulgaria. Collaboration started for building a new testing machine for rotating bending combined with constant torsion designed on the basis of an author's scheme. The experimental data obtained served for a successful IDD verification (in Chapter 5).

A Bulgarian IDD site, http://metodnaintegrala.hit.bg, was created in 2006. The method is popularized there in Bulgarian language. The thesis is also exposed there together with computer programs and files. As well, a Volume II is exposed containing expansions, supplements, details, etc. References to the IDD site are done for everything which belongs to the thesis or is its continuation but cannot be included in the thesis due to its limited volume.

In English, the same site is http://www.freewebs.com/fatigue-life-integral. It became main means for popularizing IDD abroad and for establishing contacts with many colleagues throughout the world.

As a result, collaboration with Dr. Jan Papuga and his colleagues from Czech Republic was established. Dr. Papuga is a young scientist who has a present and a future of a world authority on fatigue of materials, mainly for a site he had created: http://www.pragtic.com/. There, an ambitious so-called PragTic Project is exposed. It contains a large fatigue strength data bank, a lot of methods and software, communication in a PragTic society, PragTic forum, organization of regular annual PragTic conferences, and so on. On his site, Dr. Papuga proclaimed the integration of damage differentials without forming any cycles to be a revolutionary idea (http://www.pragtic.com/docu/PragTicA_Intro.pdf, p. 9).

From the collaboration with Dr. Papuga, a paper resulted which was reported on an international conference in Darmstadt, Germany. In this paper, the IDD abbreviation was suggested and accepted as a better name. The reported IDD lives under one-component random loadings computed without using the rain-flow procedure (which otherwise was expected on the conference) proved to be the most accurate (Subchapter 3.3).

In the summer 2009, a third two-month study visit to Germany was done, this time to the Fraunhofer Institute for Structural Durability and System Reliability LBF (Fraunhofer-Institut für Betriebsfestigkeit und Systemzuverlässigkeit LBF), at the invitation of Prof. C. M. Sonsino. He is one of the world-famous scientists in fatigue of materials. Thanks to him and to his interest in IDD, this visit was very fruitful. An IDD study (70 pages), with the participation of Prof. Sonsino and the LBF director, Prof. H. Hanselka, was written. This was the LBF 2009 annual report which took the character of a monograph on IDD. As well, two papers devoted to IDD verifications were written with participation of other more LBF colleagues.

The activity through the IDD site and the interest in IDD led to including the author in the Scientific Committee of the ICMFF9 (the Ninth International Conference on Multiaxial Fatigue & Fracture), Parma, Italy, June 7 – 9, 2010 (http://www.icmff9.unipr.it/). This conference is held once three years. The most known researchers in the subject come together to this conference and it is the most relevant forum for IDD. The author actively participated in the conference and reported an invited paper. Discussions on IDD and engaging the ICMFF9 audience attention to IDD were evoked. Other three more IDD papers were included in the ICMFF9 proceedings.

In the person of the ICMFF9 co-chairmen, Prof. Andrea Carpinteri from the University of Parma and Prof. Sonsino, the author found the long-expected acknowledgement and support for the importance of IDD. On their initiative, an invitation came for IDD publication in a special issue of *J. Fatigue* 2011 devoted to ICMFF9. All this turned into a good reason for finalizing and presenting the thesis.

CHAPTER 1. REVIEW ON EXISTING METHODS WITH CONCOMITANT ANALYSIS AND CONCLUSIONS IN THE VEIN OF IDD. GOAL AND TASKS OF THIS THESIS

1.1. Introductory notions, terms and symbols. Kinds of loading

In this thesis, computation of *limited life* which may prove to be *unlimited life* is considered. The fatigue damage is accumulated under *loading* (*stressing*) that is *variable* with respect to the time. One (*graph of a*) *stress-time function/ stress-time history* $s = s(t)$ or more than one represent(s) the variable stressing. The shorter term *oscillogram* for (the graph of) $s = s(t)$ is used.

Almost exclusively, *fatigue plane stressing* is considered in the engineering because fatigue crack growth usually starts from the surface of the body. Thus, two normal and one shear stresses act *at a critical point* of the body. They are usually denoted as σ_x, σ_y and τ_{xy}. Correspondingly, the loading (the stressing) is called *multiaxial* consisting of up to three components. This case is studied in the present thesis. However, IDD as a mathematical approach can be applied to six-component stressing, as well.

The loading is *uniaxial* (*simple*) if only one of the oscillograms $\sigma_x(t)$, $\sigma_y(t)$ and $\tau_{xy}(t)$ is available (non-zero), and the other two are constantly zeros. *Biaxial* loading means that two oscillograms are non-zero. In this thesis, the terms of *one-component* (uniaxial), *two-component* (biaxial) and *three-component loading* are also used. The multiaxial loading is also known as *combined* or *complex*.

The one-component loading is *cyclic* in case the stress-time function is periodical with a period (cycle) of time T, i.e. $s = s(t + T)$. Simple variation of $s(t)$ between constant $s_{\max}$ and $s_{\min}$ is understood: without any intermediate extrema (peaks, reversals). Loading which does not agree with this definition is called *non-cyclic loading* or non-stationary loading, or *variable-amplitude loading*.

The one-component cyclic loading is most often *sinusoidal*: $s = s_m + s_a \sin(\omega t + \delta)$ where s_m is *mean* (*static*) stress (component), s_a is *amplitude*, ω is *angular frequency* and δ is *initial phase* (*angle*), *phase-shift* (*angle*) or *out-of-phase angle*. The cyclic loading can also be non-sinusoidal, for example trapezoidal or triangular (or, to simplify an oscillogram, it is illustrated as triangular). Anyway, the following characteristics are introduced: $s_{\max}$, $s_{\min}$, $s_m = (s_{\max} + s_{\min})/2$, $s_a = (s_{\max} - s_{\min})/2$ and *stress ratio* $R = s_{\min}/s_{\max}$. The loading (cycle) is *alternating* (*reversed*, *symmetrical*) in case $R = -1$ i.e. $s_{\min} = -s_{\max}$ and $s_m = 0$, and *non-alternating* (*asymmetrical*) ($R \neq -1$, $s_{\min} \neq -s_{\max}$, $s_m \neq 0$). In particular, with $R = 0$ the loading is *pulsating*.

The multiaxial cyclic loading is *in-phase* when the oscillograms have the same initial phase. Otherwise, the loading is *out-of-phase*. In case the out-of-phase angle between two oscillograms is 180^0, the loading is *in-opposite-phase*. When the angular frequency ω or the *frequency* $f = 1/T$ of the oscillograms is the same, the loading is *of-equal-frequency*. Otherwise, the loading is *of-different-frequency*. The in-phase (or in-opposite-phase) of-equal-frequency loading is *synchronous*: the peaks in the oscillograms appear simultaneously. Otherwise, the loading is *non-synchronous*. In a wider meaning, synchronous loading is identified with proportional loading (defined below).

The non-cyclic loading is *random* (*stochastic*) when the peak ordinates are random, or it is *deterministic* (the peak ordinates are predetermined). The random loading is a random process and as such it is subject to the theory of random processes. Correspondingly, a great number of publications relate to the research field of fatigue under random loading. It is to remark that uniaxial random loading is meant. The multiaxial random loading as a multi-dimensional random process with multi-dimensional statistical characteristics remains, in principle, out of research (it can be in research only by means of IDD as discussed in Subchapter 2.8).

The multiaxial loading is *proportional* when all the two or three oscillograms have the same shape in different scales, i.e. the ordinates of the oscillograms are proportional. As a matter of fact, one single oscillogram $s(t)$ represents the multiaxial loading after multiplying with some constant ratios. For instance, the single oscillogram may be $\sigma'(t)$: of the first principal stress. The second principal stress is $\sigma''(t) = k\sigma'(t)$ where k = constant. *Thanks to the single oscillogram, the proportional loading, although multiaxial, allows the same treatment as uniaxial loading*. In case the oscillograms are non-proportional to each other, the multiaxial loading is *non-proportional*.

The *general loading case* is *multiaxial*, *non-proportional and non-cyclic loading* (Fig. 1.1-3a): *an arbitrarily tangled curved trajectory* (*loading path*) *is described in the* σ_x-σ_y-τ_{xy} *coordinate space* (Fig. 1.1-3b). The appearance of the trajectory depends on the choice of the stress axes x and y, i.e. the trajectory is variant (with respect to x and y). It represents *the mutual variation* (*the mutuality*) *of* $\sigma_x(t)$, $\sigma_y(t)$ *and* $\tau_{xy}(t)$. In general, *no reversals are to be distinguished in this trajectory, nor any cycles to be counted*.

But instead of cycles, (variant) differentials $\mathrm{d}s$ (with components $\mathrm{d}\sigma_x$, $\mathrm{d}\sigma_y$ and $\mathrm{d}\tau_{xy}$) are to be distinguished in the trajectory. Such a $\mathrm{d}s$ differential is shown in Fig. 1.1-3b. It ends at a current (running) t time, respectively at a current M point, and its beginning is at a preceding time $t - \mathrm{d}t$.

Arbitrary loading or *any loading* is any of the kinds of loading counted above, including the general case and primarily it (Fig. 1.1-3) since it includes the rest. As well, *arbitrariness of the variations of the oscillograms* is understood.

It is typical for any oscillogram $s(t)$ to fluctuate arbitrarily around an s_m *mean* (*static*) value (level) (in Fig. 1.1-3a, the three oscillograms have static levels $\sigma_{x,\mathrm{m}}$, $\sigma_{y,\mathrm{m}}$ and $\tau_{xy,\mathrm{m}}$). With that, a steady static level s_m = constant is supposed. In more complicated and rarer cases, the oscillograms may also have parts of different character. Then, an unsteady static level $s_\mathrm{m} = s_\mathrm{m}(t) \neq$ constant can be introduced. Correspondingly, the IDD method can be developed in a more complicated version as to account $s_\mathrm{m}(t) \neq$ constant (Section 2.3.7). But for now, loading with $s_\mathrm{m}(t) \neq$ constant will be separated into sub-loadings (individual loadings) with different steady static levels that approximate $s_\mathrm{m}(t) \neq$ constant of the whole loading. IDD will be applied to the sub-oscillograms separately (the other existing methods are applied in the same way).

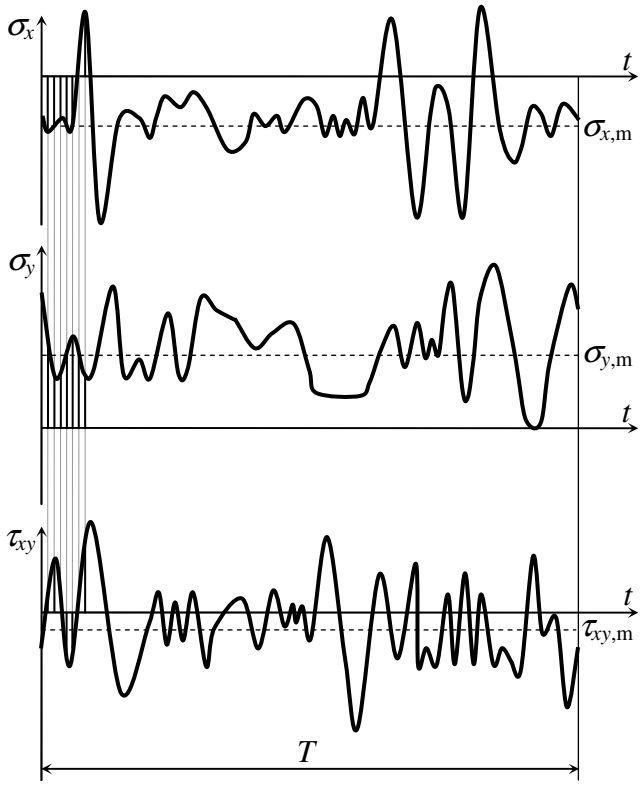

(a) Three arbitrary oscillograms $\sigma_x(t)$, $\sigma_y(t)$ and $\tau_{xy}(t)$

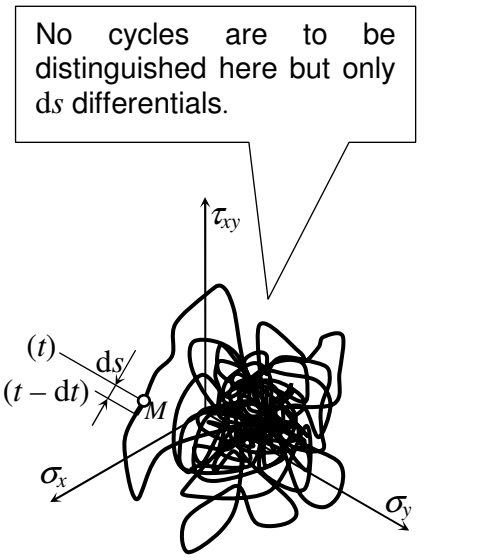

(b) Trajectory of the mutual variation (the mutuality) of the three oscillograms, and a variant loading differential $\mathrm{d}s$

Fig. **1.1-3.** Multiaxial non-proportional and non-cyclic loading (the general case of loading)

In their publications, the other researchers did not define general loading in the meaning of Fig. 1.1-3. Respectively, Fig. 1.1-3 is an original illustration (of which *J. Fatigue* has rights). The researchers did not reach the general loading case in Fig. 1.1-3 but some loading 'arbitrariness' or 'complexity' being always in the scope of some particular conditions.

In case the fatigue occurs in more than 10^4 cycles, it is called *high-cyclic fatigue*. Under 10^4 cycles, it is *low-cyclic fatigue*. The high-cycle fatigue is typically dominated by elastic strains and the Hooke's law is acceptable. Otherwise, comparatively great elasto-plastic strains entail low-cyclic fatigue. The border between low-cyclic fatigue and high-cyclic fatigue is conditional (it could be 10^3 instead of 10^4).

In this thesis, limited in volume like any other thesis, the IDD method is only verified for the (more important) high-cycle fatigue. Correspondingly, the stresses $\sigma_x(t)$, $\sigma_y(t)$ and $\tau_{xy}(t)$ are preferably treated that can be obtained by strain-gauges from strains $\varepsilon_x(t)$, $\varepsilon_y(t)$ and $\gamma_{xy}(t)$ using the Hooke's law. However, as a mathematical approach, IDD is applicable to low-cycle fatigue, as well. Then IDD is expected to be better in application directly to the strains $\varepsilon_x(t)$, $\varepsilon_y(t)$ and $\gamma_{xy}(t)$.

Supposing representative oscillograms are given in a T time-interval (Fig. 1.1-3a) and they repeat N times to fatigue failure. If the loading is random, it is supposed ergodic and a *representative loading abstract* is derived within T. The T interval plays the role of a period of time and therefore the same T symbol is adopted from the cyclic loading. Thus, *the life means N repetitions of T to fatigue failure* (to fracture or to a certain size of crack, or according to any other criterion of fatigue failure). In other words, *the life is NT* as duration. By means of a suitable multiplier, some other name can be assigned to the life, for example km run, operating hours, number of working moves, and so on. Under cyclic loading, N means, of course, *number of cycles to failure*.

In this Subchapter 1.1 in the thesis, an example follows that comes from the engineering practice in support of the discussed necessity of a universal method and of readiness for fatigue life prediction right in the general loading case (Fig. 1.1-3). In 1977, a research was carried out into the reasons for fatigue fractures of axles of a semi-trailer.

The senior colleagues leading the research declared that, under the registered combinations of non-proportional random bending and torsion, no fatigue life evaluation could be done based on any indisputable standard method to be acknowledged by the affected party i.e. the manufacturer of such semi-trailers. That is why the colleagues did standard procedures only on $\sigma_x(t)$ oscillograms from bending: schematization (cycle counting), building an amplitude spectrum, composing an *S-N* line, and then fatigue life evaluation based on the Miner rule. Even in this way the fatigue life predicted proved to be less than (although close to) $500\,000$ km: the postulated run to scraping. Later, after developing the Integral Method (the IDD) in its first version and enabling it to application, the torsion was also involved: the IDD life prediction was approximately $100\,000$ km now.

According to latest studies, complicated, multi-spectrum and non-proportional loadings occur in the woodworking machines, as well. A large area is revealed for IDD application to scientific specialties at the University of Forestry (LTU) of Sofia. This has evoked writing the last, special Chapter 6 of the thesis.

1.2. Fatigue life under cyclic uniaxial or multiaxial proportional loading. *S-N* line

1.2.1. General notes

Under one-component loading or proportional multiaxial (multi-component) loading, the running M point (Fig. 1.1-3b) oscillates on a radial straight line. It passes through the coordinate origin and serves as s axis. Under uniaxial state of stress, $s \equiv \sigma \equiv \sigma_x \equiv \sigma'$ ($\sigma_y \equiv \sigma'' = 0$, $k = \sigma''/\sigma' = 0$). Under pure shear, $s \equiv \tau \equiv \tau_{xy}$, $|\tau_{xy}| = |\sigma''| = |\sigma'|$, $k = -1$. Under multiaxial state of stress, the s axis is away from the coordinate axes σ_x, σ_y and τ_{xy} at certain angles. In all cases, if the principal varying stresses $\sigma'(t)$ and $\sigma''(t)$ are computed from the proportionally varying stresses $\sigma_x(t)$, $\sigma_y(t)$ and $\tau_{xy}(t)$, then the s axis will lie in the σ'-σ'' coordinate plane. The principal axes ' and '' will stay immovable. For the s axis is radial, some characteristics under the uniaxial or proportional loading will be denoted with $_r$ index, and the loading itself will be called '*r-loading*'.

The s axis can be separately considered (Fig. 1.2.1-1a): out of the coordinate system σ_x-σ_y-τ_{xy} or σ'-σ''. If the r-loading is cyclic in particular, then the trajectory is represented by a straight-line segment of the s axis between $s_{\min}$ and $s_{\max}$. Such a segment is illustrated (as a thickened one) in Fig. 1.2.1-1a. On the right of the segment, the *trajectory* is shown as '*unfolded*' *with the time*. In this way the oscillations on the s axis are revealed.

Wöhler was the first to do systematic investigations of *S-N* diagrams (*S-N* lines, Wöhler curves) where $S \equiv s_{\max}$ and most often $s_{\max} = s_a$ ($R = -1$). In the *S-N* diagram, experimental points with coordinates ($s_{\max}$, N) are plotted. They are too scattered (Fig. 1.2.1-1b) and a correlation line is drawn among them.

Since the time of Wöhler until now, regular tests are carried out everywhere in the world for building *S-N* lines. A great number of the testing machines produce alternating loading ($R = -1$) by rotating bending. But there are also machines that hold the specimens kinematically immovable and exert on them bending, tension-compression, torsion, etc.

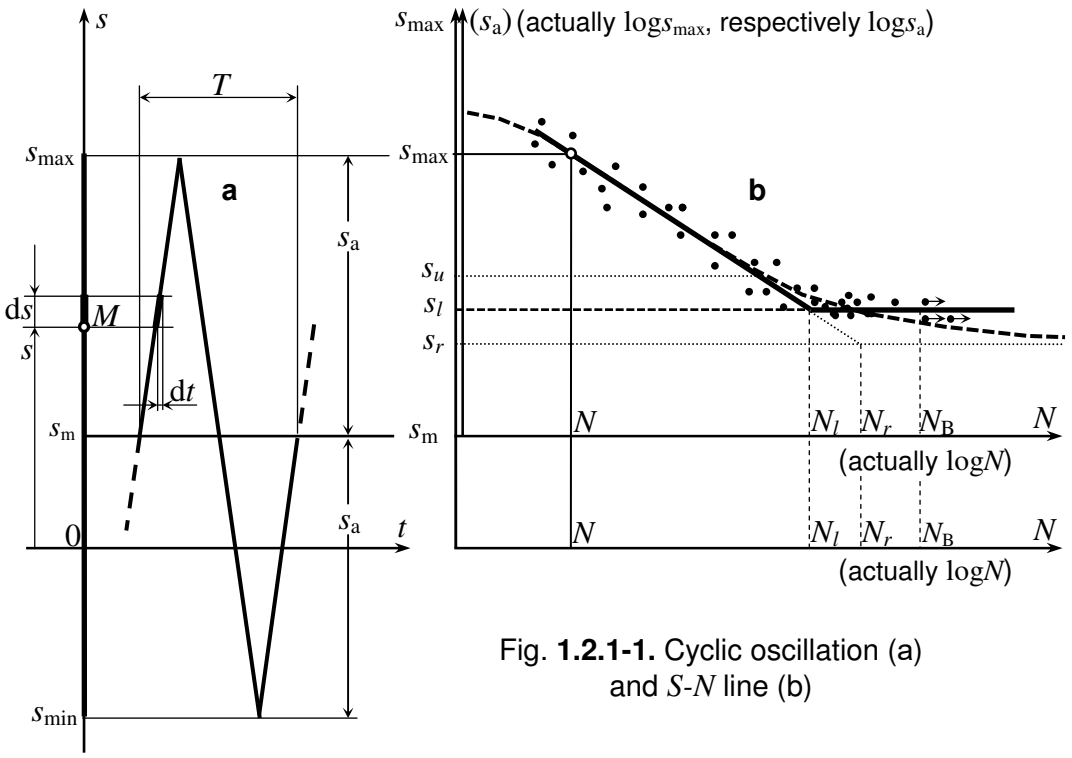

Fig. **1.2.1-1.** Cyclic oscillation (a) and *S-N* line (b)

The Wöhler curve is really a curved line if it is really drawn in (usual, decimal) *S-N* coordinates. However, the usual scale of the N coordinate axis is too unsuitable since it stretches the diagram too much: if S decreases e.g. twice, N may become one thousand times as much. That is why N is plotted in a logarithmic scale (actually $\log N$ for N in Fig. 1.2.1-1b). Basquin proposed a log scale also of the S axis (actually $\log S$ for S in Fig. 1.2.1-1b). It proved that in this way, in double-logarithmic (log-log) coordinates, the Wöhler curve can be represented as a straight line very well: the mean-square deviation of the experimental points from the line is well minimized. In fact, a straight line of regression can be drawn according to the method of least squares. Thus, the most popular equation of the *S-N* line of (high-cycle) fatigue is

$$m\log s_{\max} + \log N = \text{const} = \log A, \qquad \text{i.e.} \qquad s_{\max}{}^{m} N = \text{const} = A \tag{1.2.1-1}$$

where m is the (*indicator of the*) *slope* of the line. The greater m is, the less slanting the *S-N* line is. The m slope varies widely: from 3 to 20 and more, most often between 6 and 15. With that, a five-percent change in $s_{\max}$ (respectively, a five-percent error in measuring $s_{\max}$) can lead to a change in the life e.g. twice (respectively, an error of twice in evaluating the life). That is why, an error in the computed life in the order of twice or three times (*error factor of* 2 *or* 3), even more, is acceptable.

The *S-N* line is usually assumed to 'break in two' at the *fatigue* (*endurance*) *limit* s_l (Fig. 1.2.1-1b, in particular $s_l \equiv \sigma_{-1}$) and go horizontally to unlimited life (in the thesis, the $_l$ subscript is generally used as an index of limiting stress). Thus, Eq. 1.2.1-1 describes the sloping part of the *S-N* line and is valid for $s_{\max} \geq s_l$. In other words, Eq. 1.2.1-1 is of the limited life and gives both the function $s_{\max} = s_{\max}(N)$ and the inverse function $N = N(s_{\max})$ at $s_{\max} \geq s_l$. For IDD, the inverse function $N = N(s_{\max})$ will be used.

In historical retrospection, unlimited life was first required for the simple cyclic one-component loading (with constant amplitude). In other words, $s(t)$ should not exceed the endurance limit, i.e. $s(t) < s_l$ was required, conservatively, with a safety factor (ratio) $n = s_l/s_{\max}$. Later on, the question of evaluation of limited life was always prompted. Indeed, when

the oscillogram $s(t)$ is not with constant amplitude, then the condition $s(t) < s_l$ is not acceptable yet: provided that the highest peak is lower than s_l, then the most of the rest peaks will be unnecessarily much lower than s_l. In general, the present-day fatigue calculation is understood as not only providing the classic safety factor $n = s_l/s_{\max}$ but acting on a higher level of methods for computing limited life. For this purpose, not only the endurance limit s_l but also the other two parameters m and A in Eq. 1.2.1-1 are to be involved. With that, $A = s_l^m N_l$ where N_l is the number of cycles at the break of the S-N line (Fig. 1.2.1-1b). A popular N_l number is 2.10^6 (two millions) cycles.

Breaking an S-N line into a horizontal line is a simplified and controversial conception. The idea is also assumed of change of the slope at $s_{\max} < s_l$, respectively at $N > N_l$: m increases significantly but not to infinity (corresponding to a horizontal line). As well, a smooth bend of the S-N line is envisaged from an upper level s_u (Fig. 1.2.1-1b) and an asymptotic approach to a lower level s_r: a limit under which there is a no-damage area of r-loading. The s_l level is somewhere in the middle between s_u and s_r.

In the present IDD version, Eq. 1.2.1-1 is accepted for the straight part of the S-N line. Downwards, the S-N line will be treated in two modes: the classic 'breaking' mode at s_l to a horizontal line, and a 'smoothing' (more accurate) mode with bending smoothly to $s_r < s_l$. A conditional number of cycles N_r will correspond to s_r after extrapolating the straight S-N line to s_r (Fig. 1.2.1-1b).

1.2.2. Influence of a static (mean) stress

Tests are done and an S-N line is built mostly for symmetrical (reversed) cycle, i.e. the S-N line is valid for $s_m = 0$ and $R = -1$. Then, $s_{\max} = s_a$, $s_l \equiv s_{\max,l} \equiv s_{a,l}$ where $s_{\max,l}$ is the fatigue limit in terms of $s_{\max}$, and $s_{a,l}$ is the fatigue limit in terms of s_a. As well, although less, tests are done and S-N lines are built as valid for $s_m \neq 0$. The experimental points are plotted in coordinates $\log s_{\max}$-$\log N$ or $\log s_a$-$\log N$. When the coordinates $\log s_{\max}$-$\log N$ are replaced by the coordinates $\log s_a$-$\log N$ or vice versa, the experimental points will be re-plotted (in Fig. 1.2.1-1b, the points have the same plotting only conditionally). Correspondingly, the parameters m and A in Eq. 1.2.1-1 will change since $s_{\max}^m N = (s_m + s_a)^m N = A$ will not entail $s_a^m N = A$ under the same m and A.

The experimental investigation of the influence of $s_m \neq 0$ on the fatigue limit and on the whole S-N line requires building a family of $s_{\max}$-N lines or s_a-N lines valid for different values of $s_m \neq 0$. If the different fatigue limits $s_l \equiv s_{\max,l}$ are plotted as ordinates versus the corresponding different s_m abscissae, then a failure locus is formed known as Smith diagram (Fig. 1.2.2-1). And if the corresponding fatigue limits in terms of amplitudes $s_l \equiv s_{a,l}$ are plotted as ordinates versus the same s_m abscissae, then a failure locus is formed known as Haigh diagram (Fig. 1.2.2-2). Additional, more universal and simple names are s_m-$s_{\max}$ diagram (more precisely written with the $_l$ index: $s_{m,l}$-$s_{\max,l}$) and s_m-s_a diagram (more precisely: $s_{m,l}$-$s_{a,l}$). Figs. 1.2.2-1 and 1.2.2-2 present concrete example diagrams (a steel with yield strength $s_Y = 320$ MPa is meant).

If all the limiting stresses in Figs. 1.2.2-1 and 1.2.2-2 are valid for one and the same N_l (for example 2.10^6), then the two figures represent diagrams s_m-$s_{\max}$ and s_m-s_a of equal N_l life. Then, the diagrams can also be considered as representing restricted (related-to-life) fatigue limits. For the purposes of IDD and in general, diagrams s_m-$s_{\max}$ and s_m-s_a for any limited equal N life can be discussed. In Fig. 1.2.2-1, two more *lines of equal lives* ($N = 10^5$ and $N = 10^4$) are illustrated (by dashed lines) in the s_m-$s_{\max}$ coordinates.

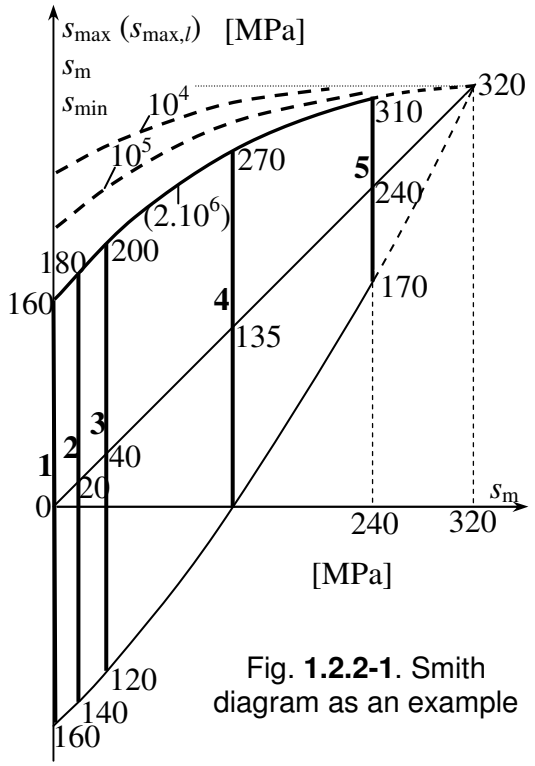

Fig. **1.2.2-1**. Smith diagram as an example

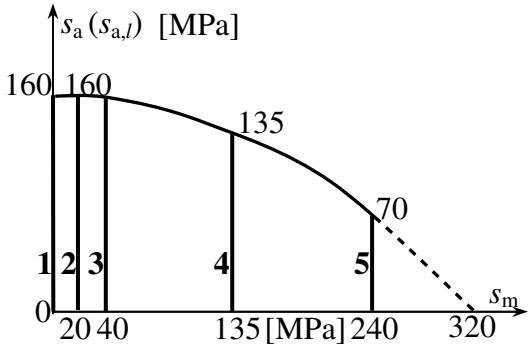

Fig. **1.2.2-2**. The corresponding Haigh diagram

According to the s_m-s_{max} diagram, an increase in the static s_m stress increases the fatigue strength in terms of s_{max}. The reversed cycle with $s_m = 0$ is the most dangerous to the fatigue strength in terms of s_{max}. The s_{max}-N lines are situated in their family next above previous with increasing s_m. Thus, at the same s_{max} and different s_m values, the life will increase with increasing s_m.

This interpretation is carried into the vein of IDD as follows. Let dD be the damage differential per the loading differential ds during dt (Fig. 1.2.1-1a). Suppose $dD = R ds$ where $R = dD/ds$ is the intensity (the derivative) of the damage $D = D(s)$. It is obvious that $R = R(s)$ is an increasing function. It has some values for reversed cycle ($s_m = 0$). Yet let a static stress $s_m \neq 0$ be set. Then, the values of $R = R(s)$ will be less. That is, s_m comes as a second argument on which the R function depends: $R = R(s, s_m)$. With increasing s_m from zero, $R(s, s_m)$ decreases.

Different descriptions of the relation $s_{a,l}(s_m)$ are used. Gerber was the first to propose a parabola. Later, in many cases the Gerber parabola was considered to be a too convex curve. Goodman replaced the parabola with a straight line. However, this straight line eliminates any convexity while the experimental data testify for such. That is why additional proposals were advanced that are 'in between' the Gerber parabola and Goodman line.

Interestingly, no proposal was found for a limiting curve passing right in the middle in between the parabola and the straight line. Therefore, also in addition to previous papers, such a proposal is done. The equation (Eq. 1.2.2-1) of that limiting curve can be seen in the thesis. Eq. 1.2.2-1 or any other equation with the same purpose serves to present not only the limiting line but also every line of equal N life in the s_m-s_a coordinates. Then, based on such an equation, the S-N line for any $s_m \neq 0$ can be hypothetically obtained from the basic S-N line for $s_m = 0$ (R = –l) (what is done further in the thesis) or vice versa.

The existing fatigue life assessment methods based on counting cycles with amplitudes $s_{a,i}$ and mean stresses $s_{m,i}$ also need some selected analytical description of the s_m-s_a diagram. It is applied to every $_i$ and thus the mean stress effect, i.e. the effect from every $s_{m,i} \neq 0$, is accounted while using the basic S-N line for $s_m = 0$ (R = –l). Depending on what

analytical relation $s_a(s_m)$ is selected, the mean stress effect and the life are evaluated differently.

1.2.3. About the *S-N* line under multiaxial state of stress

It stands to mind that the approach of using an equivalent stress under static stresses could also be used under time-varying stresses. In other words, it is possible to write $\sigma_{equ}(t) = \sigma_{equ}[\sigma_x(t),\ \sigma_y(t),\ \tau_{xy}(t)]$. However, such an approach comes in for serious criticism under arbitrary non-proportional $\sigma_x(t)$, $\sigma_y(t)$ and $\tau_{xy}(t)$. This will be shown in Subchapter 1.4.

Yet, let $\sigma_x(t)$, $\sigma_y(t)$ and $\tau_{xy}(t)$ be proportional and cyclic. Then, an equation of the kind $\sigma_{equ}(t) = \sigma_{equ}[\sigma_x(t),\ \sigma_y(t),\ \tau_{xy}(t)]$ decomposes into two proportional equations of the same kind separately for the mean (static) stresses and the amplitudes. The equation of $\sigma_{equ,a}$ can be replaced by the proportional equation $\sigma_{equ,max} = \sigma_{equ,max}[\sigma_{x,max}(t),\ \sigma_{y,max}(t),\ \tau_{xy,max}(t)]$.

The notion of *lines of equal lives* is a basic one in the thesis for *reproducing S-N lines* under any state of stress (multiaxial and uniaxial). Such a term was not introduced and established as basic before. Lines if equal lives in the σ'-σ'' coordinate plane according to the Von Mises criterion are proportional (centrally similar) ellipses.

In this Section 1.2.3 in the thesis, other more equivalence criteria (not only of Von Mises) are involved. The most treated criterion relates to the Gough and Pollard ellipse. It is shown that this ellipse corrects the Von Mises ellipse by substituting the actual σ_l/τ_l ratio for the hypothetical ratio $\sqrt{3} = \sigma_l/\tau_l$. The Gough and Pollard ellipse is usually associated with a safety factor n. But in the IDD vein, such an ellipse is more interesting as suggesting elliptic lines of equal lives in general. How to obtain then the *S-N* line at any k from such elliptic lines will be thoroughly considered in Section 2.4.7.

1.2.4. Composing an *S-N* line

Engineering books and manuals give a lot of data, graphs, factors and ratios reflecting the influences of not only s_m and k on a real object's *S-N* line but also of: the geometrical shape of the body and available stress concentrator; dimensions of the object; condition of the body surface; treatment of the body surface for strengthening; heat treatment; welding; corrosion; temperature; loading frequency; distribution of the stresses inwards along the z axis; and so on.

One of the most important factors is the stress-concentration. The possibilities for determination of local stresses have much increased nowadays. More and more developed software is used for stress analysis based on finite-elements (FE) method. Researchers go more and more 'inward into local stresses' where stressing is multiaxial as a rule. Correspondingly, this would result in more interest in IDD. The technology for manufacturing of smaller and smaller strain-gauge rosettes, and for more precise strain-gauge measurement, has also become higher. Thus, researchers can also experimentally go more and more 'inward into the local stresses' by means of strain-gauge measurement. When the oscillograms $\sigma_x(t)$, $\sigma_y(t)$ and $\tau_{xy}(t)$ are of concentrated stresses, different than the remote stresses, then the fatigue life assessment is expected to be more accurate.

After all, the problem of fatigue life assessment especially under cyclic r-loading is considered as conceptually solved: composing the corresponding *S-N* line based on a lot of experimental and theoretical experience accumulated in the engineering. IDD has nothing to add to that experience but will use it. *S-N* lines at different k values will be applied (in a way shown in Subchapter 2.4). It is obvious that the truthfulness of the used *S-N* lines will depend on the competence of the researcher who composes them. Thus, even from here it becomes

apparent that the IDD fatigue life assessment accuracy will depend also on the IDD user's competence.

1.3. Fatigue life under non-cyclic uniaxial or multiaxial proportional loading

1.3.1. Cycle counting (schematization). Miner rule. Amplitude spectrum

As understood from Preview, following the conservative notion of loading cycle, numerous methods appeared for replacing a non-cyclic oscillogram $s(t)$ by a step-sequence of cycles with different $s_{a,i}$ amplitudes at the same mean (static) stress s_m. This sequence is called spectrum of the $s_{a,i}$ amplitudes (Fig. 1.3.1-2a in the thesis). Next, the Miner rule is applied.

The assumption for this rule is: the same damage $D_T = \text{constant} = 1/N$ is brought in per any repetition of the same cycle with the same s_a amplitude until the fatigue failure occurs in N repetitions. This represents a hypothesis for constant damage intensity among the repeated cycles, i.e. *hypothesis for linear summation of the fatigue damage* (shortly called just *linear hypothesis*). It means that on the amplitude spectrum's i-step the damage per cycle $D_{T,i} = \text{constant} = 1/N_i$ remains the same as in the case of keeping constant $s_{a,i}$ amplitude to failure. N_i is the abscissa of the S-N line versus the $s_{a,i}$ ordinate.

In case the loading is random, the step-sequence actually represents a histogram of statistical distribution of the amplitudes. When the number of the $s_{a,i}$ steps is great enough, the histogram turns into a practically smooth graph of the amplitude spectrum as a function (law) of distribution of the amplitudes. And if versus every $s_{a,i}$ amplitude the statistical frequency n_i of its appearance is plotted, then the density of distribution of the amplitudes will be formed. It is a derivative of the function of distribution.

Hence, a large field was opened for numerous statistical studies of random uniaxial or proportional loading. Various distributions laws known from the mathematical statistics found application. The probabilistic representation of the loading in relation to the probabilistic representation of the S-N line, involving also the mathematical theory of random processes, compiles the comprehensive probabilistic approach to fatigue life assessment.

1.3.2. Cycle counting methods. Rain-flow method

After Miner, the schematization (distinguishing cycles and grouping them in a spectrum) was definitely and absolutely accepted as an inevitable preliminary procedure for fatigue life evaluation. Every researcher was convinced that cycles must be introduced in a non-cyclic oscillogram for using an S-N line that is namely valid for cycles. Large-scale investigations started for enabling the schematization (in different manners). Many electronic cycle counting devices were invented for automation of the schematization.

Retrospectively known methods for distinguishing and counting cycles are of: *peaks*, *ranges*, *crossings*, and many other or their modifications. The variety of methods indicates that it is difficult to achieve equivalency of the original and schematized loading, and some error is always admitted. Researchers demonstrate in many publications how a certain standard cycle counting method is not relevant under a specific type of random process, and some modification is proposed.

When the cycles are not put at one and the same s_m level but at different $s_{m,i}$ mean stresses, this procedure is called *two-parameter schematization*. Then, a correlation table is used or two-dimensional distribution of both amplitudes and static (mean) stresses is built.

With the two-parameter schematization, not only one *S-N* line but a family of different *S-N* lines should be used for the different $s_{m,i}$ mean (static) stresses. This requires application of the knowledge from Section 1.2.2 after accepting certain formulation of the s_m-s_a diagram i.e. of the $s_a(s_m)$ function. Such an approach seems to be more truthful. However, it immediately leads to a lot of different methods and to publications of many comparative studies depending on the choice of the $s_a(s_m)$ function. In this Section 1.3.2 in the thesis, other more problems are analyzed. They increase the number of the methods proposed leading to differing fatigue life assessment results.

The very transformation of $s_{a,i}$ in dependence on $s_{m,i}$ requires calculations that are only possible by means of a computer. Respectively, different computer programs proposed nowadays can be used for different ways of $s_{a,i}(s_{m,i})$ transformation. Besides, the loading statistical analysis in reference to both $s_{a,i}$ and $s_{m,i}$ is much more complicated and more varying in solutions than the one-parameter schematization (where no $s_{m,i}$ means stresses are introduced).

That is why, in the previous decades there was a more popular approach of putting all the cycles with their non-transformed amplitudes at one and the same s_m level of the whole oscillogram. This approach has a solid ground: the material is certainly 'getting accustomed' to s_m of the whole oscillogram and can hardly 'react immediately' to the prescribed sudden transformation of $s_{a,i}$ at each shift of $s_{m,i}$ from one range to the next one.

Before the era of computerization and analogue-to-digital converters for digitizing analogue signals, the method of crossings was the most convenient to be electronically enabled by means of the cycle counting electronic devices mentioned above. But later, thanks to the computers, the figuratively called *Rain-Flow* cycle counting method started dominating. It was accepted as a state (government) standard in the US, Russia and many other countries including Bulgaria. It is discussed in hundreds of publications.

With the rain-flow method, the notion of cycles in a non-cyclic oscillogram is visualized and realized as indisputable on the basis of the strain-stress hysteresis loops (Fig. 1.3.2-1). In this Section 1.3.2 in the thesis, many clarifications on Fig. 1.3.2-1 are done accompanied by essential remarks.

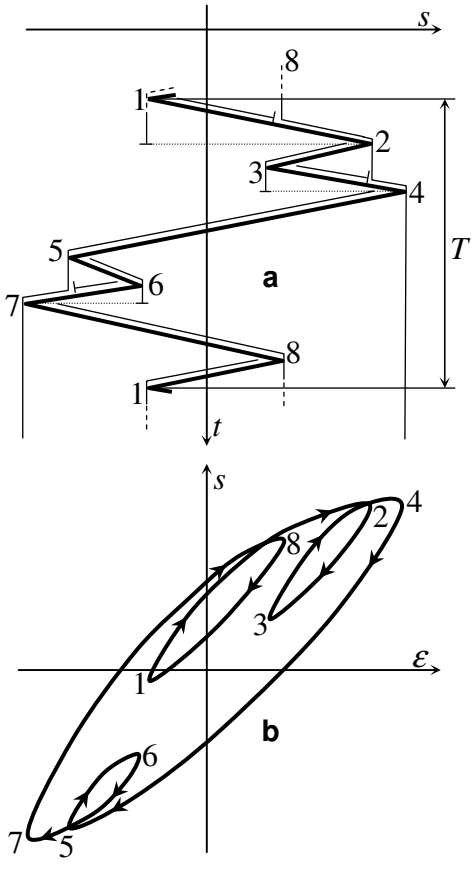

Fig. **1.3.2-1**
Illustration to the Rain-Flow procedure

1.3.3. Is it possible not to divide the loading into cycles and count them?

After Miner, no one has ever raised the question of whether another way of fatigue life computation is possible instead of CCA (instead of the cycle counting approach, i.e. instead of preliminary dividing the loading into cycles and counting them). As already mentioned in Preview, the referees of *Int. J. Fatigue* did not admit such a question to be discussed and published in the 90s of the previous century. A trial was also done for publication in *Int. J. Fatigue & Fracture* and it was not successful, either (see this Section 1.3.3 in the thesis for more details, including curious ones).

But, as already mentioned in Preview, the Bulgarian reviewers of *J. Theoretical and Applied Mechanics* acknowledged the possibility for fatigue life computation without CCA and admitted the author's paper on the subject to publication. An additional paper treating the same subject was also published in Bulgaria. Next, there was a publication on an international level (see this Section 1.3.3 in the thesis for more details).

The question of whether it is possible not to divide the loading into cycles and count them has its simple answer from the IDD point of view: the accumulated damage $D_{\Sigma,T}$ can be represented as $\Sigma\Delta D$, respectively as an integral of $\mathrm{d}D$ differentials, instead of using the Miner rule in the form $\sum(n_i/N_i)$. And thus, the $\mathrm{d}D$ differentials can be integrated directly now, without any preliminary loading schematization (decomposition) into cycles grouped into any amplitude spectrum.

1.3.4. "History", "future", continuity, static level

When cycles are sought instead of dealing with the instantaneous (running, current) ordinates of the $s(t)$ oscillogram, any possibility is excluded to determine the current (instantaneous) value of the damage $D_\Sigma(t)$ accumulated till the current t time. Damage per a part of a range cannot be determined, either. The material 'does not know' the future of the loading after t: the appearance of the next peak, its level, and so on. Not the material but the seekers of cycles are who want to know future peak(s) because they want to complete next cycle(s) after the last known peak. There is a logical paradox here: some damage has already been done but for its CCA evaluation researchers need to preliminarily know the next development of the loading.

IDD is the method able to avoid such a 'paradox of dipping into the future' of the loading. As a mathematical approach, IDD allows determination of $D_\Sigma(t)$ only based on the loading history till the t time, since damage differentials $\mathrm{d}D$ per time differentials $\mathrm{d}t$ are determined and can be integrated from 0 to t.

The introduced damage intensity $R = R(s) = \mathrm{d}D(s)/\mathrm{d}s$ throws new light on the CCA problem mentioned in Section 1.3.2: whether the amplitudes should be arranged at one and the same s_m or at different $s_{\mathrm{m,i}}$ levels. In other words: whether one-parameter or two-parameter schematization should be done. From the IDD point of view, if suddenly changing the damage per a range (a half-cycle) to another value per the next range due to a sudden change in $s_{\mathrm{m,i}}$, then the damage intensity $R(s)$ will discontinue. Indeed, during the infinitely small increase $\mathrm{d}s$ of s at the transition from the previous range to the next one, the intensity $R(s)$ will go through a finite increase i.e. discontinuity. However, $R(s)$ implies some physical damage intensity which should be mathematically continuous.

1.3.5. Linear and non-linear damage accumulation

An essential remark to CCA is that to count cycles and group them in an amplitude spectrum excludes application of any hypothesis of non-linear damage accumulation. Indeed, the real sequence of the cycles in the schematized oscillogram, i.e. the loading history, is lost. In other words, the numerous statistical investigations of non-cyclic loading make sense only based on the linear hypothesis that is otherwise known from far back as conditional and not very accurate. After all, it proves that to take into account the non-linearity of cumulative damage is practically incompatible with CCA. Hence, none of the proposed non-linear hypothesis was established in the engineering.

Anyway, the existing methods are able, though, to fairly predict fatigue life based on the linear hypothesis. It is clear that they succeed thanks to some successful averaging the real non-linear damage accumulation to a linear one. As a matter of fact, the studies in this aspect are sooner aimed at finding out the conditions for validity of the linear hypothesis and its possible modifications. But they do not transform the linear hypothesis into non-linear one. True non-linear damage summation, especially for the general case of loading, is

mathematically only possible by means of IDD. Indeed, by summing damage differentials directly till a current t time, just the real sequence of actual fluctuations of stress is followed, i.e. the loading history is strictly kept. The non-linearity of accumulation of the damage computed will be achieved by setting the very cumulative damage $D_\Sigma(t)$ as a new additional argument of the integrand (Section 2.3.7). This means, the integral result $D_\Sigma(t)$ should immediately go into the integrand. Such mathematical reversibility can enable desired non-linear summation.

1.4. Fatigue life under multiaxial non-proportional loading

1.4.1. Reduction (decomposition) of the loading

As already emphasized, no cycles could be distinguished in the original trajectory (Fig. 1.1-3b) of general non-proportional loading. Respectively, any knowledge of fatigue damage under loading cycles cannot be used directly. It could be applied but separately for any of the oscillograms $\sigma_x(t)$, $\sigma_y(t)$ and $\tau_{xy}(t)$ (Fig. 1.1-3a) with the idea to obtain next some 'equivalent' amplitude spectrum, or to reduce somehow the three oscillograms to a single one in which cycles could be counted by the rain-flow procedure, etc. Thus, a lot of researchers looked for some criteria for reduction of multiaxial loading to something that is one-component, simplified, containing some reduced parameters, etc.

However, if thinking with the IDD notions, the following objection of principle will immediately arise: the separate treatment of the oscillograms $\sigma_x(t)$, $\sigma_y(t)$ and $\tau_{xy}(t)$ (Fig. 1.1-3a) instead of their mutuality (Fig. 1.1-3b) will not be logical. Indeed, the damage differential $\mathrm{d}D$ per the loading $\mathrm{d}s$ differential (Fig. 1.1-3b) will obviously and primarily depend on the coordinates of the M point. This is dependence on the simultaneously and mutually appearing σ_x, σ_y and τ_{xy} at every t time. In other words, the original trajectory of the mutual variation of the three oscillograms (Fig. 1.1-3b) as original composition of the loading must remain into consideration.

This logic seems to be not always advanced: some authors separately do cycle counting on the oscillograms, build separate amplitude spectra, and so on. However, such an approach takes the risk to lose the influence of the mutuality: with the same computed life, the same procedure can be reversely so done as to lead to a quite different trajectory with a quite different actual life. In other words, the reversed one-to-one correspondence will be lost if trying to reduce (decompose) the multiaxiality.

In other words, the approach of reduction of loading multiaxiality has the weakness that *the original oscillograms are mathematically not retrievable in one-to-one correspondence. Under the same 'reduced thing', infinitely many possibilities are left for varying the loading between two extreme cases: a maximized and a minimized one. Each criterion of reduction should be verified in both extreme cases, or in any refuting case, under the same 'reduced thing'*. Nevertheless, too many criteria are proposed without such verification and their authors do not consider at all any necessity of it.

In this Section 1.4.1 in the thesis, other more serious remarks are entailed.

1.4.2. Reduction to an equivalent stress

Obviously, the first researchers of a varying multiaxial state of stress were under the influence of the classic strength theories for reducing a static multiaxial state of stress to an equivalent static stress σ_{equ}. In an inductive way of thinking, such reducing was transmitted to variable stresses. However, the reduction that transforms functions instead of constants will

entail an immense increase of mathematical poly-variety. Even this fact only is already disturbing because a way will be opened for a great number of methods.

If a 'reduced', 'equivalent' stress-time function $\sigma_{\text{red}}(t) \equiv \sigma_{\text{equ}}(t) = \sigma_{\text{equ}}[\sigma_x(t), \sigma_y(t), \tau_{xy}(t)]$ is composed, the first objection will be: $\sigma_{\text{equ}}(t)$ may be set to be a constant, great enough, without any fluctuations, nor any amplitudes:

$$\sigma_{\text{equ}}[\sigma_x(t), \sigma_y(t), \tau_{xy}(t)] = \text{constant}. \qquad (1.4.2\text{-}1)$$

Then, keeping this constant, various $\sigma_x(t)$, $\sigma_y(t)$ and $\tau_{xy}(t)$ can be composed. It is mathematically easy: in Eq. 1.4.2-1, two arbitrary stress-time functions, for example $\sigma_y(t)$ and $\tau_{xy}(t)$, can be set, and the equation is solved for $\tau_{xy}(t)$. Such $\sigma_x(t)$, $\sigma_y(t)$ and $\tau_{xy}(t)$ can cause fatigue failure although σ_{equ} is a constant.

In this Section 1.4.2 in the thesis, there are other more remarks. According to them, no classic static equivalent stress can directly take the role of varying criterional stress for fatigue life assessment in case the loading is non-proportional. Such a role can only be played under proportional loading. This is easy to understand considering also the fact that, under non-proportional loading, the principal axes rotate and no immovable material plane remains always criterional.

1.4.3. The concept of a critical plane and corresponding methods

What was said in the previous section makes clear that if a critical criterional plane is to be defined, then all the immovable planes at a location of a point of the material should be examined. On every plane of any orientation, a normal stress and a shear stress act. They are denoted as σ_n and τ_n where n is the normal line of the plane. Following some criterion proposed, researchers should evaluate which plane is extremely stressed. It will be a critical plane on which the material is likely to break into a crack.

An idea was established that the cracking process is led by the shear stress on the critical plane. The normal stress there has only a secondary, although necessary at the beginning, role for opening the crack but later the shear stress is what causes the crack growth. Determination of the critical plane as a plane where Maximum Shear Stress or Strain Range is located is known as MSSR concept established first. Next researchers paid more attention to the normal stress σ_n beside the shear stress τ_n. It was also expected that the total stress $\boldsymbol{p}_n = \boldsymbol{\sigma}_n + \boldsymbol{\tau}_n$ (as a vector sum) is decisive. There are also two rupture modes investigated based on the normal and shear stress.

For searching over the planes, Euler angles are used as angles of rotation of the x-y-z coordinate system about its origin which is a common point of the differently orientated planes. The determination of τ_n and σ_n depending on those angles is not an easy problem. Matrix and tensor manipulations are done and heavy mathematical expressions are obtained. In this Section 1.4.3 in the thesis, continuation of the respective analysis can be seen. But it is impossible to represent thoroughly the criteria and methods reviewed. Such representation would take too large volume and would have been worthy if the proposed IDD method had been on such a basis.

In order to partly give an idea of the existing critical plane criteria, three of them are shown in Table 1.4.3-1 in the thesis: of Findley, Dang Van and Spagnoli. Accompanying clarifications are presented. The criteria are subject, however, to serious remarks formulated in the thesis.

1.4.4. Integral methods over the planes

The critical plane approach has its opponents. It cannot distinguish if a plane is solitary in being the most stressed or whether there are (a multitude of) other planes, as well, which are equally stressed to the same extent. On this occasion, the author made the fourth publication in *J. Fatigue* that was not in favor of the concept of one critical plane (discussed in Sections 2.6.5 and 2.6.6). Besides one critical plane, the stressing of the rest planes will also influence the fatigue life. Thus, researchers developed the idea that the damage should be formed by means of an integral over all the planes, i.e. by means of averaging through damages from all the planes.

In order to give, partly again, an idea of the integrals proposed, two of them are shown in Table 1.4.4-1 in the thesis: of Liu & Zenner and of Papadopoulos. Double and triple integration is done over the Euler angles. To show this in details requires writing a separate large scientific work.

The remarks in the previous Section 1.4.3 in the thesis are also valid in this Section 1.4.3, now to the integral methods. Besides, a basic question is to be addressed to the integral methods as follows. After they start from $\sigma_x(t)$, $\sigma_y(t)$ and $\tau_{xy}(t)$ and reach at the end some (double and triple) integral, and go through $\tau_n(t)$ and $\sigma_n(t)$ by different combinations of the Euler angles, without any one-to-one correspondence with $\sigma_x(t)$, $\sigma_y(t)$ and $\tau_{xy}(t)$ (thus the mutual variation of the oscillograms is lost), and scatter into different versions of the different controversial concepts of what to take into account, how to integrate, how to form amplitudes, how to involve static stresses, how to generalize also for random loading and possibly use the Miner rule, and so on and so on, then: is it not much simpler, canalizing and more productive as an idea to formulate an integral for universal direct integration over the mutual variation of the initial oscillograms $\sigma_x(t)$, $\sigma_y(t)$ and $\tau_{xy}(t)$ in which the stressing of all the planes is encoded, and therefore there is no need of searching over them?

The IDD method proposed develops namely such an idea. But it is not an integral method in the meaning of integration over the planes. Instead, the $\mathrm{d}D$ differentials of the fatigue damage are integrated. The 'IDD' name was subsequently introduced to avoid misunderstanding, as well: the old name 'Integral Method' often evoked wrong expectations that it must be an integral method over the planes.

1.4.5. Non-proportional $\sigma(t) \equiv \sigma_x(t)$ and $\tau(t) \equiv \tau_{xy}(t)$

Fatigue tests under sinusoidal out-of-phase bending and torsion with equal frequency are much popular. They are comparatively easy for implementation and are convenient for verification of criteria. The beginning of such tests dates back to the 40s of the previous century and is associated with Nishihara & Kawamoto. They found out that for many materials the fatigue life increases with increasing the out-of-phase angle from 0^0 to 90^0. However, in many other cases just the opposite effect appears: the out-of-phase angle decreases the life.

Fatigue tests under sinusoidal bending and torsion (out-of-phase or in-phase) with different frequencies are also popular. Besides, experimental studies under random non-proportional $\sigma(t)$ and $\tau(t)$ are carried out. In some investigations, peculiar oscillograms are also produced in order to obtain special trajectories in the σ-τ plane. Cyclic sinusoidal out-of-phase or/and of-different-frequency $\sigma(t)$ and $\tau(t)$, as well as non-proportional peculiar or random $\sigma(t)$ and $\tau(t)$, are produced not only by bending and torsion but also by pull-push and torsion. Further on (in Chapter 5), IDD verifications will be shown under non-proportional cyclic $\sigma(t)$ and $\tau(t)$.

Even in the previous thesis, IDD approbation under non-proportional $\sigma(t)$ and $\tau(t)$ was done. Both data of other researchers and author's own experimental data were used. The own tests were carried out by a unique testing machine created. It produced vibrations of masses of an inertial device as explained and shown (in Figs. 1.4.5-1 and 1.4.5-2) in the

thesis. The specimen transmitted the vibrations and thus it was subjected to torsion and bending: both proportional and non-proportional, and having different interesting fluctuations.

1.4.6. Rotating bending with steady torsion

This subject is a particular case from the previous section but is individually presented here since the author took some special engagement in it.

In rotating machine shafts, $\sigma(t) \equiv \sigma_x(t) = \sigma_a \sin \omega t$ occurs due to the rotating bending together with $\tau_{xy}(t)$ due to torsion. In the simplest (and very popular) case, the torsion is steady (constant, static): $\tau_{xy}(t) = \text{constant} \equiv \tau \equiv \tau_m$. And although this combination of adding a static τ_m to $\sigma_a \sin \omega t$ is so often met in the engineering, it is not paid with priority and special attention in the books and manuals.

To make up for this deficiency at least in Bulgaria, B. Stoychev developed his Ph.D. thesis consulted by the author as his first director (there was also a second doctorand's director). A unique testing machine for rotating bending with steady torsion was created. Its design is based on a two-shaft statically indeterminate scheme adopted from the author. In this Section 1.4.6 in the thesis, a picture of the machine (Fig. 1.4.6-1 there) and additional clarifications can be seen. As well, a series of other more notes are exposed. Bulgaria, besides Portugal, was recognized on ICMFF9 as a European country having experience in fatigue studies under rotating (or rotated) bending with steady (or variable) torsion. A series of results from these studies are presented and used for IDD verifications further on in the thesis (in Chapter 5).

It proves that τ_m added to σ_a may exert weaker negative influence on the fatigue strength than the expectations are, or even null influence, or even positive influence. Then, the question arises of why such an interesting and important effect remains somehow out of the range of vision of the researchers and why it is not traditional for them to verify their criteria in the loading case considered. A possible answer is: this loading combination of $\sigma(t) = \sigma_a \sin \omega t$ and $\tau = \tau_m = \text{constant}$ looks simple but would be tough and a failure for any criterion which needs searching over the planes. Indeed, this becomes apparent according to the analysis made in this Section 1.4.6 in the thesis.

B. Stoychev tried to apply the Papadopoulos criterion. However, a new separate Ph.D. thesis should be written for that purpose. In contrast to this, the universal IDD method was immediately applicable to the concrete loading investigated. Hence, Stoychev put himself in the positive mood for IDD, and collaboration was established. He noticed that the Integral Method is much more rational and simple as a concept: it does not relate to searching over all the planes and facing the many controversial points but relates to direct integration over the loading trajectory (in which all the planes are encoded). The asymmetry of the loading is taken into account only once by means of $\sigma_{m,equ}$ (Section 2.4.2) and such a question of asymmetry does not arise any more at every plane. What solely remains to do is to set good-approbated and adequate IDD parameters.

1.4.7. Non-proportional $\sigma_x(t)$ and $\sigma_y(t)$

The fatigue investigations under non-proportional $\sigma_x(t)$ and $\sigma_y(t)$ are less than under non-proportional $\sigma_x(t)$ and $\tau_{xy}(t)$ since more technical difficulties are faced and the tests are more expensive. But in the recent decades, the technical possibilities were as developed as to stimulate more and more researches to do experiments under non-proportional stresses $\sigma_x(t)$ and $\sigma_y(t)$. A prerequisite for this is the development of the aircraft, spacecraft and marine engineering where the shell structural model is involved. It is typical for a shell to be in a biaxial stress state with components $\sigma_x \equiv \sigma'$ and $\sigma_y \equiv \sigma''$, and with immovable principal axes ' and ''. By comparison, the beam model and rotating principal axes were discussed in the previous two sections.

In this Section 1.4.7 in the thesis, a series of notes can be found. Many criteria were applied under loadings with $\sigma_x(t)$ and $\sigma_y(t)$, but they were not verified also under loadings with $\sigma_x(t)$ and $\tau_{xy}(t)$.

1.5. Conclusions from the Review

Conclusions were already done concomitantly while presenting the literature Review. Some more generalizing conclusions are to be added as follows.

It looks it has become traditional that each author develops his own fatigue life criterion and verifies it by his own experimental data. Then some other author's data are not satisfied by that criterion, and a new one is suggested. Thus too many proposed criteria have been accumulated. Most of them have remained isolated each from other, without any option for comparison and competition.

This conclusion is shared by other authors, as well. Dr. Papuga had even taken the text of the previous paragraph published in *J. Fatigue* and put it as a motto in his Ph.D. thesis.

The existing criteria are nearly as many as the researches of established reputation are. All the criteria stay far from arbitrary $\sigma_x(t)$, $\sigma_y(t)$ and $\tau_{xy}(t)$, i.e. far from the real objects. There was no universal method that could link the separate criteria and provide a bridge to each other and to the general loading case. The great number of the criteria published is a fact which, by itself, obviously does not testify in favor of the approaches of decomposition, reducing, searching over the planes, etc.

Thus, an engineer, even a competent one who primarily deals with fatigue life evaluation, would frustrate under the great number of quite different methods proposed for specific loadings and being often incompatible or contradicting to each other. There is not any universal and generally acknowledged method for the general case of loading under arbitrary oscillograms. But the engineer sharply needs such a universal method namely in terms of the loading. He would prefer some software as a 'black box' enabling the respective method under simple instructions and requiring few universal parameters to be set with easily understandable influence on the result. With that, the engineer will not be obliged to know the 'black box mechanism'. He will not have to turn every fatigue life assessment into writing a scientific work of his or of a professor attracted for collaboration.

Hence, as already understood, as an alternative to the existing methods, IDD with corresponding software is proposed to take the role of the missing universal approach for fatigue life computation. There is a Fig. 1.5-1 in the thesis which figuratively illustrates the difference between the other methods and IDD while looking for the cumulative relative damage D_Σ. The principal IDD advantage is visualized: the direct summation of damage differentials $\mathrm{d}D$ under any $\sigma_x(t)$, $\sigma_y(t)$ and $\tau_{xy}(t)$.

Of course, with the new treatment new questions arise. How to introduce $\mathrm{d}s$ and $\mathrm{d}D$ under general loading? What is the relation between them? How will IDD be practically enabled? Based on what input data? And so on.

1.6. The goal and tasks of this thesis

The goal of the thesis was: *to develop theoretically and practically and advance the new* IDD *concept as a new research line for fatigue life assessment that is integration of fatigue damage differentials* $\mathrm{d}D$ *per loading* (*stressing*) *differentials* $\mathrm{d}s$ *to a critical accumulated damage by an integral computed universally under any sort of loading* (*under any integration conditions*) *and directly* (*without any preliminary, considered equivalent, transformation of the original loading done by forming and counting cycles, decomposition, reduction, etc.*)

For achieving this goal, the following tasks are fulfilled which represent a concrete IDD method (the author's IDD version).

1. *Formulating the differential ds of the loading (the plane stressing) under any oscillograms of its components $\sigma_x(t)$, $\sigma_y(t)$ and $\tau_{xy}(t)$.*
2. *Formulating the differential dD of the relative fatigue damage by involving input S-N lines as traditional empirical fatigue life characteristics.*
3. *Building the mathematical theory of the integration of the dD differentials.*
4. *Creating the basis of IDD application in statistical (probabilistic) interpretation under random loading.*
5. *Developing a reduced version of the method under a single oscillogram s(t): under uniaxial or multiaxial proportional loading.*
6. *Creating software to make the method work by means of a computer.*
7. *Approbation (verifications, tests) of the method with published experimental data of other authors. Creating an initial data bank of the empirical factors f_c and f_τ of loading non-proportionality, as well as for prescriptions for setting the N_c and N_τ parameters.*

CHAPTER 2. IDD THEORY

2.1. Loading (stressing) differential

2.1.1. Stress differentials $\mathrm{d}\sigma_x$, $\mathrm{d}\sigma_y$ and $\mathrm{d}\tau_{xy}$

Fig. 2.1.1-1c shows (the projection of) an infinitesimal cubic volume (cuboid, orthogon, parallelepiped) on which the stresses $\sigma_x(t)$, $\sigma_y(t)$ and $\tau_{xy}(t) = \tau_{yx}(t)$ act. They compose, at the current t time, the state of stress denoted as (s). The increment $\mathrm{d}t$ from t can be introduced as the usual mathematical style is and as it is accepted in other sections of the thesis. But $\mathrm{d}t$ can also be introduced from the preceding (previous, old) time $t_\mathrm{p} = t - \mathrm{d}t$ to the current t time. This was preferred in the general case of (non-proportional) loading as more convenient for algorithmization. The preceding state of stress at the preceding time $t_\mathrm{p} = t - \mathrm{d}t$ is shown in Fig. 2.1.1-1a and is denoted as (s_p). Respectively, the stressing (loading) differential $(\mathrm{d}s)$ appears in Fig. 2.1.1-1b.

The physical meaning of $(\mathrm{d}s)$ is the state of stress that is the infinitesimal change of the

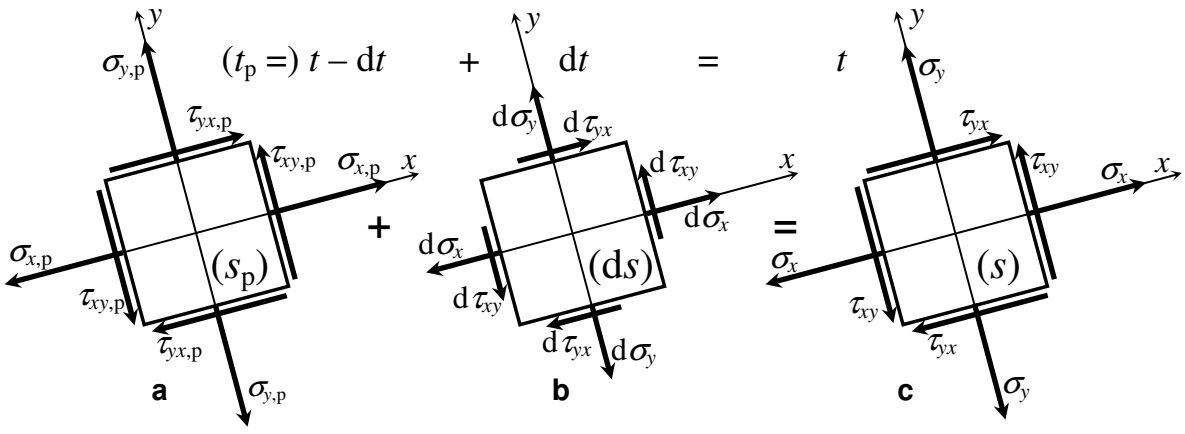

Fig. **2.1.1-1**. (a) The variant (s_p) state of stress at the previous time $t_\mathrm{p} = t - \mathrm{d}t$;
(b) the variant loading (stressing) $(\mathrm{d}s)$ differential during $\mathrm{d}t$;
(c) the variant (s) state of stress at the current t time

(s_p) state of stress during dt. After adding (ds) to (s_p), the current (s) state of stress is obtained (Fig. 2.1.1-1c). The following notation will also be used: $(s_p) \equiv (\sigma_{x,p}, \sigma_{y,p}, \tau_{xy,p})$, $(ds) \equiv (d\sigma_x, d\sigma_y, d\tau_{xy})$ and $(s) \equiv (\sigma_x, \sigma_y, \tau_{xy})$. Thus, the equation $(ds) = (s) - (s_p)$ can be written that means $d\sigma_x = \sigma_x - \sigma_{x,p}$, $d\sigma_y = \sigma_y - \sigma_{y,p}$ and $d\tau_{xy} = \tau_{xy} - \tau_{xy,p}$.

On the other hand, the components $d\sigma_x$, $d\sigma_y$ and $d\tau_{xy}$ form the infinitesimal ds element of the trajectory (Fig. 1.1-3b). Correspondingly, the ds label (not in parentheses) will represent a geometrical form of the loading (ds) differential.

The problem arises as already mentioned in Preview: all the stresses in Fig. 2.1.1-1, as well as ds and the whole trajectory in Fig. 1.1-3b, depend (are variant) on the orientation of the axes x and y. Indeed, if changing the x-y orientation by an α angle, then σ_x, σ_y and τ_{xy} will change according to well-known equations from the textbooks:

$$\sigma_x \to \sigma_\alpha = \frac{\sigma_x + \sigma_y}{2} + \frac{\sigma_x - \sigma_y}{2}\cos 2\alpha + \tau_{xy}\sin 2\alpha\,, \tag{2.1.1-1}$$

$$\sigma_y \to \sigma_{\alpha+\pi/2} = \sigma_x + \sigma_y - \sigma_\alpha\,, \tag{2.1.1-2}$$

$$\tau_{xy} \to \tau_{\alpha,\alpha+\pi/2} = -\frac{\sigma_x - \sigma_y}{2}\sin 2\alpha + \tau_{xy}\cos 2\alpha\,. \tag{2.1.1-3}$$

In these equations, σ_x, σ_y and τ_{xy} are on an original (initial) cuboid with normal lines x and y; σ_α, $\sigma_{\alpha+\pi/2}$ and $\tau_{\alpha,\alpha+\pi/2}$ are on a cuboid with different orientation: turned (around z) at the α angle against the original cuboid; α is measured from x. In Eqs. 2.1.1-1 – 2.1.1-3, all the stresses are functions of t (the t argument in parentheses is considered as present although not written explicitly).

2.1.2. Invariant loading differential $(d\sigma', d\sigma'', d\tau)$

Obviously, the principal cuboid with its principal stresses in the principal directions (principal axes, principal normal lines) should be used in some way. These stresses, cuboid and axes are invariant: they appear the same with any choice of the x-y orientation, i.e. they are independent of α.

In the Bulgarian and other textbooks, the labels of the three principal stresses are σ_1, σ_2 and σ_3 so that $\sigma_1 \geq \sigma_2 \geq \sigma_3$. This rule is inconvenient to IDD since the two principal stresses will change their labels and axes under non-proportional loading. They will be now σ_1 and σ_2, now σ_2 and σ_3, now σ_3 and σ_1, now on the one principal axis, now on the other. Therefore, the labels σ' and σ'' are preferred: the principal stresses *bound constantly* (*without interchange*) with their own principal axes which are correspondingly denoted as ' and " (Fig. 2.1.2-1c further below).

There is a well-known equation for the principal stresses represented in the following form here:

$$\left.\begin{matrix}\sigma' \\ \sigma''\end{matrix}\right\} \text{ or } \left.\begin{matrix}\sigma'' \\ \sigma'\end{matrix}\right\} = \frac{\sigma_x + \sigma_y}{2} \pm \sqrt{\left(\frac{\sigma_x - \sigma_y}{2}\right)^2 + \tau_{xy}^2}\,. \tag{2.1.2-1}$$

In fact, Eq. 2.1.2-1 represents two equations: the plus sign yields $\max\{\sigma', \sigma''\}$ and the minus sign gives $\min\{\sigma', \sigma''\}$. However, it is not known whether $\max\{\sigma', \sigma''\} = \sigma'$ and $\min\{\sigma', \sigma''\} = \sigma''$ or vice versa. That is why, the 'or' option is involved in Eqs. 2.1.2-1. This problem will be thoroughly analyzed later (Sections 2.4.4, 4.1.2 – 4.1.5).

Another well-known equation gives the angle $(\alpha =)\ \alpha_0$ at which the principal cuboid is found out (Fig. 2.1.2-1c):

$$\mathrm{tg}2\alpha_0 = \frac{2\tau_{xy}}{\sigma_x - \sigma_y}. \qquad (2.1.2\text{-}2)$$

According to Eq. 2.1.2-2, α_0 can vary between -45^0 and $+45^0$ and go through an 'arctg jump' by $\pm 90^0$ when the denominator goes through 0. In Fig. 2.1.2-1c, the α_0 angle is shown as α'. This does not mean $\alpha_0 = \alpha'$ always: at another time, the equalities $\alpha_0 = \alpha'' = \alpha' \pm 90^0$ may be valid.

At first sight, it would be a good idea to replace the variant $\sigma_x(t)$, $\sigma_y(t)$ and $\tau_{xy}(t)$ with the invariant $\sigma'(t)$ and $\sigma''(t)$. This would entail replacing the variant 3D trajectory in the σ_x-σ_y-τ_{xy} coordinate space and $\mathrm{d}s$ in it (Fig. 1.1.3b) with the simpler invariant plane trajectory and plane $\mathrm{d}s$. However, then the transformation of the three original oscillograms $\sigma_x(t)$, $\sigma_y(t)$ and $\tau_{xy}(t)$ into only two principal ones $\sigma'(t)$ and $\sigma''(t)$ will not be in reversible one-to-one correspondence (and will be analogous to the approach of reduction criticized in Chapter 1). The rotation of the principal axes and its influence on the fatigue life will be omitted. In this Section 2.1.2 in the thesis, it is proved that the influence in question is not negligible at all.

That is why *the following idea is advanced*. Fig. 2.1.2-1a shows, at the previous time $t_\mathrm{p} = t - \mathrm{d}t$, that cuboid $(s_{\mathrm{p},0})$ which will be principal at the current t time and stays *immovable during* $\mathrm{d}t$ *at the angle* α_0 valid for the t time. Hence, since the cuboid is non-principal, a *shear stress* $\tau_{xy,0}$ acts on it together with normal stresses $\sigma_{x,0}$ and $\sigma_{y,0}$. This $\tau_{xy,0}$ is infinitesimal since the cuboid $(s_{\mathrm{p},0})$ is nearly principal. Fig. 2.1.2-1b shows the appearance of $\mathrm{d}\sigma'$, $\mathrm{d}\sigma''$ and $\mathrm{d}\tau$ during $\mathrm{d}t$ which compose the invariant loading differential $(\mathrm{d}s)$ in physical meaning. By adding $(\mathrm{d}s)$ to $(s_{\mathrm{p},0})$, the invariant (s) state of stress results (Fig. 2.1.2-1c), i.e. the same cuboid becomes already principal at the t time. Respectively, $(\mathrm{d}s) = (s) - (s_{\mathrm{p},0})$ i.e. $\mathrm{d}\sigma' = \sigma' - \sigma_{x,0}$, $\mathrm{d}\sigma'' = \sigma'' - \sigma_{y,0}$ and $\mathrm{d}\tau = -\tau_{xy,0}$.

The next loading differential $(\mathrm{d}s)$ from the time t to the time $t + \mathrm{d}t$ will look similar to Fig. 2.1.2-1b *but valid for another immovable cuboid* with an infinitesimally different orientation: the α_0 angle will be computed again from Eq. 2.1.2-2 but for the time $t + \mathrm{d}t$. The new σ_x, σ_y and τ_{xy} at the time $t + \mathrm{d}t$ will come in the role of current stresses while those from the t time will take the part of previous stresses, and so on.

Thus, consecutive invariant loading differentials are considered in the sense that lots of immovable cuboids at one and the same body's point are observed at consecutive values of α_0 *during consecutive time differentials* $\mathrm{d}t$. In fact, the continuous smooth function $\alpha_0(t)$ (excluding arctg jump by $\pm 90^0$) is replaced with a stepped one.

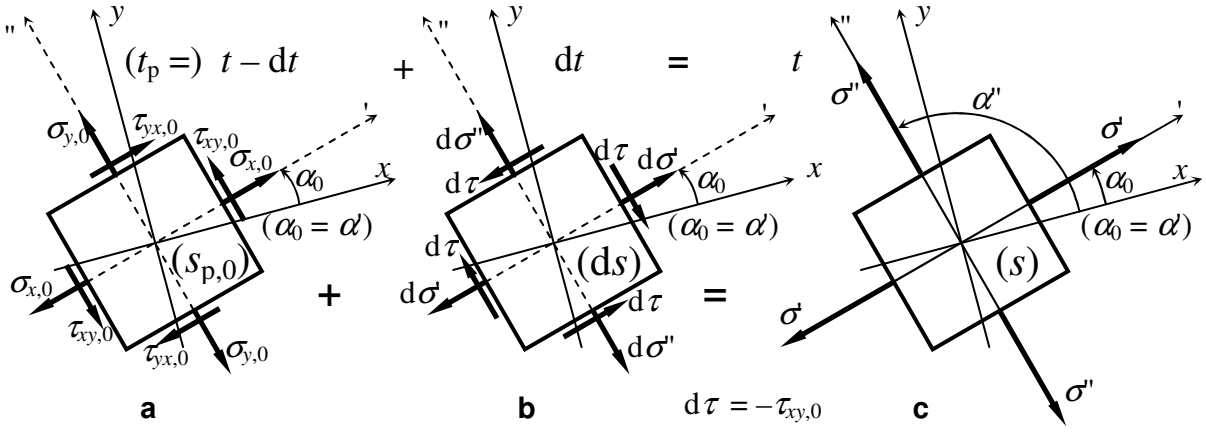

Fig. **2.1.2-1**. (a) The state of stress $(s_{\mathrm{p},0})$ (at the previous time $t_\mathrm{p} = t - \mathrm{d}t$) of the cuboid which will be principal at the current t time and is orientated at the angle $\alpha_0(t)$; (b) the invariant stressing (loading) differential $(\mathrm{d}s)$; (c) the invariant (s) state of stress of the same cuboid already principal at the t time

Thanks to the idea described, a third component $\mathrm{d}\tau = -\tau_{xy,0}$ of $(\mathrm{d}s)$ also appears in Fig. 2.1.2-1b together with $\mathrm{d}\sigma'$ and $\mathrm{d}\sigma''$. This $\mathrm{d}\tau$ is owing to, and namely takes into account, the rotation of the principal axes during $\mathrm{d}t$.

2.1.3. Geometrical form of the invariant loading differential ds

The physical invariant loading differential $(\mathrm{d}s)$ introduced in the previous section is subject to geometrical interpretation represented below. The IDD method can be developed without this interpretation but only using equations relating to physical cuboids and the stresses on them. However, IDD is developed much more convenient and demonstrative by means of the interpretation below.

It is based on the following statements. The stress transformation according to Eqs. 2.1.1-1 – 2.1.1-3, including with $\alpha = \alpha_0$, geometrically means the following: the point $M(\sigma_x,\sigma_y,\tau_{xy})$ of the σ_x-σ_y-τ_{xy} trajectory (Fig. 1.1-3b) goes along a *transforming ellipse* (*ellipse of transformation*) shown in Fig. 2.1.3-1, and reaches the σ_x-σ_y coordinate plane that becomes σ'-σ'' plane. Each such an ellipse is always parallel to the ξ-τ_{xy} plane where ξ is the bisector of the quadrants II and IV of opposite algebraic signs (Fig. 2.1.3-1). The major (big) axis of the ellipse is parallel to the ξ coordinate axis and the minor (small) ellipse's axis is parallel to the τ_{xy} axis. The ratio between the ellipse's axes (or half-axes) is always $\sqrt{2}$. The center of the ellipse (0 point) is on the bisector η of the quadrants I and III of equal algebraic signs.

The proof of these statements can be seen in this Section 2.1.3 in the thesis.

Now, Fig. 2.1.3-1 is to be seen again. The determination of σ' and σ'' by Eqs. 2.1.2-1 at the t time means that the current (new) end of the current variant element ds in the σ_x-σ_y-τ_{xy} space is brought to a contact with the plane σ'-σ'' at the point $M'(\sigma',\sigma'',0)$ (or M'' if interchanging σ' and σ'' what will be additionally discussed in Sections 2.4.4 and 4.1.2 – 4.1.5 as a large subject). And the determination of $\sigma_{x,0}$, $\sigma_{y,0}$ and $\tau_{xy,0}$ by the Eqs. 2.1.1-1 –

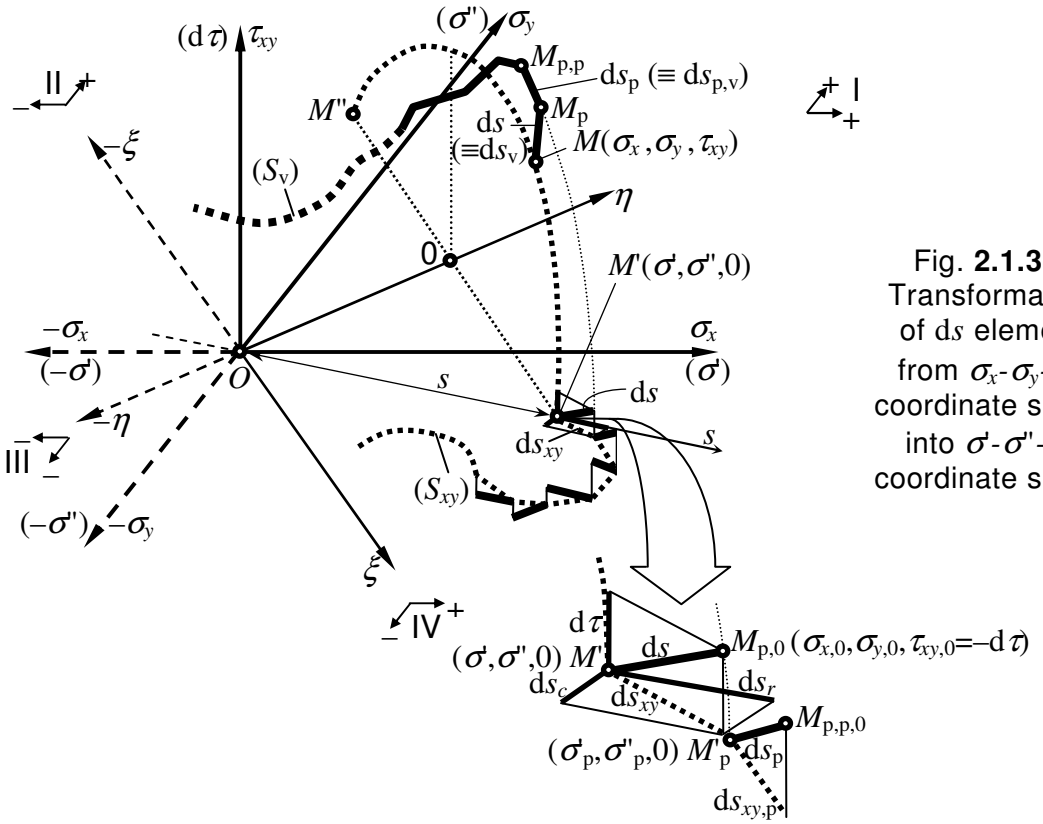

Fig. **2.1.3-1** Transformation of ds element from σ_x-σ_y-τ_{xy} coordinate space into σ'-σ''-dτ coordinate space

2.1.1-3 at the time $t_p = t - dt$ means that the preceding end of the transformed and already invariant element ds is obtained: the point $M_{p,0}(\sigma_{x,0},\sigma_{y,0},d\tau)$. With that, the preceding M_p end goes along its similar transforming ellipse, replaced infinitesimally aside, to the point $M_{p,0}$. It remains at the infinitesimal distance $d\tau$ above (or below) the σ'-σ'' plane. The so-transformed current element ds is already invariant of the choice of the original axes x and y.

At the previous time $t_p = t - dt$, the M_p point went along its ellipse (see the magnified fragment in Fig. 2.1.3-1) to the M'_p point in the role of a current invariant point in the σ'-σ'' plane; the pre-previous variant point $M_{p,p}$ followed M_p to the position $M_{p,p,0}$; and so on back in the time. Thus, the previous invariant ds_p element is disconnected from the current ds element. That the consecutive invariant elements appeared disconnected is for they relate to differently orientated immovable cuboids which are principal for instants only.

The so-built sequence of the invariant ds elements is denoted as (S) and is called invariant 'trajectory' (although it is torn in fragments) or trajectory in the σ'-σ''-$d\tau$ space. The length of (S), i.e. the sum (the integral) of the ds lengths, is S. The fragmentation of the invariant (S) trajectory is not disturbing (besides, it is to remind that the geometrical interpretation is not a must). There is nothing disturbing that the rotating principal cuboid should be 'stopped for a little while' to have the ds element appeared as invariant (together with appearance of $d\tau$) what will later enable the determination of dD independently of the x-y orientation.

The component (projection) of any invariant ds element onto the σ'-σ'' plane is labeled as ds_{xy} (Fig. 2.1.3-1). All the ds_{xy} elements form a trajectory (S_{xy}). Its length S_{xy} is the sum (the integral) of the ds_{xy} lengths. The current ds_{xy} element and the previous $ds_{xy,p}$ element are as connected as the infinitesimal projective vertical $d\tau$ segment through $M_{p,0}$ coincides with the transforming ellipse through $M_{p,0}$. For the previous ds_p element, that ellipse brought $M_{p,0}$ into M'_p with some deviation from the projection of $M_{p,0}$. This deviation is a negligible infinitesimal of second order. That is, $\sigma_{x,0}$ and $\sigma_{y,0}$ converge to the previous σ'_p and σ''_p of the preceding differentials ds_p and $ds_{xy,p}$: $\sigma_{x,0} \to \sigma'_p$, $\sigma_{y,0} \to \sigma''_p$. It turns out that the infinitesimal ds_{xy} differentials are connected with the allowance of the second-order infinitesimal deviations. Respectively, the (S_{xy}) trajectory is a smooth curved line (or a straight one in particular). The same (S_{xy}) trajectory is directly presented by Eq. 2.1.2-1 without accounting the rotation of the principal axes.

The d differentials will be replaced with finite Δ differences (finite Δ elements) and therefore $\sigma_{x,0}$ and $\sigma_{y,0}$ will visibly deviate from σ'_p and σ''_p. Nevertheless, the following (second) possibility for forming $\sigma_{x,0}$ and $\sigma_{y,0}$ is available: equalizing them directly to σ'_p and σ''_p. In other words, this is the possibility to neglect the finite smaller deviation of M'_p from the projection of $M_{p,0}$. The current and the previous Δs_{xy} elements will be connected at M'_p. Then, Eqs. 2.1.1-1 and 2.1.1-2 will not be used for computing $\sigma_{x,0}$ and $\sigma_{y,0}$. The other (already described above) first possibility is: $\sigma_{x,0}$ and $\sigma_{y,0}$ are computed by Eqs. 2.1.1-1 and 2.1.1-2. Then, the current and the previous Δs_{xy} elements appear disconnected due to the above-mentioned deviation (which is always in the ξ direction). With both possibilities considered, $\tau_{xy,0} = -\Delta\tau$ is computed by using Eq. 2.1.1-3.

Together with the trajectories (S) and (S_{xy}), it is also to introduce a 'trajectory' (S_τ) built of the $d\tau$ elements. Its length S_τ is the sum (the integral) of the $d\tau$ lengths. So, if the principal axes rotate, the ds elements disconnect from each other since their $d\tau$ components appear. In case the principal axes are immovable, the $d\tau$ elements disappear and the elements $ds \equiv ds_{xy}$ are connected. Then, they compose a continuous smooth trajectory $(S) \equiv (S_{xy})$ which entirely lies in the σ'-σ'' plane. This means the loading differential is associated with one and the same permanently immovable principal cuboid. Of course, it is also possible that $d\tau = 0$ and $ds \equiv ds_{xy}$ not permanently but only in time intervals of immovability of the principal axes.

As a matter of fact, *a special three-dimensional coordinate space* σ'-σ''-$\mathrm{d}\tau$ *has been introduced in which the third dimension* $\mathrm{d}\tau$ *is infinitesimal*. Nevertheless, with the transition from the original three dimensions σ_x-σ_y-τ_{xy} to the new dimensions σ'-σ''-$\mathrm{d}\tau$, again three, no loading information is lost. This transition provides a reversible one-to-one correspondence: the original variant continuous trajectory can be restored from the invariant fragmented trajectory in a single-valued way. On the other hand, as the third dimension is infinitesimal, the invariant trajectory presentation is practically two-dimensional: the further *analysis is actually two-dimensional*. This is a significant convenience, also for computer visualization: the (S_{xy}) trajectory will only be displayed on the computer screen that represents the σ'-σ'' plane, and, on a separate screen's place, the corresponding $\Delta\tau$ element will be displayed simultaneously with the appearance of every current Δs_{xy} element.

Meanwhile, another index was also introduced in Fig. 2.1.3-1 and will be often used from now on: $_{\mathrm{v}}$ for 'variant'. Examples: the variant $\mathrm{d}s$ element is denoted additionally as $\mathrm{d}s_{\mathrm{v}}$ in order to be differed from the invariant $\mathrm{d}s$ element, the variant trajectory is denoted as (S_{v}), etc. In case the $_{\mathrm{v}}$ index is surely understood, it can be skipped: for instance, in Fig. 2.1.3-1, $M \equiv M_{\mathrm{v}}$, $M_{\mathrm{p}} \equiv M_{\mathrm{p,v}}$, $M_{\mathrm{p,p}} \equiv M_{\mathrm{p,p,v}}$, etc.

In particular, *if the original variant* (S_{v}) *trajectory coincides with a transforming ellipse, then the* $\mathrm{d}\tau$ *elements only exist, i.e.* $\mathrm{d}s \equiv \mathrm{d}\tau$ *and* $(S) \equiv (S_\tau)$. *All the* $\mathrm{d}\tau$ *elements gather onto one point* $M'(\sigma',\sigma'',0)$ (*or* M''). *This is the case of constant principal stresses in rotating principal directions* (it is a kind of maximized case and will be thoroughly treated in Subchapter 2.6).

2.1.4. Components of the loading differential. Basic IDD types of loading. Resolution of the loading differential

Fig. 2.1.3-1 suggests resolution of the loading differential $(\mathrm{d}s)$ into three components in a way which is confirmed as expedient by the whole IDD experience so far. The resolution is 'zoomed in' in Fig. 2.1.3-1: $\mathrm{d}s$ is resolved into a radial component $\mathrm{d}s_r$, a circumferential component $\mathrm{d}s_c$, and $\mathrm{d}\tau$. Actually, apart from $\mathrm{d}\tau$, $\mathrm{d}s_{xy}$ is additionally resolved into $\mathrm{d}s_r$ and $\mathrm{d}s_c$ that are perpendicular to each other. Correspondingly, two other 'trajectories' are introduced: (S_r) of length S_r as a sum (integral) of the $\mathrm{d}s_r$ elements, and (S_c) of length S_c as a sum (integral) of the $\mathrm{d}s_c$ elements. *Trajectory ratios* $t_r = S_r/S$, $t_c = S_c/S$ and $t_\tau = S_\tau/S$ are also introduced. Each of them is ≤ 1.

Hence, the IDD method suggests three basic types of loading.

First type: proportional loading (including uniaxial stressing and pure shear) with a trajectory $(S) \equiv (S_r)$. It is called *r-loading*. Radial elements $\mathrm{d}s_r$ exclusively appear and the ratio $k = \sigma''(t)/\sigma'(t)$ remains constant. The elements $\mathrm{d}s \equiv \mathrm{d}s_r$ lie on a radial line (axis) s through the coordinate origin in the σ'-σ'' plane (Fig. 2.1.3-1). Each element is at a distance s from the coordinate origin. Each proportional loading has its own k radial axis on which the trajectory $(S) \equiv (S_r)$ oscillates. All the elements $\mathrm{d}s \equiv \mathrm{d}s_r$ are connected, all the elements $\mathrm{d}\tau$ are zeros, $t_r = S_r/S$ is exact 1, and the principal axes are permanently immovable. The ratio $t_r = S_r/S$ may also be close to 1: the loading is nearly proportional. In case $t_r = S_r/S$ is exact 1, the proportional loading will also be emphatically called 'pure' r-loading.

Second type: non-proportional loading with immovable principal directions and a trajectory $(S) \equiv (S_c)$ that is on a circumference in the σ'-σ'' plane. It is also called circumferential loading or *c-loading*. In laboratories, cruciform or thin-wall tubular specimens

can be exposed to such loading (see Section 1.4-7). As a simplest case, sinusoidal 90^0-out-of-phase symmetrical $\sigma_x(t)$ and $\sigma_y(t)$ with equal amplitudes $\sigma_{x,a}$ and $\sigma_{y,a}$ can be produced. Then, a central (centrally located) circumference is described as a trajectory. This is the 'pure' second type of loading with $t_c = S_c/S = 1$. Otherwise, every non-proportional loading with immovable principal axes relates to the second type if $t_c = S_c/S$ is close to 1.

Third type: non-proportional loading with constant principal stresses in rotating principal directions having $(S) \equiv (S_\tau)$. It is also called $\mathrm{d}\tau$- *or* $\Delta\tau$-*loading*. This type was revealed just thanks to the IDD point of view. So formulated, the third type had not been introduced before. However, it proves to be of first-rate importance now. It is a maximized case, a 'touch stone', an 'acid test' that could invalidate many of the fatigue life theories proposed (this will be discussed in Sections 2.6.2 – 2.6.5). Correspondingly, the question of how to implement in laboratories this loading in pure form with $t_\tau = S_\tau/S$ exact 1 was not treated as it deserves. Again from the IDD point of view, an answer to that question is found out (Section 2.6.2). Here it is to mention that the well-known experiments under cyclic out-of-phase bending and torsion, or pull-push and torsion (Section 1.4.5), may cause intensive rotation of the principal axes. Thus, a ratio $t_\tau = S_\tau/S$ relatively close to 1 could be achieved.

This Section 2.1.4 in the thesis continues with several equations and illustrations in reference to the resolution of the $(\mathrm{d}s)$ loading differential, including in its physical meaning.

2.2. Basic damage differentials and basic damage intensities

Of course, while the stress state (s_p) changes by a differential $(\mathrm{d}s)$, some damage differential $\mathrm{d}D$ is added to the cumulative damage $D_\Sigma(t - \mathrm{d}t)$.

How should $\mathrm{d}D$ be defined? In this Subchapter 2.2 in the thesis, it is grounded that so far the single possible option is to propose a phenomenological (empirical) IDD approach.

Let the case $(\mathrm{d}s) \equiv (\mathrm{d}s_r)$ be considered first, i.e. a basic loading r-differential (Fig. 2.1.4-3a in the thesis illustrates its physical meaning). The corresponding basic damage differential is $\mathrm{d}D \equiv \mathrm{d}D_r$. The derivative $R_r = \mathrm{d}D_r/\mathrm{d}s_r$ is introduced: basic damage intensity under r-loading. It is some function of the principal stresses σ' and σ'', i.e. it relates to a certain point in the σ'-σ'' plane: $R_r = R_r(\sigma',\sigma'')$. Then, basic damage differentials $\mathrm{d}D_r = R_r\mathrm{d}s_r$ will be integrated.

How to determine $R_r(\sigma',\sigma'')$? The idea is simple: this damage intensity should satisfy given (input) S-N lines under cyclic r-loadings with different values of $k = \sigma''(t)/\sigma'(t) = \mathrm{constant}$. IDD does not deal with the origin or composition of the input S-N lines. They are the most treated characteristics of fatigue life and for them there is a lot of accumulated experimental and theoretical experience (including for their accelerated determination: a respective study done is presented in Section 1.2.5 of Volume II). The input S-N lines can be both experimental and partly or entirely hypothetical. For their composition, any existing suitable and confirmed methods and criteria will be used, i.e. IDD incorporates them, actually. The very determination of $R_r(\sigma',\sigma'')$ based on the input S-N lines, i.e. the development of the above-mentioned simple idea, requires mathematical treatment that is not as simple. It is carried out in the next two Sections 2.3 and 2.4.

Analogously, basic damage differentials $\mathrm{d}D_c$ and $\mathrm{d}D_\tau$ per the basic loading differentials $(\mathrm{d}s_c)$ and $(\mathrm{d}\tau)$ (shown in physical meaning in Fig. 2.1.4-3b and Fig. 2.1.4-3c in the thesis) are introduced together with corresponding basic damage intensities $R_c = \mathrm{d}D_c/\mathrm{d}s_c = R_c(\sigma',\sigma'')$ and $R_\tau = \mathrm{d}D_\tau/\mathrm{d}\tau = R_\tau(\sigma',\sigma'')$. Differentials $\mathrm{d}D_c = R_c\mathrm{d}s_c$ and $\mathrm{d}D_\tau = R_\tau\mathrm{d}\tau$ will be integrated.

By the way, since the damage is considered relative (a part of 1), i.e. dimensionless, then each R function has a dimension of $[\mathrm{Pa}^{-1}]$.

Similarly to the idea of determining R_r, R_c could be also determined in a way as to satisfy experimental or/and hypothetical fatigue life data under c-loadings ('circumferential' loadings). In the world, there is accumulated experimental and theoretical experience in fatigue life under non-proportional loadings with immovable principal axes. Such loadings are close to the circumferential type although they had not been considered in this way. Now, IDD emphasizes *the necessity of doing such tests that trajectories are obtained oscillating on central circumferences* in the σ'-σ'' plane. Only then will more reliable data be available for determination of R_c. For the time being, R_c will be found in agreement with life data under loadings having trajectories in which differentials $\mathrm{d}s_c$ dominate. R_c will be also considered in comparison to R_r. On this occasion, the empirical ratio $f_c = R_c/R_r$ will serve in the role of an (averaged) empirical factor of loading non-proportionality. In other words, $f_c = R_c/R_r$ will testify for the material's sensitivity to non-proportionality of loading with immovable principal axes. With that, $f_c \geq 1$ is expected, i.e. $R_c \geq R_r$, according to physical and other considerations that follow in this Subchapter 2.2 in the thesis.

The third intensity R_τ is to be determined in a way as to satisfy life data under constant principal stresses acting onto rotating principal directions (pure $\mathrm{d}\tau$-loading). IDD reveals the importance of this $\mathrm{d}\tau$-loading and *emphasizes the necessity of doing tests that provide trajectories in* σ_x-σ_y-τ_{xy} *coordinates oscillating on ellipses which transform* $\sigma_x(t)$, $\sigma_y(t)$ *and* $\tau_{xy}(t)$ *into* σ' = constant *and* σ'' = constant. Then, every loading differential is $(\mathrm{d}s) \equiv (\mathrm{d}\tau)$ and looks in physical meaning like shown in Fig. 2.1.4-3c in the thesis. The ratio $f_\tau = R_\tau/R_r$ is introduced in the role of an (averaged) second empirical factor of loading non-proportionality: of material's sensitivity to principal axes rotation. In this Subchapter 2.2 in the thesis, expectation for $R_\tau \geq R_r$ is grounded.

The next, main question is: how are the basic $\mathrm{d}D_r$, $\mathrm{d}D_c$ and $\mathrm{d}D_\tau$ combined (and changed) into a general damage differential $\mathrm{d}D$ in case $\mathrm{d}s_r$, $\mathrm{d}s_c$ and $\mathrm{d}\tau$ appear simultaneously as components of a mixed (general) loading differential $\mathrm{d}s$? The development of this subject is carried out in Subchapter 2.7.

2.3. Determination of $R \equiv R_r$ and application of IDD to one value of k

2.3.1. Determination of $R(s)$ based on the Newton-Leibniz formula

For shorter notation, the $_r$ index is omitted (but is implied) in this section: $R(s) \equiv R_r(s) = \mathrm{d}D_r(s)/\mathrm{d}s \equiv \mathrm{d}D(s)/\mathrm{d}s$.

The s argument of $R(s)$ and $D(s)$ is the distance from the coordinate origin to the oscillating M point at the t time. The s radial axis (Fig. 2.1.3-1) on which M oscillates is individually illustrated after taking it outside the σ'-σ'' plane and is shown vertical (Fig. 1.2.1-1a) just for convenience. Let the simplest, cyclic oscillation of M point between $s_{\min}$ and $s_{\max}$ (Fig. 1.2.1-1a) be available. The distance s as an argument of $R(s)$ and as an operand will be treated in absolute value (always positive). Moreover, s will be later raised to a real power. *The meaning of D with s argument is accumulated damage* (*accumulated differentials* $dD = Rds$) *during moving the M point from* 0 *to* s.

The derivative R and the primitive D with the s argument correspond to f and F with the x argument in the Newton-Leibniz theorem in Preview in the thesis. As noticed there, if $x_{\min}$ is constant, then

$$\frac{\mathrm{d}}{\mathrm{d}x_{\max}} \int_{x_{\min}}^{x_{\max}} f(x)\mathrm{d}x = \frac{\mathrm{d}F(x_{\max})}{\mathrm{d}x_{\max}} - 0 = f(x_{\max} \equiv x). \qquad (2.3.1\text{-}2)$$

In other words, if the integral is a function of its upper limit $x_{\max}$ and is differentiated with

respect to it, then the integrand $f(x)$ is obtained, and the upper limit $x_{\max}$ takes the part of the integrand's argument x. Although this interpretation is well-known, it is worth reminding here, since no researcher had used it for obtaining the damage intensity as done below.

Now, $R(s)$ and $D(s)$ come to replace $f(x)$ and $F(x)$ in Eq. 2.3.1-2. These $R(s)$ and $D(s)$ will be considered the same regardless of the location of s on either side from the coordinate origin (this postulation will be discussed in Section 2.3.7). While the point M is oscillating one cycle, it travels twice the distance between $s_{\min}$ and $s_{\max}$. With that, the damage D_T per one cycle is accumulated. Then, the integration of the differentials $\mathrm{d}D$ to D_T is done according to the following understandable procedure (see Fig. 1.2.1-1a):

$$D_T = \int_{(S)} \mathrm{d}D = 2\int_{s_{\min}}^{s_{\max}} R(s)\mathrm{d}s = 2\left[\int_{0}^{s_{\max}} R(s)\mathrm{d}s \pm \int_{0}^{s_{\min}} R(s)\mathrm{d}s\right]. \qquad (2.3.1\text{-}3)$$

The plus sign is valid when the peaks $s_{\min}$ and $s_{\max}$ are on both sides of zero; otherwise, the minus sign is valid. The indices $_{\min}$ and $_{\max}$ are assigned to $s_{\min}$ and $s_{\max}$ in a way that $s_{\min} < s_{\max}$ in absolute values (the $s_{\max}$ peak is farther from zero than the $s_{\min}$ peak).

$R(s)$ is expected to be an exponential function steeply growing with increasing s. Therefore, the second integral in the brackets in Eq. 2.3.1-3 can be neglected at first stage. On the other hand, according to the linear hypothesis (Section 1.3.1), $D_T = 1/N(s_{\max})$ where the function $N(s_{\max})$ is represents by an S-N line. Hence,

$$\frac{1}{2N(s_{\max})} = \int_{0}^{s_{\max}} R(s)\mathrm{d}s\,. \qquad (2.3.1\text{-}4)$$

Thus, a remarkable possibility is available for application of the Newton-Leibniz theorem for obtaining the integrand similarly to Eq. 2.3.1-2: both sides of Eq. 2.3.1-4 are differentiated with respect to the upper variable limit $s_{\max}$ and R is obtained with the argument $s_{\max} \equiv s$:

$$R(s) = \frac{\mathrm{d}}{\mathrm{d}s_{\max}}\left(\frac{1}{2N(s_{\max} \equiv s)}\right). \qquad (2.3.1\text{-}5)$$

Next step is to introduce the analytical expression of the function $N(s_{\max})$, i.e. of the S-N line, to be differentiated with respect to $s_{\max} \equiv s$. In Section 1.2.1, Eq. 1.2.1-1 of the S-N line for $s_{\max} > s_l$ was indicated as the most popular. Thus,

$$s_{\max}{}^m N = A,\ \ N = N(s_{\max}) = \frac{A}{s_{\max}^m},\quad \frac{1}{N(s_{\max})} = \frac{s_{\max}^m}{A},\quad \frac{1}{2N(s_{\max} \equiv s)} = \frac{s^m}{2A}\,. \qquad (2.3.1\text{-}6)$$

By differentiating the last expression and according to Eq. 2.3.1-5, $R(s)$ is obtained:

$$R(s) = \frac{ms^{m-1}}{2A}\,. \qquad (2.3.1\text{-}7)$$

This equation is valid for $s > s_l$ in case the fatigue limit s_l is entered. For $s < s_l$, R is supposed to be zero but this will be additionally discussed later (Section 2.3.3).

It is to notice that IDD uses an S-N line as $s_{\max}$-N diagram whereas CCA uses an S-N line as s_a-N diagram.

2.3.2. The functions $R(s)$ and $D(s)$ containing i^* divisor

If checking out Eq. 2.3.1-7 with an actual slope, e.g. with $m = 10$, it becomes apparent

that $R(s)$ really grows steeply with increasing s. Nevertheless, the error admitted above for neglecting the integral between the limits 0 and $s_{\min}$ can be compensated. For this purpose, a constant divisor denoted as i^* is put at the place of 2 in Eq. 2.3.1-7:

$$R(s) = \frac{ms^{m-1}}{i^* A}. \tag{2.3.2-1}$$

For determination of i^*, Eq. 2.3.2-1 is to be substituted in Eq. 2.3.1-3 without neglecting the second integral in the brackets now. As well, $D_T = 1/N(s_{\max})$ is substituted. The following is obtained:

$$\frac{1}{N(s_{\max})} = 2\left[\int_0^{s_{\max}} \frac{ms^{m-1}}{i^* A}\mathrm{d}s \pm \int_0^{s_{\min}} \frac{ms^{m-1}}{i^* A}\mathrm{d}s\right] = \frac{2}{i^* A} s_{\max}^m \left[1 \pm \left(\frac{s_{\min}}{s_{\max}}\right)^m\right]. \tag{2.3.2-2}$$

This operation is actually IDD reproduction of the input (given) *S-N* line represented by the third of the Eqs. 2.3.1-6, after the *R* function is determined from the same *S-N* line according to Eq. 2.3.2-1. By equalizing the reproduced function $N(s_{\max})$ to the input one, i.e. by equalizing the last term of Eq. 2.3.2-2 to the right side of the third of the Eqs. 2.3.1-6, and meanwhile canceling out, the following is obtained:

$$i^* = 2\left[1 \pm \left(\frac{s_{\min}}{s_{\max}}\right)^m\right]. \tag{2.3.2-3}$$

The sign plus or minus appears according to the same rule that related to Eq. 2.3.1-3.

Eq. 2.3.2-3 really yields i^* as a constant if the *S-N* line is valid for $\mathrm{R} = s_{\min}/s_{\max} = \text{constant}$. Then, thanks to i^* from Eq. 2.3.2-3, IDD exactly reproduces such an input *S-N* line. For pulsating loading cycle ($s_{\min} = 0 = \mathrm{R}$), Eq. 2.3.2-3 yields exact 2 for i^*. For alternating (reversed) loading cycle ($s_{\min} = s_{\max}$, $s_{\mathrm{m}} = 0$), i^* is exact 4.

If the *S-N* line is valid not for $\mathrm{R} = \text{constant}$ but for $s_{\mathrm{m}} = \text{constant} \neq 0$ which is the case mostly met, then the stress ratio $\mathrm{R} = s_{\min}/s_{\max}$ varies along the whole *S-N* line. Correspondingly, Eq. 2.3.2-3 will give different values of i^* for exact reproducing individual N abscissae of the *S-N* line. If one and the same $i^* = \text{constant}$ is used, the whole *S-N* line will not be reproduced perfectly.

It will be shown later (Section 2.3.6) that $i^* = \text{constant}$ can always be taken within the interval $4 \geq i^* \geq 2$ and this will provide enough accuracy, practically. Moreover, nearly for every non-zero s_{m}, the input *S-N* line will be reproduced precisely enough with $i^* = 2$. Anyway, the problem of satisfactory reproduction of an input *S-N* line is solved. The final expression of the *R* function is Eq. 2.3.2-1.

The primitive $D(s)$ of $R(s)$, i.e. the function obtained by integration of Eq. 2.3.2-1, is

$$D(s) = \frac{s^m}{i^* A}. \tag{2.3.2-4}$$

Both Eq. 2.3.2-1 and Eq. 2.3.2-4 is valid for $s > s_l$ in case a fatigue limit s_l is entered. For $s < s_l$, $R(s)$ and $D(s)$ are supposed to be zeros but this will be additionally analyzed in the next section.

Let Eq. 2.3.2-4 be compared to the third of the Eqs. 2.3.1-6 that represent the *S-N* line. It is seen that $D(s)$ is the function $1/N(s \equiv s_{\max})$ which can be called 'reciprocal Wöhler function' divided by i^*: $D(s) = 1/[i^* N(s)]$. Thus, $1/N(s \equiv s_{\max})$ represents $D(s)$ proportionally through the constant i^* divisor. This would be also valid for *any different S-N line equation* which another IDD follower would prefer instead of Eq. 2.3.1-6. Of course, if Eq. 2.3.1-6 is

not used, then Eq. 2.3.2-3 for i^* will be different (but again there will be $i^* = 4$ if $s_m = 0$ and $i^* = 2$ under pulsating loading).

2.3.3. *S-N*, *S-R* and *S-D* lines. 'Breaking' (impulse) mode and 'smooth' mode

Now, example graphs of the functions $N(s)$ (the *S-N* line), $R(s)$ and $D(s)$ according to Eqs. 2.3.1-6, 2.3.2-1 and 2.3.2-4 can be illustrated all together. They are figuratively overlapped in Fig. 2.3.3-1 (which is in addition to Fig. 1.2.1-1b). The vertical coordinate axis, along which the trajectory oscillates, plays now the role of the abscissa axis while the horizontal coordinate axis takes the ordinates of the three functions. These three lines, *S-N*, *S-R* and *S-D*, are straight in double-logarithmic coordinates.

As mentioned more than once above, necessary specifications relating to the conditions $s > s_l$ and $s < s_l$ are to be introduced. What exactly happens at $s = s_l$? Then, the *S-N* line abruptly breaks (refracts) to a horizontal and $N \to \infty$ (Fig. 2.3.3-1b). With the *S-D* line, a sudden jump occurs from $D = 0$ to $D(s_l) = 1/(i^* N_l) = s_l^m/(i^* A)$. With the derivative *S-R*, this means an instantaneous infinite *impulse*. Upon integrating that impulse on a single infinitesimal element $\mathrm{d}s$ at s_l, the finite value $D(s_l) = 1/[i^* N(s_l)] \equiv 1/(i^* N_l)$ results. It is a sudden addend to the damage. Practically, the impulse will be finite and will cause the same addend but per a finite Δs element.

It turns out that as soon as the oscillating M point crosses the s_l level, $1/(i^* N_l)$ should be added to the damage accumulated to that time. If the addend $1/(i^* N_l)$, correspondingly the impulse $R(s_l)$, is skipped during the computation, then the (output) *S-N* line reproduced by IDD will deviate from the input straight *S-N* line. A smooth bend to the horizontal asymptote at s_l will occur (Fig. 2.3.3-1). Hence, for exact reproduction of an input *S-N* line which breaks in two at s_l, the addend $D(s_l) = 1/(i^* N_l)$ should be included at each crossing the s_l level.

Such an option is called breaking mode or impulse mode and is provided in the IDD software for users who want to use a breaking *S-N* line. The author is skeptic about setting discontinuity as a jump in $D[s(t)]$, respectively in $D_\Sigma(t)$. More strictly the rule should be

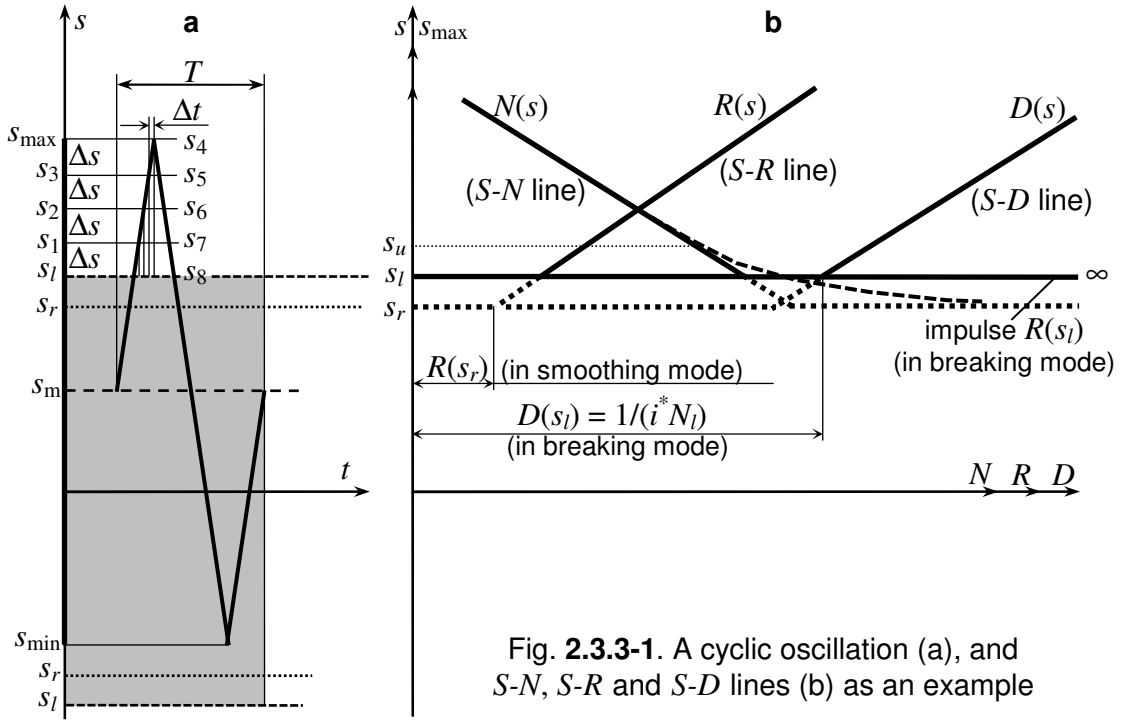

Fig. **2.3.3-1**. A cyclic oscillation (a), and *S-N*, *S-R* and *S-D* lines (b) as an example

followed that physical functions are continuous on principle. Then, finite jumps should not be admitted in primitives, and, moreover, infinite jumps (impulses) should not be admitted in their derivatives. The impulse $R(s_l) \to \infty$ is another IDD 'discovery'. It does not advocate the idealization of breaking S-N line. The opponents of the impulse mode would prefer a less jumping idealization as follows.

A kind of new limit $s_r < s_l$ is introduced (Fig. 2.3.3-1). It is a border between areas of $R(s) > 0$ and $R(s) = 0$. The non-zero $R(s)$ is determined by Eq. 2.3.2-1 for $s > s_r$, whereas $R(s)$ is zero for $s \le s_r$. There will be no impulse $R(s_r)$. An input S-N line is first extrapolated below s_l to s_r and is called input R-*prototype*. A conditional number of cycles N_r corresponds to s_r (illustrated in Fig. 1.2.1-1b). Thus, while doing IDD reproduction of $N(s_{\max})$, a smoothed output S-N line results. It follows quite close the straight input prototype to some s_u level and then bends to a horizontal asymptote at s_r (Fig. 2.3.3-1b).

Hence, the option is given to the IDD user to select the breaking mode or the smooth mode. In both cases, a straight line is entered in $\log s_{\max}$-$\log N$ coordinates and is called R-*prototype*. Its equation is $s_{\max}{}^m N = A$. If the breaking mode is selected, N_l (respectively s_l) will be entered. Then, the given S-N line will be reproduced as coinciding with the input R-prototype and breaking in two. If the smooth mode is selected, N_r (respectively s_r) will be entered. Then, the given S-N line will be reproduced (more realistically) as smoothly bending (its equation will be presented in the next section). If the IDD user does not want at all to have any distinct interval of no damage round the coordinate origin of the s axis, then N_l or N_r will be entered as sufficiently great (respectively, s_l or s_r will be sufficiently low).

2.3.4. Numerical examples. Equation of 'bending' (smooth) S-N line

Demonstratively, with concrete numerical data, the N life of the oscillation in Fig. 2.3.3-1a is reproduced by IDD in this Section 2.3.4 in the thesis. $D_{\Sigma,T} = \Sigma \Delta D = \Sigma R(s) \Delta s$ and then $N = 1/D_{\Sigma,T}$ is calculated. It proves that the N life from the S-N line is reproduced very well in breaking mode even if the Δs elements are comparatively big. Then the reproduction of a smoothed S-N line is demonstrated and its equation is:

$$(s_{\max}{}^m - s_r{}^m) N = A. \qquad (2.3.4\text{-}5)$$

Eq. 2.3.4-5 is able to describe a bending S-N line (also apart from IDD) and agree with the scattered experimental points better than the classic equation $s_{\max}{}^m N = A$ with breaking in two. The IDD user will prefer the smooth mode in case the input S-N line is formed namely as bending. Such an S-N line will be put in agreement with Eq. 2.3.4-5 and thus the parameters m and A of the input prototype's equation $s_{\max}{}^m N = A$ will be obtained.

2.3.5. The opportunity for fatigue life computation without cycle counting, in impulse 'peak' and 'range' mode, and in smooth mode

The same R intensity (Eq. 2.3.2-1)*, through which input lives are reproduced under cyclic proportional oscillations with different* $s_{\max}$ *values, may also be used directly for life prediction under non-cyclic proportional loading* according to $D_{\Sigma,T} = \Sigma R(s) \Delta s$ and $N = 1/D_{\Sigma,T}$. In other words, an input S-N line that CCA uses through the Miner rule will also be used now, however directly, *without any preliminary looking for cycles and counting them*.

There is a main algorithm of the IDD software named *Ellipse* (the name is for often involved elliptical mathematical expressions). This algorithm is for the general loading and does not differ whether the stressing is proportional or not. *Ellipse* performs $N = 1/\Sigma\Delta D$ where R_r, R_c, R_τ, Δs_r, Δs_c and $\Delta\tau$ are all together included in the expression of ΔD in a way discussed further on (Subchapter 2.7).

But particularly under *r*-loading, the simplification $R_c = R_\tau = \Delta s_c = \Delta\tau = 0$ is available. It enables the other simplification: the possibility to use the primitive $D \equiv D_r$ function and the Newton-Leibniz equation instead of the derivative $R \equiv R_r$. Then, the computational procedures with the elements $\Delta s \equiv \Delta s_r$ are not needed. This opportunity is analyzed further in the same Section 2.3.5 in the thesis. It proves that the impulse mode can be 'peak impulse mode' or 'range impulse mode'. The difference between these two impulse mode versions is insignificant. Anyway, it is again confirmed that the smooth mode is to be preferred.

After demonstrating simple examples of composition of $D_\Sigma(t)$, an algorithm for impulse and smooth damage accumulation emerges. It was developed for practical application under any single oscillogram and was named *Integral*. It is much simpler than *Ellipse*. The *Integral* development is taken out to Chapter 3.

2.3.6. An example for the values of the i^* divisor with $s_m \neq 0$ and for the possibility to directly set $i^* = 2$

In continuation of Section 2.3.2 it is to verify the statement there which, in other words, says: the N abscissae of an input S-N line versus s_{max} ordinates at one and the same $s_m \neq 0$ will be reproduced as approximate, but exact enough, if directly setting one and the same $i^* = 2$ in case s_m is comparatively far from zero; and if s_m is too close to zero, then one and the same (averaged) i^* value will be calculated within the interval $4 \geq i^* \geq 2$. Below in this Section 2.3.6 in the thesis, calculations of i^* follow providing reproduction of five input example S-N lines with different $s_m \neq 0$ values.

Based on the example considered, a rule is to be stated that if the ratio s_m/s_l exceeds at least $0{,}11$, then $i^* = 2$ can be directly set. Otherwise i^* should be calculated and averaged between 2 and 4, and hence the reproduction error factor can be reduced close enough to 1.

The demonstrated manual calculations (using a calculator) are not the practical manner of evaluating and setting i^*. Instead, the very software *Ellipse* or *Integral* will be used: by means of it, it is always possible to check how precisely input lives are reproduced with the selected value of i^*.

2.4. Determination of R_r in the whole σ'-σ'' plane. Concomitant issues

2.4.1. Introducing lines of equal lives

In the *Ellipse* algorithm, *at least two R_r-prototypes are entered* under cyclic *r*-loadings for two radial lines in the σ'-σ'' plane (Fig. 2.4.1-1). For example, the lines with $k = \sigma''/\sigma' = 0$ of uniaxial stress state and $k = \sigma''/\sigma' = -1$ of pure shear will often be involved. In Fig. 2.4.1-1, two radial lines are shown with values k_i and k_{i+1} of the ratio $k = \sigma''/\sigma'$. The $_i$ index is introduced since *Ellipse* can accept *more than two R_r-prototypes* for radial lines: *up to $n \leq 9$ in number*. This is more than enough for the practical application of IDD.

As already known, the R function at each point of any radial line is determined according to Eq. 2.3.2-1. The latter takes now the form $R_r(s_i \equiv s_{max,i}) = m_i s_{max,i}^{m_i - 1}/(i^* A_i)$ where m_i and A_i are the parameters of the input $R_{r,i}$ prototype having the equation $s_{max,i}^{m_i} N_i = A_i$.

Instead of the A_i parameter, it is more convenient to enter the $s_{max,i}$ ordinate and the N_i abscissa of a point through which the prototype passes as an S-N line having the m_i slope. Such a point will shortly be called 'through-point'. It is also more convenient to exchange $s_{max,i}$ with $\sigma'_{max,i}$ accompanied by the corresponding k_i. After all, the parameters of an input prototype are $\sigma'_{max,i}$, N_i, m_i and k_i. To avoid writing the $_i$ index at each of the parameters, the contents of the $R_{r,i}$ prototype will be simpler denoted so: $(\sigma'_{max}, N, m, k)_i$.

In Fig. 2.4.1-1, a trajectory is shown as a segment of the radial k_i line. It is a cyclic oscillation between $s_{min,i}$ and $s_{max,i}$ and its life is N cycles. Let a second segment of the radial k_{i+1} line represent another cyclic oscillation having the same N life. And, on the radial k line, let a third oscillation have the same N life. The k value is in the interval between k_i and k_{i+1} in Fig. 2.4.1-1 but otherwise it may be out of this interval, especially if only two input prototypes are entered. The peaks of the three oscillations, where the oscillating points M_i, M and M_{i+1} are put, lie on the same *line of equal N life under r-loadings*. Its label is $l_N \equiv l_{N,r}$.

The places of the peaks M_i and M_{i+1} (Fig. 2.4.1-1) for any N are determinable from the input prototypes $R_{r,i} \equiv (\sigma'_{max}, N, m, k)_i$ and $R_{r,i+1} \equiv (\sigma'_{max}, N, m, k)_{i+1}$. If the line of equal life through the points M_i and M_{i+1} is described mathematically, then the place of M will be determined as a point of intersection of l_N and the radial k line. This will result in a mathematical expression for determination of N for s_{max} and k. That expression will represent the function $N(s_{max})$ (with k parameter). And, as already known from Section 2.3.2, from differentiation of $1/[i^* N(s_{max})]$ the intensity $R_r(s \equiv s_{max})$ will be obtained at any k now, i.e. in the whole σ'-σ'' plane.

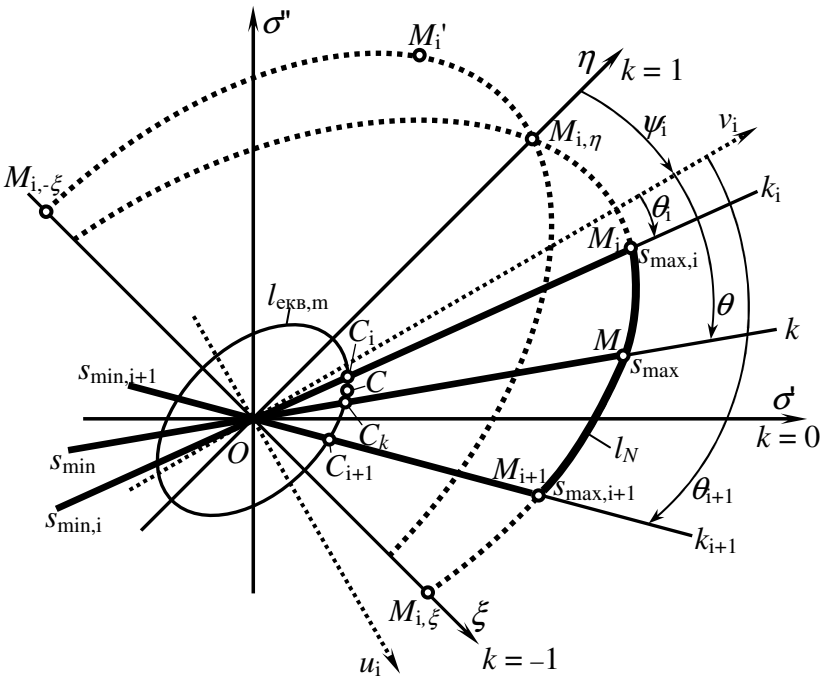

Fig. **2.4.1-1**. Elliptic arc of a line of equal life

2.4.2. Taking static stresses (or R stress ratios) into consideration

Before developing the above idea of deriving $N(s_{max})$ from the lines of equal lives at any k, the next concomitant question should be answered. What relation should bind the mean (static) stresses of the straight-line segment trajectories in Fig. 2.4.1-1? Correspondingly, *for what* $\sigma'_{m,i}$ *should each input* $R_{r,i}$ *prototype be valid* according to the static stresses $\sigma_{x,m}$, $\sigma_{y,m}$ and $\tau_{xy,m}$ of the input oscillograms $\sigma_x(t)$, $\sigma_y(t)$ and $\tau_{xy}(t)$?

Since referring to static stresses, the classic approach of reduction of $\sigma_{x,\mathrm{m}}$, $\sigma_{y,\mathrm{m}}$ and $\tau_{xy,\mathrm{m}}$ to an equivalent static stress $\sigma_{\mathrm{equ,m}}$ is acceptable. For this purpose, some of the classic or recent criteria can be used. An author's criterion is also proposed in this Section 2.4.2 in the thesis. After each input $R_{r,\mathrm{i}}$ prototype at $k \equiv k_{\mathrm{i}}$ receives its $\sigma'_{\mathrm{m}} \equiv \sigma'_{\mathrm{m,i}}$ in agreement with $\sigma_{\mathrm{equ,m}}$, next step is agreeing the prototype's parameters $\sigma'_{\mathrm{max,i}}$, N_{i} and m_{i} with $\sigma'_{\mathrm{m,i}}$. And after that, the prototype is ready for entering in the IDD software.

In a summary: the input $R_{r,\mathrm{i}}$ prototypes should relate to lives of straight-line segment trajectories with the same $\sigma_{\mathrm{equ,m}}$ of the trajectory subjected to life computation. If the input oscillograms (the 'current' input data) $\sigma_x(t)$, $\sigma_y(t)$ and $\tau_{xy}(t)$ are pulsating ($\mathrm{R} = 0$), then the input prototypes should also be valid for $\mathrm{R} = 0$.

2.4.4. Exchanging the values of the principal stresses (switching over the signs ±). First, second and third condition

It is to recollect from Section 2.1.2 the following. The α' angle always determines the instantaneous position of the ' principal axis and α'' is always the angle of the '' principal axis. The principal stresses σ' and σ'' are always and correspondingly bound with the principal axes ' and ''. At any t time, the principal stresses can be computed from Eqs. 2.1.2-1 but it is not known which is σ' and which is σ''. They cannot be recognized, either, by the α_0 angle from Eq. 2.1.2-2.

Then, the following question arises: how to correctly recognize σ' and σ'' in the connection with their own axes ' and '' in order not to admit their wrong exchange (interchange)? Otherwise, incorrect discontinuities (jumps) of $\alpha'(t)$, $\sigma'(t)$ and $\sigma''(t)$ may occur. Correspondingly, the invariant (S_{xy}) trajectory will be torn: its next part will be suddenly carried out from e.g. the M' point to the distant M'' point (Fig. 2.1.3-1).

The equation of $\alpha'(t)$ (or $\alpha''(t)$) is is involved:

$$\alpha'(t) = \operatorname{arctg}\frac{\sigma'(t) - \sigma_x(t)}{\tau_{xy}(t)} \qquad \left(\text{or} \quad \alpha''(t) = \operatorname{arctg}\frac{\sigma''(t) - \sigma_x(t)}{\tau_{xy}(t)}\right) \qquad (2.4.4\text{-}1)$$

where $\sigma'(t)$ and $\sigma''(t)$ are computed first from Eqs. 2.1.2-1. The so-called first condition for switchover (of the $\pm$ signs) is formulated: $\sigma' \geq \sigma''$ if $\tau_{xy} \geq 0$ and $\sigma' \leq \sigma''$ if $\tau_{xy} < 0$. If $M(\sigma_x, \sigma_y, \tau_{xy})$ is out of the η-τ_{xy} plane, a second condition applies: the variant point $M(\sigma_x, \sigma_y, \tau_{xy})$ (Fig. 2.1.3-1) goes into that of the two points $M'(\sigma', \sigma'', 0)$ and $M''(\sigma'', \sigma', 0)$ which is closer. This condition prevails upon the first one and may disable it by causing a new switchover.

The second condition makes the variant trajectory 'attract' the invariant trajectory to 'its own' side from the η-τ_{xy} plane. The so-'attracted' invariant trajectory may pass over to the other side of the η axis without bouncing off it but crossing it naturally. However, whether the invariant trajectory will be 'allowed' to pass over to the other side or not, the following third condition determines: no discontinuity of $\alpha'(t)$ must occur in the order of $\pm 90^0$. If such a discontinuity is found out after the first and second condition, then the third condition will produce a (new) switchover.

This idea of an 'angular' third condition for switchover is developed in Section 4.1.3 in the thesis. There are too many details to be elaborated. They mostly relate to how much close to each other the points of the variant trajectory are, especially in the immediate proximity to the η axis. The $\alpha'(t)$ angle has its own finite change from point to point and this change can be great especially if the points are very close to the η axis. In order to recognize if such a change is indeed 'its own' i.e. not commingled with a 'wrong jump by $\pm 90^0$', certain additional conditions should be observed. As well, the possible interference of the arctg-jump

by $\pm 180^0$ should be taken into account. By solving the problem of the correct switchover controlled by $\alpha'(t)$ according to the third angular condition, the very problem of determination of the $\alpha'(t)$ function is solved, in fact.

The very $\alpha'(t)$ function, except for its possible role to control the switchover according to the third condition, is not directly needed for IDD at this stage. Therefore, eventually, another controlling third condition has been preferred. It will be presented later (in Section 4.1.4 in the thesis). There will be other more considerations involved in terms of the continuity of the participating functions, the rotation of the principal axes, and a necessity of specific dividing the current variant element into two sub-elements (Section 4.1.5). That is all a large and complicated subject which engaged much time and effort for the correct mathematical solution, algorithmization and programming in *Ellipse*. Corresponding differential analysis was done as an essential IDD part that belongs, on principle, to Chapter 2. But for the bulky mathematical and algorithmic details, the subject in question was carried out to Chapter 4.

2.4.6. Composition of the lines of equal lives

The segment M_iMM_{i+1} (Fig. 2.4.1-1) was postulated to be an arc of a central ellipse having axes v_i and u_i. The v_i axis deviates from η at an angle ψ_i. In *Ellipse*, input ψ_i angles between -45^0 and 45^0 are entered. A positive ψ_i is accepted clockwise as shown in Fig. 2.4.1-1. The input prototypes follow each other also 'clockwise' at k_i from 1 to -1, and therefore $k_{i+1} < k_i$ in algebraic values. In other words, the prototypes are entered from up to down; $2 \le n \le 9$ or, what is the same, $1 < n < 10$. An example: $n = 3$, $k_1 = 1$ (biaxial equal stressing with $\sigma' = \sigma''$), $k_2 = 0$ (uniaxial stressing with σ' while $\sigma'' = 0$), and $k_3 = -1$ (pure shear, $\sigma' = -\sigma''$).

Thanks to the ψ_i angle, the segment M_iMM_{i+1} is more flexible. It is able to be as convex (curving outwards from the coordinate origin) as desired, or its convexity can decrease so that it may practically turn into a straight-line segment. Thereafter, transition to concavity (curving inwards to the coordinate origin) would occur. That is, for certain values of ψ_i and at certain places of the points M_i and M_{i+1} no ellipse could pass through them but a hyperbola having the axes v_i and u_i. Thus, the sought equation of an ellipse would turn into an equation of a hyperbola.

Concavity of a line of equal life does not correspond to any theoretical criterion. Moreover, in contrast to an ellipse as a geometrically closed figure, a hyperbola can go to infinity. This would block the *Ellipse* algorithm. Therefore, a subprogram is included that examines ψ_i, k_i, k_{i+1} and the other parameters of the input $R_{r,i}$ and $R_{r,i+1}$ prototypes for possible appearance of a hyperbola (Section 4.1.8). If the M_iM_{i+1} segment should be hyperbolic instead of elliptical, the subprogram will alarm and suggest to the user intervals for different ψ_i values that ensure an ellipse.

In this connection, the following remark is appropriate. When finding out published experimental *S-N* lines at different k_i values, their authors usually drew each line for itself through the scattered experimental points. For this purpose, some statistical way was used, usually based on the minimum-square method. And any observing lines of equal lives i.e. any observing mutual relations of the *S-N* lines at different k_i values was usually not done. Thus, too different m_i slopes are often obtained what results in appearance of somewhat 'strange', 'zigzagging' lines of equal lives.

Whenever *Ellipse* alarms, though, for hyperbolas, it is always due to 'strange' input prototypes. Even then, by means of relevant changes of ψ_i or/and n (entering also intermediate prototypes if necessary), again a fully satisfactory agreement with experimental data is achieved. With adding ψ_i, the parameters of an input prototype become 5: (σ'_{max}, N,

$m, k, \psi)_i$. Only the last prototype entered for the last k_n radial line will miss the parameter $\psi_i \equiv \psi_n$ since no next radial k_{n+1} line is involved.

Next details relating to this Section 2.4.7, in view of their mathematical and algorithmic difficulty, are carried out to Subchapter 4.1.

2.4.7. Determination of $N(s \equiv s_{max})$ and $R_r(s)$ at any k

Now, the mathematical solution of the problem of deriving $N(s \equiv s_{max})$ and $R_r(s)$ from the lines of equal lives can be presented in an initial outline. The equation of the ellipse to which the M_iMM_{i+1} segment belongs is used. As well, the angles θ_i, θ and θ_{i+1} shown in Fig. 2.4.1-1 are involved. After series of complicated deductions (Section 4.1.7), the following equation is obtained:

$$aN^{\frac{2}{m_i}} + bN^{\frac{2}{m_{i+1}}} - s^{-2} = 0. \qquad (2.4.7\text{-}1)$$

Large mathematical expressions indicated as a and b (Section 4.1.7) participate here. The parameters of the i^{th} and $i+1^{st}$ prototype are included in a and b, as well as $k = \sigma''/\sigma'$ of the radial line on which the point $M \equiv M(\sigma', \sigma'')$ instantaneously falls; s is the distance OM to the coordinate origin:

$$s = \sqrt{\sigma'^2 + \sigma''^2} = \sigma'\sqrt{1 + k^2}\,. \qquad (2.4.7\text{-}2)$$

Meanwhile it is to remind that, according to the Newton-Leibniz theorem, s is treated as $s \equiv s_{max}$ (as well as $\sigma' \equiv \sigma'_{max}$). Thus, Eq. 2.4.7-1 represents the sought $N(s_{max})$ function containing the k parameter. It is also to recollect (from Sections 2.3.1 and 2.3.2) that $R(s \equiv s_{max})$ will be derived by differentiation of $1/[i^* N(s \equiv s_{max})]$ with respect to s_{max} at constant k. By the way, since k = constant, a and b in Eq. 2.4.7-1 also participate as constants in the differentiation.

Eq. 2.4.7-1 is not directly solved for N and therefore $N(s \equiv s_{max})$ is an implicit function. Hence, the differentiation will be implicit. For this purpose, Eq. 2.4.7-1 is first represented in the following form:

$$a\left(\frac{1}{N}\right)^{\frac{2}{m_i}} + b\left(\frac{1}{N}\right)^{\frac{2}{m_{i+1}}} = s_{max}^{-2}. \qquad (2.4.7\text{-}3)$$

Next, the implicit differentiation follows, with respect to s_{max} through $1/N$:

$$\left[-\frac{2}{m_i}a\left(\frac{1}{N}\right)^{\frac{2}{m_i}-1} - \frac{2}{m_{i+1}}b\left(\frac{1}{N}\right)^{\frac{2}{m_{i+1}}-1}\right]\frac{\mathrm{d}}{\mathrm{d}s_{max}}\frac{1}{N} = -2s_{max}^{-3}. \qquad (2.4.7\text{-}4)$$

Here, $\mathrm{d}(1/N)/\mathrm{d}s_{max}$ is substituted with $i^* R(s \equiv s_{max})$ and the R_r function is obtained:

$$R \equiv R_r(s,k) \equiv R_r(\sigma', \sigma'') = \frac{s^{-3}}{i^*}\left[\frac{a}{m_i}\left(\frac{1}{N}\right)^{\frac{-2}{m_i}-1} + \frac{b}{m_{i+1}}\left(\frac{1}{N}\right)^{\frac{-2}{m_{i+1}}-1}\right]^{-1}. \qquad (2.4.7\text{-}5)$$

This equation needs substitution of the numerical N value which has to be preliminary computed from Eq. 2.4.7-3 for the corresponding value of $s \equiv s_{max}$. As already stated above, Eq. 2.4.7-3 is not directly solved for N. Therefore, a sub-algorithm in *Ellipse* has been

created for solution by two numerical methods of successive approximations. The final solution is reached quickly (for example, in 5 or 6 approximations only).

The mathematical and algorithmic details relating to this Section 2.4.7 are also carried out to Subchapter 4.1.

2.4.8. Initial description of procedures in the *Ellipse* algorithm

The computation according to Eq. 2.4.7-3 (in successive approximations) and Eq. 2.4.7-5 repeated for a great number of trajectory's points (from tens to millions of them) is immense. However, the contemporary computers perform it for insignificant time.

In this Section 2.4.8 in the thesis, a summary is presented clearing the sequence of the computational procedures in the *Ellipse* algorithm in the general loading case. Further details are treated in Section 2.7.7, Subchapter 4.1 and further on.

2.5. The R_c damage intensity in the whole σ'-σ'' plane. Concomitant issues

2.5.2. Introducing R_c-prototypes compared to R_r-prototypes

After all, the following was only possible to create at the present stage of the IDD development: the R_c function is set in the same way like the R_r function by means of (conditional) input R_c prototypes $(\sigma'_{\max}, N, m, k, \psi)_i$ $(i = 1, 2, \ldots, n)$.

These prototypes will be determined by adaptation so that they should agree with given (experimental or hypothetical) lives under non-proportional loadings with immovable principal axes and with trajectory ratios $t_c = S_c/S$ close to 1. The R_c prototypes are entered for the same values of k_i and are of the same n number like the R_r prototypes. And setting $f_c = R_c/R_r = \text{constant}$ in the whole σ'-σ'' plane will mean that each input R_c prototype will have the same parameters which the corresponding R_r prototype has, with the exception of the N parameter: it will be f_c times as low.

In this Section 2.5.2 in the thesis, analysis is done which shows that every R_c-prototype at k_i is expected to be replaced downwards from the corresponding R_r-prototype.

2.6. The R_τ damage intensity in the whole σ'-σ'' plane. Concomitant issues

2.6.1. The pure $d\tau$-loading. The rotating disk of Findley et al.

The pure $d\tau$-loading (a 'discovery' of IDD at $ds \equiv d\tau$), when the principal stresses remain constant while the principal axes rotate, should have been noticed, discussed and written down into the chronic of the fatigue strength studies long ago. Respectively, *it should have been established long ago as one of the basic laboratory tests* in the role of a 'touch stone' (an 'acid test') for examining the fatigue life criteria proposed.

Many quantities introduced in Strength of Materials such like equivalent stress, strain energy, and others, expressed by the principal stresses, remain also constants, altogether and simultaneously. Hence, if fatigue life criteria are created based on variation of these quantities, such criteria will be all canceled since no variation is available.

In 1960, Findley et al. published the following experiment: compressing a rotating disk by two constant forces P with a common line of action through the disk's center (Fig. 2.6.1-1 in the thesis followed by remarks). This is the single known case of implementing $d\tau$-loading.

2.6.4. Introducing R_τ-prototypes compared to the R_r-prototypes

Again due to the lack of experimental (and even hypothetical) data from which R_τ could be derived, the S-N approach is accepted again to R_τ as it was applied to R_c. In other words, again conditional input prototypes $(\sigma'_{\max} \equiv \sigma', N, m, k, \psi)_i$ $(i = 1, 2, \ldots, n)$ are introduced in the form of 'S-N lines' called R_τ prototypes now. They are analogous to the R_r and R_c prototypes and are valid for the same radial k_i lines. The R_τ intensity will be again computed according to Eqs. 2.4.7-3 – 2.4.7-5. It will be studied in comparison to the R_r intensity by involving the factor $f_\tau = R_\tau/R_r$.

According to the IDD experience so far and according to the physical and other considerations, $R_\tau \geq R_r$ is expected at a given k_i value. Correspondingly, the R_τ prototype is expected to be located below the R_r prototype. Analogously to the R_c prototypes, a conditional 'extrapolated number of cycles' $N_{ex} \equiv N_{ex,\tau} \equiv N_\tau$ is introduced; $N_\tau \geq N_r$ is expected.

2.6.5. The pure $\mathrm{d}\tau$-loading as maximized case and other cases of 'weaker' loading
2.6.6. Comparative fatigue life assessments in the cases considered (not in favor of the critical plane concept)

These two sections in the thesis will be read with a great interest by every researcher who has created some fatigue life criterion based on the concept of one critical plane. Due to the restricted volume of this Author's Summary, abstracts are spared here.

2.7. The damage differential $\mathrm{d}D$ in the general case of combined loading. Versions of the IDD method

2.7.1. Searching for an empirical formula for $\mathrm{d}D$

In the general case of mixed (combined) loading, all the three components $\mathrm{d}s_r$, $\mathrm{d}s_c$ and $\mathrm{d}\tau$ of the $\mathrm{d}s$ loading differential appear simultaneously. If $\mathrm{d}s_r$, $\mathrm{d}s_c$ and $\mathrm{d}\tau$ appeared separately, the corresponding basic damage differentials $\mathrm{d}D_r = R_r\mathrm{d}s_r$, $\mathrm{d}D_c = R_c\mathrm{d}s_c$ and $\mathrm{d}D_\tau = R_\tau\mathrm{d}\tau$ would be produced. Now, the key question arises: how to formulate the damage differential $\mathrm{d}D$ per $\mathrm{d}s$? An empirical answer to this question will be sought as already grounded in Subchapter 2.2 in the thesis. The S-N approach will be followed and the $\mathrm{d}D$ differential will remain as a relative fatigue damage differential without any concrete physical sense. Any remark about the lack of such sense would belittle not the present IDD method but the S-N approach in general which involves fatigue damage summation. All the cycle counting methods would actually be belittled together with the mass-scale used Miner rule: in it, the damage $D_T = 1/N$ per a cycle does not have any physical meaning, either.

Thus, for now IDD is developed within the frames of empirical systematization and tries to enable the S-N approach at its 'weak point': under the general non-cyclic, multiaxial and non-proportional loading. The empirical S-N approach is brought up now to the most covering level that is integral both in its mathematical meaning and in the meaning of encompassing any sorts of loading. Of course, the various possible physical considerations for treatment the fatigue are not neglected in the thesis but, just the contrary, they are used.

2.7.3. The generalization using three damage intensities

After the previous PhD thesis, the decision was taken that, anyway, the method is subject to next development and improvement, and preferably in the σ'-σ''-$\mathrm{d}\tau$ coordinate sys-

tem. In this Section 2.7.3 in the thesis, certain considerations and limiting conditions lead to

$$\mathrm{d}D = \sqrt{\mathrm{d}D_r^{\,2} + \mathrm{d}D_c^{\,2} + \mathrm{d}D_\tau^{\,2}} = \sqrt{(R_r\,\mathrm{d}s_r)^2 + (R_c\,\mathrm{d}s_c)^2 + (R_\tau\,\mathrm{d}\tau)^2}\,. \qquad (2.7.3\text{-}1)$$

2.7.5. IDD equation with the R_r-intensity and the factors f_c and f_τ. First and second practical category of non-proportional loadings

Upon looking at Eq. 2.7.3-3, the following question certainly arises: do the intensities R_r, R_c and R_τ combined in the equation remain the same basic ones as they are under the pure r-loading, c-loading and $\mathrm{d}\tau$-loading? Or they are already different for their mutual influence? And, if they really influence one another, how do they change in combination?

There is no reason to expect that the three simultaneously participating intensities would remain equal to the basic ones without any influencing on each other. The crack growth mechanisms are too different under the pure r-loading, c-loading and $\mathrm{d}\tau$-loading, and would hardly remain the same in combination. The differences would be thoroughly cleared only after implementing experiments for determining the basic R_c and R_τ as described in Sections 2.5.1, 2.6.2, 2.6.3, 2.7.4 etc., and only after engaging efforts of many researchers interested in these sections.

So far, IDD verifications could only be done for combined non-basic intensities, and separately (according to Sections 1.4.5 – 1.4.7): on the one hand, under non-proportional $\sigma_x(t)$ and $\tau_{xy}(t)$, and, on the other hand, under non-proportional $\sigma_x(t)$ and $\sigma_y(t)$. Correspondingly, the first and second practical categories of non-proportional loadings are introduced. The first one is more important since it relates to a beam (including a shaft) as the most popular model, and the second category relates to the model of shell (including the plate). Cases where the three oscillograms $\sigma_x(t)$, $\sigma_y(t)$ and $\tau_{xy}(t)$ are all non-zero and all non-proportional are very rarely met in the engineering.

In this Section 2.7.5 in the thesis, the expectation is grounded that R_c for the first practical category will be lower than for the second one. In general under mixed loading, drawing the intensities R_c and R_τ closer to the basic R_r is assumed. This is conditioned by the continuity (the smoothness) of the damage accumulation. After all the discussions, and missing data from purposeful investigations of the basic intensities R_c and R_τ according to Sections 2.5 and 2.6, and facing always such problems put for the first time, then for the time being IDD remains to be performed and verified based on the following IDD life equation:

$$N = \left[\sum_{(S)} R_r \sqrt{\Delta s_r^{\,2} + f_c^{\,2}\Delta s_c^{\,2} + f_\tau^{\,2}\Delta\tau^2}\right]^{-1}. \qquad \textbf{(2.7.5-1)}$$

This Eq. 2.7.5-1 comes from Eq. 2.7.3-1 where $R_c = f_c R_r$ and $R_\tau = f_\tau R_r$ are substituted, and then $N = 1/D_{\Sigma,T} = [D_{\Sigma,T}]^{-1}$ is formed. R_r is the basic, 'proportional' damage intensity (under r-loadings i.e. uniaxial and proportional multiaxial loadings) determined according to Subchapter 2.4; f_c and f_τ assume the role of factors of (material's sensitivity to) loading non-proportionality. Thanks to these factors, the basic 'proportional' R_r intensity from the cyclic r-loadings becomes conveniently usable for life computation under non-proportional loadings.

The f_c and f_τ factors are new empirical fatigue parameters which can become as popular as the empirical parameters of an S-N line. According to the assumption of drawing the three intensities closer, it is to accept that f_c and f_τ would not differ too much under non-proportional loadings of the first practical category. As to the second practical category, f_c is only needed. Anyway, empirical data banks for f_c and f_τ should be built separately for the first and the second practical categories of non-proportional loadings.

2.7.7. No-damage areas and lines that surround them

An area round the coordinate origin of the X-Y plane (the generalized plane which is the σ'-σ'' plane in particular) containing assumed zero values of a given R damage intensity is called no-damage area. Let L be a general symbol of such an area. Simultaneously, L will also serve as a label of the curved line which surrounds the no-damage area. This line will be called surrounding line, border line, limiting line or L line. When the R intensity is specified as R_r, R_c or R_τ, then L will be L_r, L_c or L_τ.

The three lines L_r, L_c and L_τ are illustrated in Fig. 2.7.7-1 just as an example without any claiming for their actual disposition one to another. But, as a rule, the condition is kept that L_τ and L_c are more inward to the coordinate origin than L_r. This corresponds to the expected location of the R_τ and R_c prototypes below the R_r prototype. Fig. 2.7.7-1 relates to the plane X-$Y \equiv \sigma'$-σ''. The illustration for the plane X-$Y \equiv \varepsilon'$-ε'' will look similarly.

Only one quarter of each L line will be used: located in the first quadrant of the symmetry axes ξ and η (like in Fig. 2.4.1-1). The IDD user may draw for himself the L line as consisting of asymmetrical quarters but he should decide by himself which quarter is to be used depending on whether the loading is primarily tensile or primarily compressive, etc. That quarter is put in the first quadrant of the symmetry axes and is symmetrically reproduced in the rest of the three quadrants. This is in accordance with averaging and approximation discussed in the thesis.

Any L line is not fixed under every loading but varies if the loading is changed: if the latter is substituted by another with greater $\sigma_{\text{equ,m}}$, then each L area will 'swell out'.

It is very convenient to approximate the lines L_r, L_c and L_τ by the lines $l_{N,r}$, $l_{N,c}$ and $l_{N,\tau}$ of equal lives $N_r \equiv N_{\text{ex},r}$, $N_c \equiv N_{\text{ex},c}$ and $N_\tau \equiv N_{\text{ex}\,\tau}$. *In fact, instead of apparent lines L_r, L_c and L_τ, the numbers N_r, N_c and N_τ will be entered.* In this Section 2.7.7 in the thesis, additional considerations motivate the intention stated in Sections 2.5.2 and 2.6.4 to use only the smooth mode for the computation of $D_{\Sigma,c}$ and $D_{\Sigma,\tau}$. And if this mode is also preferred for $D_{\Sigma,r}$, then the accepted approximation of the lines L_r, L_c and L_τ by the lines $l_{N,r}$, $l_{N,c}$ and $l_{N,\tau}$ is additionally grounded.

Another IDD follower can, of course, prefer forming and entering each L line apparently, separately and independently of a corresponding line of equal life. However, this is hardly worth at the present stage of the IDD development.

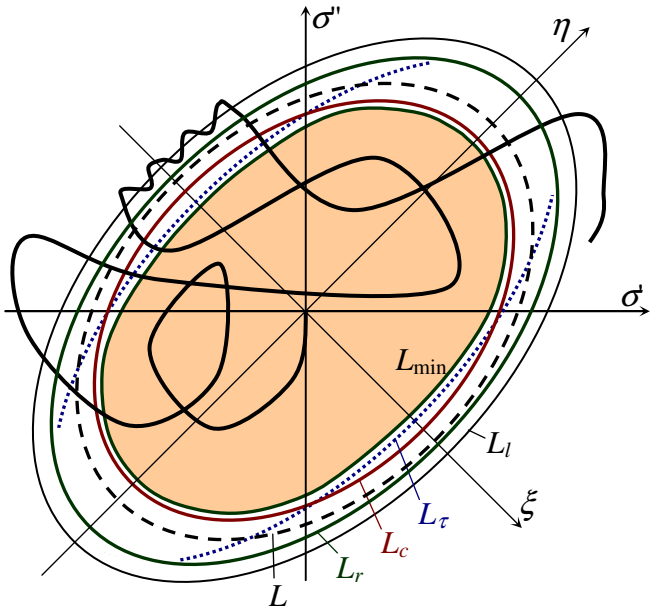

Fig. **2.7.7-1**. L lines (areas) and an (S_{xy}) trajectory (as an example)

The discussion up to here leads to the following: together with the empirical factors f_c and f_τ in Eq. 2.7.5-1, the IDD user will have to select and enter empirical parameters N_c and N_τ, as well. *They substitute any controversial notions of fatigue limits under non-proportional loadings*. Thus, in fact, the empirical data bank built so far (in Chapter 5) for the first category of non-proportional loadings includes four IDD parameters: f_c, f_τ, N_c and N_τ. With that, N_c and N_τ are set in comparison to N_r, and N_r comes from the input prototypes.

2.8. IDD in statistical (probabilistic) interpretation under random loading

This Subchapter 2.8 in the thesis lays a basis which, regarding its importance, complexity and scientific contribution, can grow into a separate thesis or theses. Due to the restricted volume of the present Summary, no abstracts from the subchapter are included here. The researchers interested in the subchapter can study it in the thesis. They will be the researchers who had worked on statistical and probabilistic distributions of amplitudes and had never imagined the following: without any need of involving amplitudes, one-dimensional and two-dimensional distribution densities of current (instantaneous) stresses can directly serve for IDD fatigue life assessment.

2.9. Interpolation for IDD

2.9.1. The necessity of interpolation. A number for interpolation

The *Ellipse* software must be able to generate, if necessary, intermediate ordinates of the input oscillograms $\sigma_x(t)$, $\sigma_y(t)$, $\tau_{xy}(t)$ (or others) by interpolation among their originally entered ordinates. Thus the Δs elements will be composed as short as to sufficiently represent the $\mathrm{d}s$ differentials.

Let ΔT be the interval between two input successive ordinates of every oscillogram within T before the interpolation. A so-called *number for interpolation* n_i is introduced: ΔT is divided into n_i equal parts Δt. Every original ordinate of every input oscillogram $s(t)$ will be reproduced (regenerated) by the interpolation and will be followed by $n_i - 1$ generated intermediate ordinates of the oscillogram (the graph) of an interpolation polynomial. In particular, $n_i = 1$ will be entered if any interpolation is not needed.

2.9.2. Trigonometric interpolation

Trigonometric interpolation means substitution of a periodic stress-time function $s(t)$ by a Fourier trigonometric polynomial. This notion evoked by IDD is again new. The trigonometric interpolation is close to the harmonic nature of the fluctuations (waves) in $s(t)$. Such interpolation is set in the IDD software as original working out.

2.9.3. Cubic-spline interpolation

In the last decades of the previous century, different kinds of software for computer drawing entered the engineering on a mass scale. The necessity of smooth connecting separate points by some curved line, the so-called spline, became one of the key problems. For the specificity of the *Ellipse* software, an author's own original programming version of the cubic-spline interpolation was developed and included in *Ellipse* during the 90s. This required managing many mathematical, algorithmic and programming details that are spared in the thesis.

The cubic-spline interpolation is envisaged for the general non-cyclic loading and can substitute the trigonometric interpolation in all the cases. As to the cycle loadings, the trigonometric interpolation is more convenient.

2.10. Conclusions

The tasks 1 – 4 formulated in Subchapter 1.6 have been carried out. Thus, an original theory has been built to enable the new IDD concept, respectively the new IDD research line, for fatigue life assessment.

In contrast to the large scattering of the existing methods that are often contradictory and incompatible, and difficult to select among them, a uniform and universal fatigue life equation has been proposed (as a main IDD version): Eq. 2.7.5-1. At its input, the following data are: arbitrary oscillograms $\sigma_x(t)$, $\sigma_x(t)$ and $\tau_{xy}(t)$, S-N lines in the form of R_r prototypes under cyclic r-loadings, empirical factors of loading non-proportionality f_c and f_τ (respectively, R_c and R_τ prototypes), and empirical numbers N_c and N_τ for no-damage areas.

The input oscillograms do not need any preliminary processing like reducing to a single oscillogram, schematization and counting cycles, distribution (spectrum) of amplitudes, distribution of means stresses, and so on. This sounds surprisingly to every CCA follower who is not familiar with IDD. Every next ordinate of each oscillogram, respectively every next oscillogram's fluctuation, comes directly, as it is, into the integration process. The ordinates of the oscillograms take turns in their actual mutuality, and the latter's influence on the fatigue life is automatically accounted.

The f_c and f_τ factors participate (only) under non-proportional loading (only f_c takes part in the second practical category, and none of the two f_c and f_τ factors participates under cyclic, non-cyclic or random r-loading). The many scattered CCA comparative studies cannot, anyway, give a basis for universal selection of one of the existing methods; but now they can be canalized in building a data bank for f_c, f_τ, N_c and N_τ.

It is also to state that each of Subchapters 2.1 – 2.9 represents, as well, an individual study which could be a separate investigation with individual conclusions. In this regard, Subchapter 2.8 can be especially mentioned: IDD is represented, as well, in a statistical (probabilistic) interpretation. The opportunity has been revealed for probabilistic fatigue life assessment based on densities of distributions of instantaneous stress values instead of stress amplitudes. This opportunity is also surprising, now to every follower of the existing methods for probabilistic fatigue life assessment.

The enabled connection of the individual studies from Subchapters 2.1 – 2.9 makes Chapter 2 sufficiently important for revealing the new research line. This thesis could have been restricted up to here since the conceptual problems have been solved. However, every fatigue life researcher will want to see practical results from IDD. For this purpose, IDD software is needed. Therefore, a tough part of the thesis will be (partly) presented in Chapter 3 and (especially) in Chapter 4: creating the IDD software.

CHAPTER 3.
SOFTWARE AND VERIFICATIONS OF IDD UNDER A SINGLE OSCILLOGRAM

3.1. The *Integral* algorithm

3.1.2. Algorithmic IDD equation of the fatigue life

Let consecutive s-ordinates ... s_A, s_C, s_B, ... be entered including peak ordinates s_A and s_B. Between them, intermediate s_C ordinates can also be present (Fig. 3.1.1-1 in the thesis). The *Integral* algorithm will recognize and distinguish the peak ordinates and will operate on the entire ranges between them.

A damage D_{AB} is produced from the range AB between two successive extrema A and B. According to the Newton-Leibniz theorem, the basic equation for D_{AB} is $D_{AB} = D(s_B) - D(s_A)$ in case the range AB is out of the area L_l, respectively L_r. These areas (Fig. 2.7.7-1) are actually linear intervals now. The whole damage accumulated within T is $D_\Sigma(T) \equiv D_{\Sigma,T} = \Sigma D_{AB}$. With that, the *Integral* name is conditional: since using $D(s)$ instead of $R(s)$, no integral

of differentials is computed, in fact (such an integral is actually done by the *Ellipse* algorithm).

Eq. 2.3.2-4 for $D(s)$ is involved, as well as s_l for the (peak or range) impulse mode and s_r for the smooth mode (peak or range impulse mode is explained in the thesis). The expression of $D_{\Sigma,T} = \Sigma D_{AB}$ and its reciprocal $N = 1/D_{\Sigma,T}$ lead to

$$N = \frac{i^* A}{\sum\left\{{}^{(1)}0 \text{ or } [{}^{(2)}(s_B^m - s_A^m) \text{or}^{(3)}(s_B^m) \text{or}^{(4)}(s_B^m + s_A^m) \text{or}^{(5)}(s_B^m - s_r^m) \text{or}^{(6)}(s_B^m + s_A^m - 2s_r^m)]\right\}}. \tag{3.1.2-1}$$

Behind the Σ sign, the current addend $\{\dots\} = \{D_{AB} i^* A\}$ stays in which s_A and s_B are the previous and the current (serial) peak s-ordinates renamed so that $s_B > s_A$ in absolute values. In this addend, s_l may stay instead of s_r. The very addend is:

(1) 0, if $s_B \le s_r$ (respectively $s_B \le s_l$) (the range AB is inside the interval L_r, respectively L_l; the limits of the interval are included in it);

(2) $s_B^m - s_A^m$, if $s_A > s_r$ (respectively $s_A > s_l$) and A and B are on the same side from zero (AB is one-sidedly out of L_r, respectively L_l); or if $s_A \le s_l$ (A is inside) in range impulse mode;

(3) s_B^m, if $s_A \le s_r$ (respectively $s_A \le s_l$) (A is inside) in peak impulse mode;

(4) $s_B^m + s_A^m$, if $s_A > s_r$, (respectively $s_A > s_l$) and A and B are on the both sides from zero (AB comes out from the both sides of L_r, respectively L_l) in impulse range or peak mode;

(5) $s_B^m - s_r^m$, if proceeding in smooth mode and $s_A \le s_r$ (A is inside);

(6) $s_B^m - s_r^m + s_A^m - s_r^m$, if proceeding in smooth mode and $s_A > s_r$, and A and B are on the both sides from zero (AB comes out from the both sides of L_r).

The sudden addend $1/(i^* N_l)$ is included implicitly and automatically in the options (3) and (4). Respectively, it is excluded (by the subtraction of s_r^m) in the options (5) and (6).

3.1.3. The *Integral* computer program. Demos

The *Integral* program is much simpler than *Ellipse*. Its heart is the algorithmic Eq. 3.1.2-1. The current input s-ordinates are read from a preliminarily prepared file. In the thesis, every current-data file is accepted to have a name beginning with the C letter. Thus, 'C-file' is often said in short.

The input S-N line data, i.e. the data of the input R-prototype, are entered from the keypad. Such data are called leading data or L-data. The L-data of the input prototype are s_l (displayed as `Sl`), N_l (`Nl`) and m (`m`); s_l and N_l are the coordinates of the R-prototype's through-point. The latter is the point of breaking the S-N line in two in the peak and range impulse modes, and s_l is the fatigue limit in the algorithmic Eq. 3.1.2-1. In the smooth mode, the through-point can also be given with different coordinates, although under the same names s_l and N_l. Now, instead of s_l, s_r (`Sr`) participates in Eq. 3.1.2-1 and is given separately. The divisor i^* (`i*`) is also entered.

The program, under the name `INTEGRAL.EXE`, can be downloaded from the IDD site.

Further on in this Section 3.1.3 in the thesis, *Integral* program demos are done as a part of the IDD software manual.

3.3. Real tests and comparison (under zero static level)

3.3.1. Experimental oscillograms and S-N line

Experimental fatigue life data are used from tests of flat specimens under uniaxial tension-compression carried out by Polish authors. Nine $s(t)$ oscillograms were produced with zero expected value for the static level. Each oscillogram is within a representative interval (period) $T = 649$ s and contains $245\,760$ ordinates. About $100\,000$ of them are peak ordinates and the rest of them are intermediate ordinates. Four specimens were tested at each of the nine loading levels.

The experimental points for the S-N line, the line itself (it proved to be smoothly bending) and its R-prototype are shown in Fig. 3.3.1-4 in the thesis.

3.3.2. Experimental and computed lives

The experimental lives TN_{exp} and the computed rain-flow lives TN_{cmp} are shown in the thesis in Table 3.3.2-1 and in an N_{exp}-N_{cmp} diagram in Fig. 3.3.2-1. The rain-flow computed lives were obtained by means of the free software (freeware) on the site http:// www.pragtic.com/program.php of Dr. Papuga. He kindly and competently cooperated for the computer processing on the nine C-files. They were kindly provided by the Polish Professor Lagoda under original names 0r21 – 0r29.

The PragTic cycle counting can be done as one-parameter schematization like in Section 3.2.2: without $s_{\text{m,i}}$ mean stress effect inclusion, i.e. by putting all the cycles directly on the zero static level. Two-parameter schematization, i.e. $s_{\text{m,i}}$ mean stress effect inclusion, can also be done. Each $s_{\text{a,i}}$ amplitude is transformed (enlarged) according to $s_{\text{m,i}}$ by means of one of the following options: (a) Goodman; (b) Gerber; (c) Smith-Watson-Topper (SWT). The latter was recommended by Dr. Papuga as providing very good results. Many details on the computations are spared in the thesis but can be seen in an Excel file 3.3.2.xls on the IDD site. Below, short abstracts from this Section 3.3.2 in the thesis follow.

Only after using the rain-flow method in the two-parameter schematization (taking $s_{\text{m,i}}$ into account) based on the recommended SWT version, were improved (the best) values $1{,}11$ and $1{,}13$ obtained for averaged ratios $N_{\text{cmp}}/N_{\text{exp,m}}$. By the way, it is clear that improved CCA schemes can always be proposed and the proposals can be many. Under such variety and scattering of methods proposed, it is confirmed again that to concentrate the efforts within the IDD conceptual frame looks more reasonable.

The nine C-files are on the IDD site. The computed IDD lives are illustrated in Fig. 3.3.2-2. Nearly all the points are within the both scatter bands of the factor 2. The enlarged solid square symbols (■) relating to the mean (averaged) lives $TN_{\text{exp,m}}$ take places now on the upper side, now on the lower side of the diagonal line of the factor 1. The average of the ratios $N_{\text{cmp}}/N_{\text{exp,m}}$ (including conditionally also $0\text{r}21$ and $0\text{r}22$) proves to be $1{,}01$ i.e. very close to 1 (if excluding $0\text{r}21$ and $0\text{r}22$, then $1{,}03$ is obtained).

The comparison of the IDD life results with the rain-flow results in the one-parameter and two-parameter schematization versions indicates that this IDD verification happens to be more than successful: it gives averages of the ratios $N_{\text{cmp}}/N_{\text{exp,m}}$ which are the most favorable (nearly equal to 1). And, as well, the scattering of the ratios $N_{\text{cmp}}/N_{\text{exp,m}}$ in the meaning of the root mean square of the deviation trends to be minimal with IDD.

The computed IDD lives prove to be approximately the same if s_r and m are varied in certain limits, and if the smooth mode is replaced by the peak or range impulse mode.

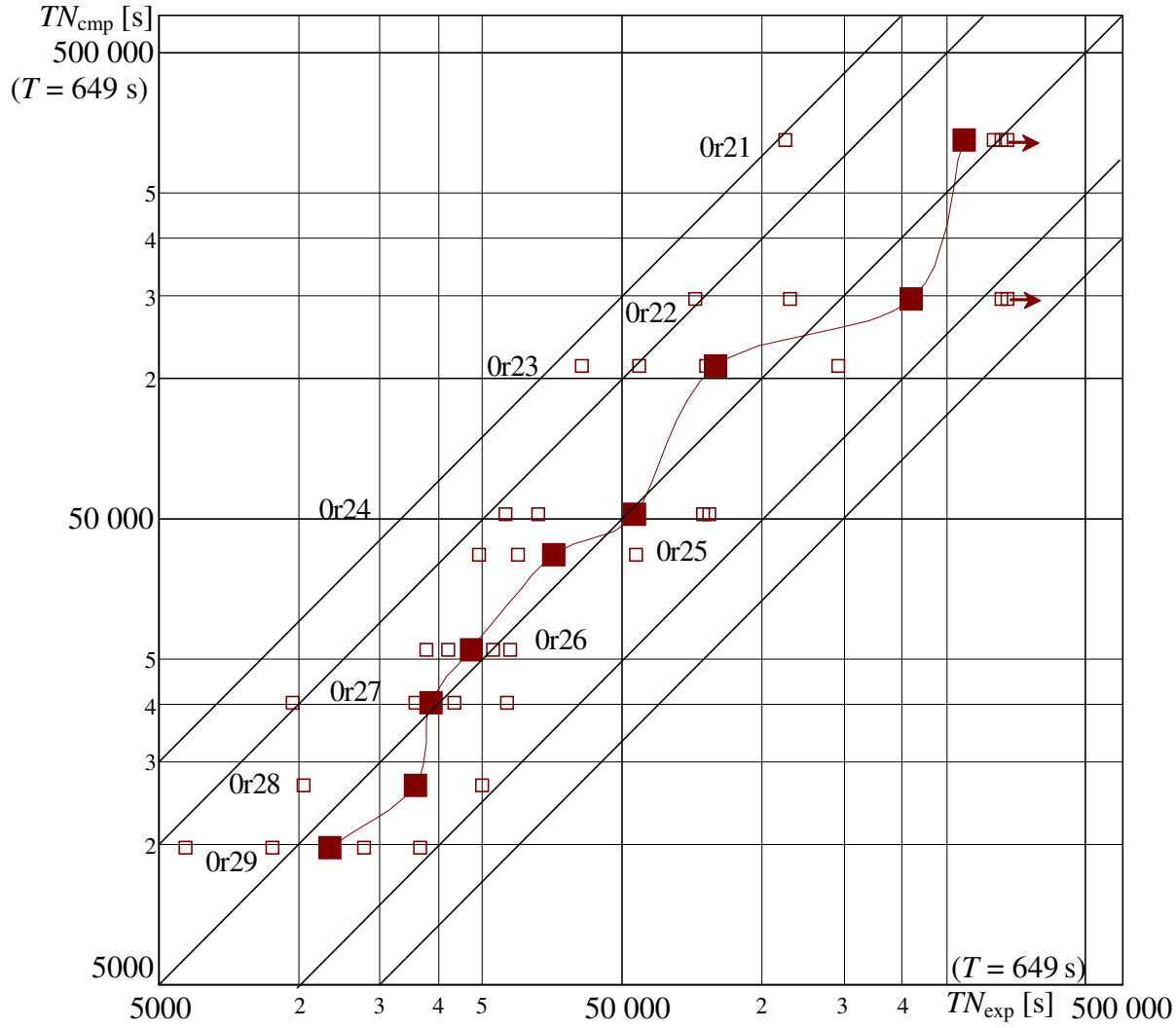

Fig. **3.3.2-2**. Diagram of the experimental lives TN_{exp} and the IDD computed lives TN_{cmp} using the smooth mode with s_r = 230 MPa

3.4. Conclusions

The reduced IDD version under a single $s(t)$ oscillogram has been worked out as implementation of the task 5 from Subchapter 1.6. For practical application of this IDD version, the *Integral* program had been created to substitute the *Ellipse* software in case there is a single non-zero oscillogram instead of three input non-proportional oscillograms envisaged. As well, the subtask of testing IDD in comparison with the rain-flow method and other CCA methods has been fulfilled.

The main final conclusion is: IDD successfully 'takes the examination' under a single arbitrary $s(t)$ oscillogram and, moreover, may predict the fatigue life better than the two-parameter schematization based on the rain-flow method with accounting the $s_{m,i}$ effect (the mean stress effect). After the 'examination taken', the re-direction of the efforts to IDD application to multiaxial non-proportional loadings can already be done.

CCA has to 'dip into the future' to look for $s_{m,i}$ and involve its influence on $D_{T,i}$, moreover in different versions without establishing any, indisputably. Whereas, the influence of different $s_{m,AB}$ values on D_{AB} from equally large AB ranges is involved automatically by Eq. 3.1.2-1: in case $s_{m,AB}$ is greater, D_{AB} is immanently obtained also greater.

CHAPTER 4. THE *ELLIPSE* SOFTWARE

4.1. The more important mathematical and algorithmic details

In the thesis, the full mathematical and algorithmic details are spared. In general, the efforts done for many years for surmounting all the math-and-algorithm problems faced during the numerous tests and applications of the software cannot be presented in detail in the thesis; neither can all the entailed complications and improvements be described. Moreover, full author's results from a programming labor are not supposed to be entirely presented in case the software is envisaged for copyright protection. Only the more important (the conceptual) details are presented. They have not been immediately obtained but after lots of other ideas, trials and rejections. A lot of algorithmic traps have been surmounted.

4.1.10. The graph mode

The graph mode is on in case the user requests it. A Fortran option is used to make the screen full and function in color graph mode 320x200. The background is set blue but the user can request it white (as it is in Fig. 4.6.1-1).

The color palette includes green, red and tan.

From the rectangle area 320x200, a square is separated right (Fig. 4.6.1-1) within which the trajectory is displayed, and left from the square a field is available for captions. The user sets the square as a part of the X-Y plane where the trajectory (S_{xy}) is expected to find place. Correspondingly, algebraic values are entered for `minX` to the left side of the square, `maxX` to its right side and `minY` to the bottom side.

Insofar falling into the square, there are displayed: (in green) the axes X, Y, ξ and η; (in

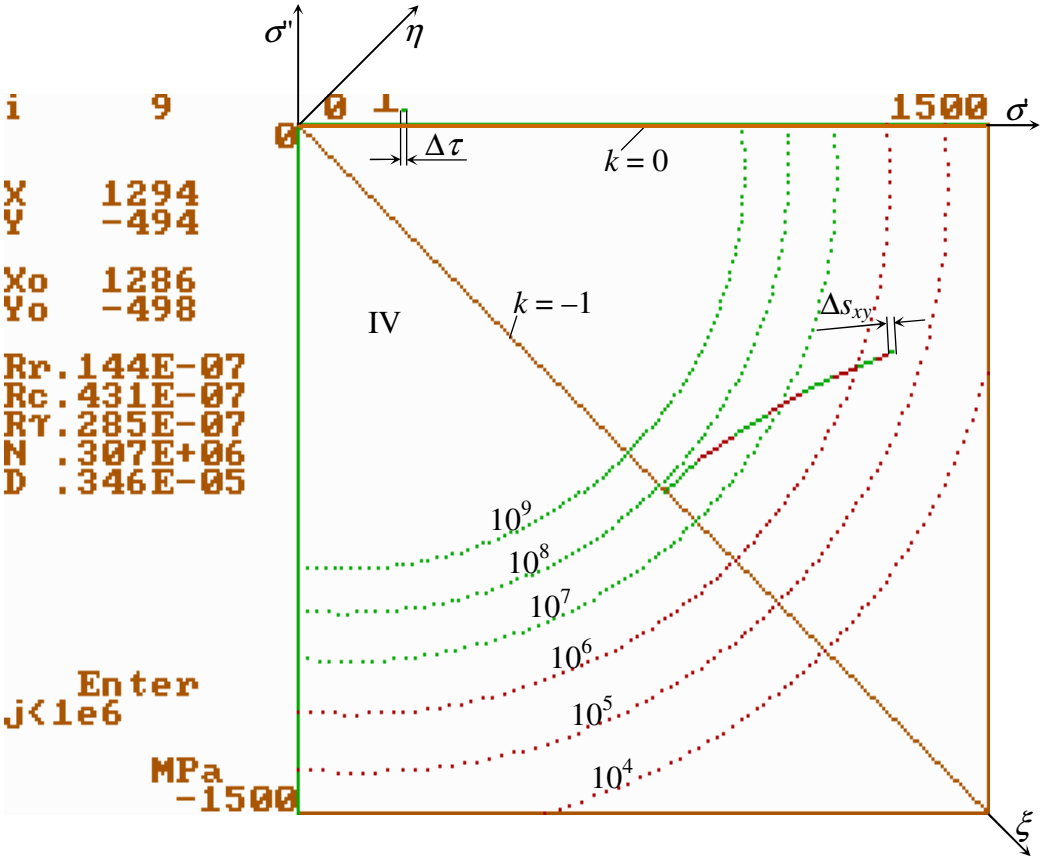

Fig. **4.1.10-1**. An example of graph mode

tan) the radial lines with k_i entered (if any of the axes X, ξ and η is also one of those radial lines, it also becomes tan).

If the user enters `minX` and `maxX` with a little difference between them i.e. a small `A`, it is zooming in: a small square from the X-Y plane is displayed on the whole screen. And if a big `A` is entered, it is zooming out. The respective scaling is an essential issue while creating the algorithm.

Fig. 4.1.10-1 represents a print-screen copy after a pause requested at `i = 9`. The user is expected to enter `j`: the number of next Δs_{xy} elements to be displayed in a group. If a great `j` is entered (up to one million), a lot of elements will quickly be displayed or the entire trajectory will be drawn. Correspondingly, the digits of the numbers left from the square will change quickly. After exhausting `j`, the next pause occurs. If the user wants to observe the elements one by one, then Enter is just pressed for each element. Thus, the changing numbers left from the square can also be observed one by one. After drawing the entire trajectory, the life prediction result will be displayed.

4.2. The *EllipseT* program

The *EllipseT* program is the basic one of the *Ellipse* software. The last *T* letter of the program's name means using trigonometric interpolation. As already known, this and any other program of the IDD software can be downloaded from the IDD site. The Fortran name of the program is ELLIPSET.EXE.

The IDD user could not immediately acquire (the work with) *EllipseT* (and the entire *Ellipse* software). Certain self-teaching is necessary by means of the demos/exercises presented further in the thesis. All the files mentioned there are available on the IDD site.

In the thesis, five sections of this Subchapter 4.2 are presented. They compose the main part of the manual for teaching how to work with the IDD software.

4.3. The cubic-spline interpolation. The program *EllipseS* (and *EllipseC*)

4.3.2. Demos with *EllipseS* (similar to sections 4.2.1 – 4.2.3)

The Fortran name of the program is ELLIPSES.EXE. It can also be downloaded from the IDD site together with the files for the demos.

In the thesis, the contents of this Section 4.3.2 and of the next Section 4.3.3 represent the next part of the manual for teaching how to work with the IDD software.

4.4. Conclusions

An original differential theory was developed for the variant and invariant non-proportionally varying stresses and strains, and for the transition from the variant to the invariant ones and vice versa in a one-to-one correspondence. A lot on new notions were involved. Within the frames of this theory, the following problems were solved: determination of the $\alpha'(t)$ function (the principal axes rotation) and switchover of the $\pm$ signs in the principal stresses and strains equations. For this purpose, three switchover conditions (the third one is angular or radial) were (for the first time) deduced, and a necessity of dividing variant elements into two subelements each was found out. The very problem of such dividing was also solved.

The 6th task (formulated in Subchapter 1.6) engaging the most efforts and time was successfully fulfilled: the software for IDD computation was created. Mathematical and

algorithmic problems were solved having such volume and difficultness which usually engage in the scientific research a whole team of mathematicians and programmers. Instead, efforts of the author were engaged for many years. A lot of algorithmic difficulties and traps were surmounted. A lot of programming work was done. A manual for using the *Ellipse* software was written.

CHAPTER 5. IDD VERIFICATIONS UNDER NON-PROPORTIONAL LOADINGS OF THE FIRST PRACTICAL CATEGORY

5.1. Strategy of the verifications

As grounded in Section 2.7.5, the IDD Eq. 2.7.5-1 will be verified in the thesis only under non-proportional loadings of the first, more important practical category relating to bending or axial loading and torsion of a beam as the most popular model of a structural component.

The strategic aim of the verifications is to build an initial data bank of the new empirical IDD parameters f_c, f_τ, N_c and N_τ. It seems attractive and possible to take the world-wide scattered fatigue life experience under proportional and non-proportional loadings and focus it universally to IDD based on such empirical parameters. The verifications will indicate insofar the IDD parameters show some clear correlation according to the material etc., some repeated appearance and predictability, so that they would really turn into popular new empirical fatigue characteristics placed in manuals, data bases, etc.

The strategy includes, as well, the opportunity for every other researcher to use the experimental data from the verifications done and try to check whether they are better covered by another proposed method than IDD. And if the result from such a trial is negative

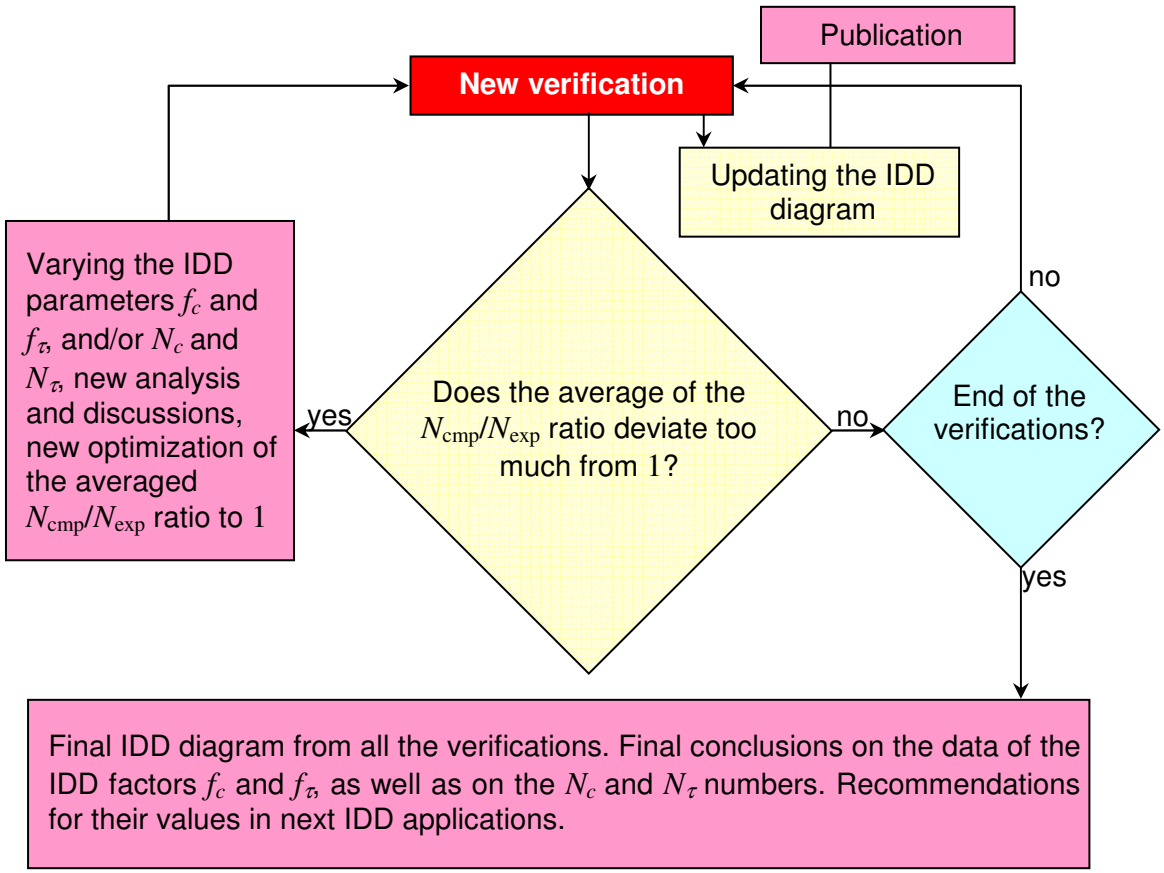

Fig. **5.1-1**. Algorithm of the verifications

(as expected), this would actually lead to establishing IDD.

In this Chapter 5 in the thesis, six verifications (1) – (6) preceded by an adaptation (0) are presented. Their descriptions, all the many illustrations to them and the individual results obtained are spared in this Summary. The verifications done are considered sufficient for finalizing the thesis and presenting it for defense. However, the work does not conclude with these verifications: before, during and after presenting the thesis, the verifications continue in Volume II. With that, there is a progress in forming an initial data bank of the (only) two IDD parameters f_c and N_c under non-proportional loadings of the second practical category.

The verifications strategy follows the algorithm shown in Fig. 5.1-1. The 'IDD diagram' in this algorithm means an N_{cmp}-N_{exp} diagram from the IDD verifications.

5.9. Conclusions from Chapter 5

5.9.1. IDD N_{cmp}-N_{exp} diagram

In Fig. 5.9.1-1, there are placed in all 49 values of N_{exp} and corresponding 49 values of

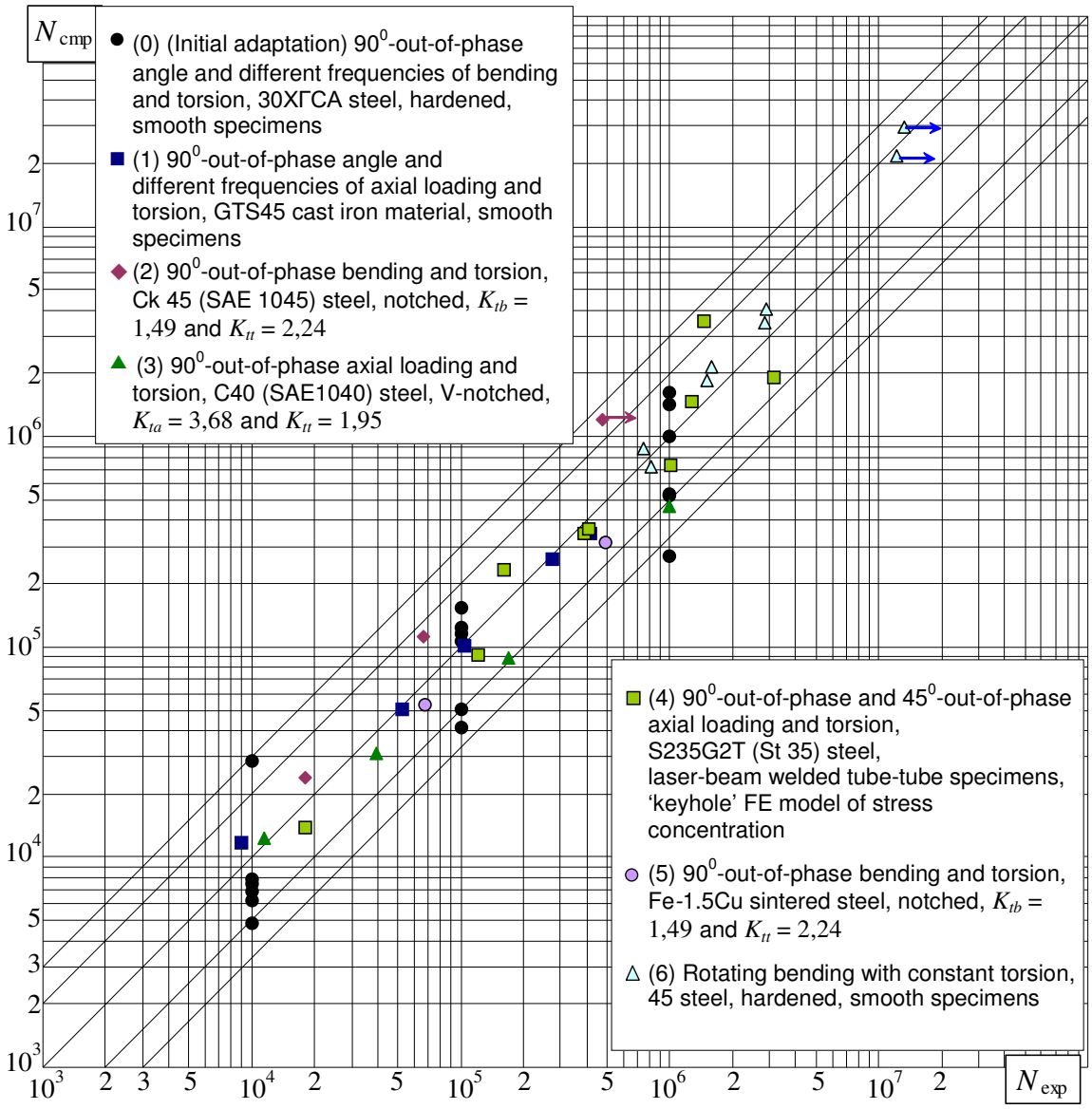

Fig. **5.9.1-1**. IDD N_{cmp}-N_{exp} diagram from the (0) initial adaptation and the (1) – (6) verifications (the $N_{\text{cmp}}/N_{\text{exp}}$ ratios have 1,02 average and 0,52 standard deviation from the average)

N_{cmp} from the adaptation (0) and the verifications (1) – (6). Three of the N_{exp} values are considered as 'greater than' for the availability of run-outs (survived specimens). For the rest 46 N_{cmp}/N_{exp} ratios the statistical data (in the Ch5.xls file) are valid as follows.

The average is $1{,}02$: an extremely good result. The standard deviation (from the $1{,}02$ average) is $0{,}52$: a very successful result. It means that in future similar IDD applications N_{cmp} will be expected to appear most probably between $1{,}54^{-1}N_{exp} = 0{,}65N_{exp}$ and $1{,}54N_{exp}$. The greatest deviations of N_{cmp}/N_{exp} are Min $0{,}27 = 3{,}68^{-1}$ and Max $2{,}86$. They have both appeared in the initial adaptation whereas in the verifications (1) – (6) Min is $0{,}47 = 2{,}14^{-1}$ and Max is $2{,}45$. By the way, the average of N_{cmp}/N_{exp} from the verifications (1) – (6) is $1{,}05$ and the standard deviation is $0{,}41$.

5.9.2. Empirical data bank of the IDD parameters and conclusions

So far, based on the thesis (and the latest studies being placed in Volume II), the following empirical data bank (Table 5.9.2-1) has been formed for the first practical category of non-proportional loadings. The bank is, of course, initial and uncompleted but is a good basis for next IDD fatigue life evaluations.

According to the previous Section 5.9.1 and speaking more generally, the expected inaccuracy of N_{cmp} would be less than 2 as an error factor (i.e. $0{,}5 < N_{cmp}/N_{exp} < 2$). This inaccuracy can always be directed to the safety side by setting proper higher values of the four IDD parameters.

Next verifications intended will precise Table 5.9.2-1 and would change its structure. So far, it seems that f_c and f_τ for steels are in correlation with the static strength: f_c and f_τ are 2 and 3 in case R_m exceeds ≈ 700 MPa, and f_c and f_τ decrease to 1 and 1 when R_m is down to about 410 MPa. It is expected that the correlation considered will be expressed later as

Table. **5.9.2-1**. Empirical data bank of the IDD parameters for the first practical category of non-proportional loadings

IDD parameters		Confirmed for		
		R_m, $R_{p0,2}$ MPa/ Materials	Specimens	Loadings
Steels	$f_c = 2$ $f_\tau = 3$ $N_c \geq N_r$ $N_\tau \geq N_r$	1490, 1300/ 45 (hardened) 1310, 1090/ 30ХГСА 1030 (welding), 350/ S235G2T (St 35) 850, 704/ Ck 45 (SAE 1045) 715, 537/ C40 (SAE 1040)	Smooth and notched (with K_t to about $3{,}68$), and welded	Non-proportional bending or axial loading and torsion with t_c to about $0{,}62$ and t_τ to about $0{,}73$, with $\sigma_{equ,m} = 0$ and $\sigma_{equ,m} > 0$, with various forms of trajectories
	$(2 > f_c > 1,$ $3 > f_\tau > 1,$ $N_c > N_r,$ $N_\tau > N_r)$	(551, 365/ 11523.1)	(Smooth)	
	$f_c = 1$ $f_\tau = 1$ $N_c > N_r$ $N_\tau > N_r$	410, 300/ Fe-1.5%Cu	Notched	
Cast iron	$f_c = 2$ $f_\tau = 3$ $N_c > N_r$ $N_\tau > N_r$	449, 305/ GTS 45	Smooth	

clearer functions $f_c = f_c(\mathrm{R_m})$ and $f_\tau = f_\tau(\mathrm{R_m})$ in intervals with lower limits about 1 and upper limits about 2 and 3. These intervals are not large and therefore even a significant scatter of the functions $f_c(\mathrm{R_m})$ and $f_\tau(\mathrm{R_m})$ in them would not deprive every new fatigue life assessment of success. So far, the data in the Specimens and Loadings columns of Table 5.9.2-1 do not seem to influence $f_c(\mathrm{R_m})$ and $f_\tau(\mathrm{R_m})$. In other words, f_c and f_τ seem to be valid for any specimens and any loadings of the first practical category, as well as for non-zero static levels of the oscillograms.

The cast iron material in Table 5.9.2-1 showed $f_c = 2$ and $f_\tau = 3$. It will be interesting and important, of course, to have data for f_c and f_τ obtained also for aluminum alloys and other materials.

The studies on the 11523.1 steel, included in the data bank, relate to smooth tubular specimens subjected to non-proportional tension-compression and torsion. These studies continue after the presented final version of the thesis and go into Volume II. They are done together with Jan Papuga and other Czech researchers. Publication of the results is envisaged for later (therefore, parentheses are used in the corresponding row of Table 5.9.2-1). Variant trajectories with various interesting forms in the σ_x-τ_{xy} plane were implemented. Computed IDD lives are obtained in a good agreement with the experimental ones in case f_c and f_τ are set by interpolation to be between the values valid for C40 (SAE 1040) and Fe-1.5%Cu. This confirms the above-mentioned decrease in f_c and f_τ due to a decrease in $\mathrm{R_m}$. Dr. Papuga has also applied other methods but so far their computed lives results significantly yield to the IDD results.

The numbers N_c and N_τ are left with some indefiniteness in Table 5.9.2-1. In fact, the areas L_c and L_τ are not strictly given. This corresponds to the opinion, already mentioned, that the notion of fatigue limit contains some uncertainty and fictitiousness especially under arbitrary non-proportional loadings. What only looks for sure is that the L_c and L_τ lines should be more inward to the coordinate origin than the L_r (or L_l) line. This can be ensured even by the equalities $N_c = N_\tau = N_r$ but only if $f_c > 1$ and $f_\tau > 1$. Otherwise, in case f_c and f_τ near 1, then $N_c > N_r$ and $N_\tau > N_r$ should be set.

As to trajectories which go farther out of the L_r area, setting N_c and N_τ to be or not to be greater than N_r cannot seriously influence N_{cmp}. However, if the trajectory does not go out of the L_r area, then the selection of N_c and N_τ to be greater than N_r becomes important. As shown in the thesis, if a trial increase of N_c and N_τ sharply changes N_{cmp}, then stronger inequalities $N_c > N_r$ and $N_\tau > N_r$ should be preferred. Generally speaking, as a tentative recommendation, N_c and N_τ should be selected in the order of $10N_r$ with possible error in favour of safety.

It is to additionally note that fatigue life assessment methods are also proposed by a part of the authors of the experimental data used in the IDD verifications. None of all the other methods has been simultaneously applied to all the experimental data of the six IDD verifications. If such a trial is done, it will be seen that the conclusions in Subchapter 1.5 are confirmed: too various methods, proved only in specific loading cases, incompatible (or inapplicable) and conflicting to each other in all the cases.

CHAPTER 6. NECESSITY AND POSSIBILITY FOR APPLICATION OF IDD TO MACHINES AND TECHNICAL EQUIPMENT IN THE FOREST INDUSTRY

6.2. First example [33]

6.2.1. Circular shaft. Kinematics of cutting

In this Section 6.2.1 in the thesis, a conclusion is drawn that for the purposes of the

next load and strength calculation, the forces on the circular blade teeth can be considered as concentrated in the tooth vertices (as shown in Fig. 6.2.1-4 in the thesis).

6.2.3. Approximate expectations of the normal and sheer stress oscillograms

In this Section 6.2.3 in the thesis, after all, the possible $\tau(t)$ and $\sigma(t)$ oscillograms shown in Fig. 6.2.3-2 are derived in a try to take into account preceding conclusions and example numerical data. Concrete stress scales in MPa are not given but only relations between fluctuations.

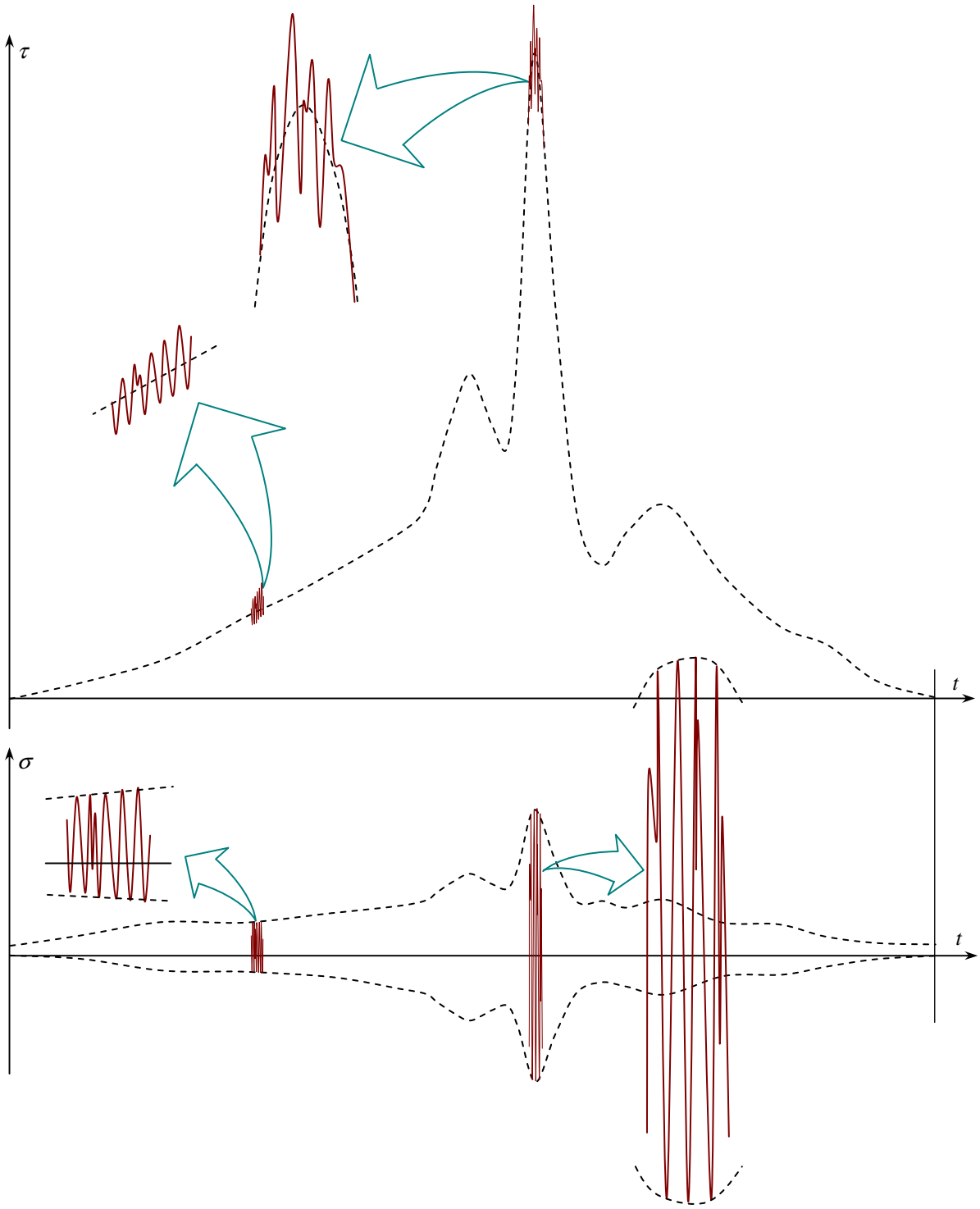

Fig. **6.2.3-2**. Possible $\tau(t)$ and $\sigma(t)$ oscillograms during a complete cut through the 160x160 mm square cross section for about 6 seconds

6.2.4. Conclusion

If involving also the other cutting regimes besides the cross cutting considered, as well as all the possible dimensions of the piece of wood and varying the many sorts of the wood, then a quite multiform spectrum of $\sigma(t)$ and $\tau(t)$ oscillogrmams will be obtained. If carrying out strain-gauge investigations, the experimental oscillogrmams obtained will have the last word. Anyway, fatigue life computation is to be done under oscillograms $\sigma(t)$ and $\tau(t)$ that are very complicated, quite specific (not met at other machine shafts), non-cyclic, random and non-proportional. Practically, it is very likely that each author of a different method for fatigue life assessment, after seeing the oscillograms in Fig. 6.2.3-2, will decline an invitation to apply that method. Whereas, the IDD method is applicable namely under such conditions and therefore it is necessary. All the knowledge from the thesis, and mainly from the verifications in Chapter 5, can be applied. Of course, this is not possible within the frames of the thesis that is already 'too swollen'. But namely based on the thesis, a large field is opened for future doctorands to obtain concrete IDD fatigue life computation results within the doctoral program '02.01.32 Machines and Technical Equipment for the Forestry, Wood Industry, Woodworking and Furniture Industry'.

6.3. Second example

6.3.1. Band-saw blade

In the books where the fatigue of materials is treated, the notion of a random oscillogram with a non-zero mean (static) stress is introduced. But no popular example is established as classic. And namely the case of the band-saw blade where the tensile stress oscillogram will vary about a static level is very suitable to become a classic example.

6.3.2. Calculation scheme

A scheme (a model) is shown in Fig. 6.3.2-1 (in a first version) in the thesis. The scheme is of a kind which is usually imagined by a professor in Strength of Materials. In the case considered, the saw band is a typical engineering example of a statically indeterminate closed contour. Such statically indeterminateness is a classic subject in any Strength of Materials course, including in the author's textbooks. There, as well as in the thesis, details, explanations, terms and symbols involved can be found.

An 'opening' in the closed statically indeterminate contour is shown in the thesis with revealing the two equal and opposite internal tensile forces with a common X magnitude. The solution of the statically indeterminate problem i.e. the determination of X can be achieved based on the deformational equation $\partial U/\partial X = \lambda - \alpha_t l \Delta t$. The equation's left side $\partial U/\partial X$ (unless it is represented in a different form) could be developed e.g. as a sum of Castigliano integrals. Besides, with the deflection of the saw band along the two half-circumferences of the band wheels, the equation $M_y(x) \approx EJ_y/R$ will participate where R is the radius of the wheels. The problem becomes very interesting. It will be developed together with students as coauthors and band-saw specialists from the Faculty of Forest Industry.

6.3.3. Expectations of the tensile stress oscillogram. Conclusion

The analysis from the previous Section 6.3.2 is already sufficient to envisage the tensile stress oscillogram as follows. The diagrams of the variable $N_x(x)$ and $M_y(x)$ along the whole length of the saw band will be obtained. Hence, the diagram of the tensile stress $\sigma(x)$ will result from $N_x(x)$ and $M_y(x)$ simultaneously. And now: while any cross-section of the band

is traveling the whole length of the moving saw band, the graph of the $\sigma(x)$ function is turning into a $\sigma(t)$ oscillogram. This is an essential point of consideration contributing to the thesis.

With that, cutting force $P = \text{constant}$ is assumed up to here. And if setting $P = P(t)$ like in the analysis in the previous Subchapter 6.2, then the $\sigma(t)$ oscillogram will prove to have complex and random variations. They will be additionally complicated if involving vibrations and other more dynamic phenomena. It will be an essential scientific achievement when obtaining a final and actual oscillogram of $\sigma(t)$ in a band-saw blade. That oscillogram will be a very good occasion for IDD application following the verification in Chapter 3. The case will be popularized to become a classic example as stated in Section 6.3.1.

The spirit of the conclusion in the previous Subchapter 6.2 (Section 6.2.4) remains here, as well. Indeed, the fatigue loadings in the machines and technical equipment in the forest industry prove to have such complicatedness and complexity as to open one of the widest fields for application and demonstration of IDD in next diploma and doctoral theses. The envisaged joint studies with the students, and the collaboration with the specialists in machines and technical equipment for the forest industry, and the IDD defence discussions, will all give the author good chances to contribute to making the Faculty of Forest Industry known as one of the most competent faculties in reference to fatigue of materials.

CONCLUSION

(Final concluding notes)

The mechanism of forming the fatigue life is too complicated and inscrutable. This provides a possibility to every researcher to propose his own CCA method (model) for fatigue life assessment which contains some partial truth and is experimentally confirmed in some limited scope. Another researcher, under different experimental data and different loadings, does not find confirmation of the previous method and, in his turn, also proposes his own model. After all, there is not any uniform, all-acknowledged and universal CCA method but there are many disputable methods comparing to each other, each one with its partial truth and that is why they tolerate each other.

Now, something radically different is proposed: not to have loading cycle as the basic notion but to have it as a particular notion, and, instead of searching for disputable cycles, to follow the indisputable differentials (Fig. 1.1-3b) of any loading and directly compute the damage differentials per the loading differentials.

Thus, it is not simply about a serial new method in expectation of a tolerant attitude. Now, a united skeptical or negative reaction is possible: considering that many thousands of fatigue life researchers in the world had searched for cycles in every loading, the IDD concept and the author's IDD method could make a lot of opponents. They could even state that IDD rejects all the accumulated fatigue life knowledge built on the basis of the notion of loading cycle. On this occasion it is to pay attention again to the contributions 2.3 and 13.4 (in Expanded Review of Contribution on the IDD site): IDD rejects nothing of the existing knowledge. The thesis has entirely been built on the basis of the existing knowledge and the main idea is to use it in another way.

It is understandable that the colleagues would express skepticism and jealousy after they have devoted theirs investigations and careers to CCA and received acknowledgements and degrees for that. It is understandable that they would look for weak points of the IDD concept and of the author's IDD method, and would raise controversial questions since the complicated and inscrutable mechanism of forming the fatigue life leaves a large place for a lot of disputation.

However, there is a possibility which leaves no place for disputation on whether IDD should be acknowledged or not, as follows.

Let any IDD opponent verify any other fatigue life evaluation method by using the same experimental data files used also by the author in the IDD verifications done in Chapter 5. Let the verification in Chapter 3 be also added. Let the verification or verifications continuing in Volume II be added, as well. All the experimental data are not of the IDD author but of other authors and therefore a partial selection of one's own experimental data is excluded. And if the IDD opponent proves that the other method is always applicable in all the mentioned cases and categorically excels the IDD method, then the disputation ends: the IDD method should withdraw. Moreover, the other method will prove to be that missed one which can claim for general validity now. But if the other method yields, the disputation ends again: the IDD method should be given the right of way. Moreover, resetting and canalizing the world investigations to IDD should be recommended.

If the other method and the IDD method turn out to be approximately tantamount, again the IDD method should be given the right of way to continue comparing and proving itself in next and next verification (Volume II). With that, the oscillograms should purposefully be diversified as much as possible: to be of both the first and second practical category of non-proportional loadings, and of mixed loading with various trajectory ratios t_r, t_c and t_τ, and of various trajectory's forms, and of both cyclic and non-cyclic loadings, and of both deterministic and random loadings, and of pure r-loadings, pure c-loadings, pure $\mathrm{d}\tau$-loadings, and so on.

Hereby the author closes and lets the colleagues and the honorable scientific jury members take the scientific responsibility for the evaluation of the thesis.